ISSN 1913-1844 (Print)
ISSN 1913-1852 (Online)

MODERN APPLIED SCIENCE

Vol. 3, No. 6
June 2009

Canadian Center of Science and Education

Editorial Board

Ahmad Mujahid Ahmad Zaidi	Universiti Tun Hussein Onn Malaysia, Malaysia
Alessandra Crosato	Delft University of Technology, the Netherlands
Hamimah Adnan	Universiti Teknologi MARA, Malaysia
J S Prakash	Sri Bhagawan Mahaveer Jain College of Engineering, India
Lim Hwee San	Universiti Sains Malaysia, Malaysia
Moussaoui Abdelkrim	University of Guelma, Algeria
Musa Mailah	Universiti Teknologi Malaysia, Malaysia
Stefanos Dailianis	University of Patras, Greece
Sujatha. C.H	Cochin University of Science and Technology, India
Sundus H Ahmed	Ministry of Science and Technology, Iraq
Susan Sun	Canadian Center of Science and Education, Canada
Sutopo Hadi	University of Lampung, Indonesia

Modern Applied Science

www.ccsenet.org/journal.html

Vol. 3, No. 6

June 2009

Contents

Visualization of Urban Transportation Data Generated by Wireless Sensor Network Using Modern Approaches 3

Manni Huang

Spatial Sound Reproduction Based on HRTF Auto-Selection Algorithm 21

Cheng Zhang, Ke'an Chen & Chao Xing

Implementation of Energy Management Structure for Street Lighting Systems 30

C.Maheswari, R.Jeyanthi, Dr.K.Krishnamurthy & M.Sivakumar

Study on Economic, Rapid and Environmental Power Dispatch Based on Fuzzy Multi-objective Optimization 38

Lubing Xie, Songling Wang & Zhiquan Wu

The Effect of Radial Swirl Generator on Reducing Emissions from Bio-Fuel Burner System 45

Mohamad Shaiful Ashrul Ishak, Mohammad Nazri Mohd Jaafar & Yehia A. Eldrainy

Study on Coating and Luminescence Mechanism of Hydrothermal Preparation of Mica-based Pearlescent Pigments 52

Daguang Li, Chao Yu, Tiehu Li, Weiqing Fu, Wenjin Ji & Fenghua Zhao

Vibration-Based Fault Diagnosis of Hydraulic Pump of Tractor Steering System by Using Energy Technique 59

Kaveh Mollazade, Hojat Ahmadi, Mahmoud Omid & Reza Alimardani

Stock Investment Value Study Based on Fuzzy Comprehensive Evaluation 67

Zongyan Xu, Zhong Liu, Feifei Zhou & Haihua Li

Purification and Partial Characterization of Esterase from Marine *Vibrio fischeri* 73

P. Ranjitha, E.S. Karthy & A. Mohankumar

The Work in Process (WIP) Control Model and Its Application Simulation in Small-batch and Multi-varieties Production Mode 83

Yaochao Wang

Mixing Process of Binary Polymer Particles in Different Type of Mixers 88

S.M.Tasirin, S.K.Kamarudin & A.M.A. Hweage

Study on the Product Symbol System for Brand R&D 96

Qin Wang

Microwave Sintering of Niobium Co-doped Yttria Stabilized Zirconia 102

S.Manisha Vidyavathy & Dr.V.Kamaraj

Research on Flocculation Property of Bioflocculant PG.a21 Ca 106

Yongzhang Pan, Bo Shi & Yu Zhang

The Application and Modeling for Conditional Heteroscedasticity Time Series 113

Wenfang Su, Rui Shan, Jun Zhang & Yan Gao

Research for Characteristics of Rotating Dipole Acoustic Source in Spatial Acoustic Field 119

Zhihong Liu, Chuijie Yi & Qian Zhang

One Type of Optimal Portfolio Selection in Birandom Environments 126

Limei Yan

Modern Applied Science

www.ccsenet.org/journal.html

Vol. 3, No. 6

June 2009

Contents

A Small Power SMP Based TOPSwitch 132

Tingjian Zhong, Hongxing Luo & Wenjin Dai

Influence on Lubricant Properties of Anti-wear Agent Containing Nitrogen, Boron and Molybdenum 136

Xuguo Huai & Shihai Zhao

Research on Vectorization of Embroidery Images Consisting of Straight Lines & Circular Arcs 141

Jinglan Li & Huaiqiang Liu

Modern Applied Science

www.ccsenet.org/journal.html

Vol. 3, No. 6

June 2009

Visualization of Urban Transportation Data Generated by Wireless Sensor Network Using Modern Approaches

Manni Huang

Department of Computer Science, Trinity College Dublin

College Green, Dublin 2, Ireland

E-mail: huangm@tcd.ie

Abstract

Distributed wireless sensor networks are one of the first real world examples of pervasive computing, the notion that small, smart, and cheap sensing and computing devices will eventually permeate the environment. Nowadays, it has proved to be useful in various applications. In a large sensor network, no matter the sensors are large or small, the data are especially complicated and unintelligible. We should make it easy to understand with the help of technologies of existence. Certainly, data visualization, which is defined as the interactive graphical presentation of data, could present data in the forms of aesthetic layout rather than traditional tables, pie charts and bar graphs, making the data more beautiful, elegant and descriptive. Attempting to visualize the data generated by wireless sensor networks, the audience will not be simply restricted to experts, but also all the people.

This dissertation aims to demonstrate the technology of both wireless sensor network and data visualization with the basis for the critical problems, challenges and future goals of development and applications. And we propose a simulative model integrated the two above technologies, emphasis on the processing. The framework is based on Google Maps; thus it allows robust navigation and communications within several different spatial ontologies. Our approach factors the problem into the following sub goals: deploying the sensors in urban crossroad, acquiring and analyzing data, and representing the data with aesthetic forms.

Keywords: Wireless sensor network, Data visualization

Abstract

This chapter introduces the motives of this research; it addresses present situation and its derivative research questions. Furthermore, it concludes with an overview of the content of the dissertation.

1.1 Motives of This Research

Over the past ten years, true, the Construction of Urban Transportation Facilities developed rapidly, but due to outdated management style and unreasonable transport infrastructure, engineers (Jaesup Lee, Randall and Michael) indicated that congestion, safety and air pollution remain as serious challenges in urban transportation systems. Facing up to the problem of increased urbanization, industrialization and changes in population density, scientists in developed countries took up research and put forward the concept of ITS (Intelligent Transport Systems) in the 1960s. With the rapid development of Computer Science and Information Technology, today's ITS have been evolved into a synergy of new information technology for simulation, real-time control, and communications networks. The system could round-the-clock monitoring at the main roads, 24 hours a day, including a series of phenomenon (e.g. overspeed, retrogradation, running a red light, parking prohibition, floating car data and Latency time). Those images, data and information are used to transmit back to the Monitoring Center as evidence to punish drivers or reference materials. Take the case of motor vehicle inspection reporting system, it could analyses vehicle flow statistic at traffic crossing, including vehicle flow rate on a time basis (year/month/day), vehicle waiting time at a traffic lane, and then generates a bar chart or table to output so that traffic management can take measures to relief the problem of traffic congestion.

Despite the growing interest in Intelligent Transport System, most of the problems concerning it only exist due to low-stability, expensive cost, complex operation and low clarity. Scientists (Professor K Soga, Professor R Mair, Dr. CR Middleton, Dr. F Stajano and Dr. IJ Wassell, 2006) predict that future monitoring system will undoubtedly comprise Wireless Sensor Network (WSN) and will be designed around the capabilities of autonomous nodes. Each node in the network will integrate specific sensing capabilities with communication, data processing and power supply.

1.2 Research Questions

The guiding research question is: How to visualize urban transportation data generated by Wireless Sensor Network

using modern approaches. This involves the following specific objectives:

- **To demonstrate how large number of sensors can be integrated into Intelligent Transport System using Wireless Sensor Network to improve performance**
- **To demonstrate how to visualize those sensing data using absolutely fascinating ways rather than using conventional ways like tables and bar charts.**

1.3 Overview of Contributions

The reminder of the dissertation comprises 5 chapters. The next two chapters overview key concepts and problems for wireless sensor network and data visualization. The 4th chapter focuses on the proposed model based on the existing technology.

Chapter 2 overviews fundamental concepts, critical problems, challenges and future trends of wireless sensor networks. It also illustrates applications widespread used in the field, and discusses its specific characters.

Chapter 3 presents an overview of fundamental concepts, critical problems, challenges and goals of data visualization. It also introduces applications widespread used in the field.

Chapter 4 reviews the current situations and focus on the process of deployment of sensor node and data visualization.

CHAPTER II: LITERATURE RIVIEW (i) - Wireless Sensor Network

Abstract

A wireless sensor network is wireless networks consisting of spatially distribute autonomous devices using sensors to cooperatively monitor physical or environmental conditions at different locations. This chapter introduces fundamental concepts and problems approached in the wireless sensor networks. The applications of wireless sensor network technology, which are from different areas briefly to demonstrate the most widespread used in the field, are presented. Characters of the wireless sensor networks are discussed.

2.1 Wireless Sensor Network: Introduction to Critical Problems, Challenges and Future Trends

With the vigorous development of world science and technology, and the advent of the Information Age, mankind now lives in an increasingly globalized and interconnected world. Once, as many people will agree, the achievement of the goal of seamless connection between people, objects and events were unachievable, but now this situation has been revolutionized. Due to the recent advances in sensor, computing and communication technologies, an interconnecting world is no longer confined to Internet use. Thus, it is fundamental to improve the understanding of how to integrate powerful mobile computing and wireless communication, which is complex, heterogeneous and geographically distributed.

Ubiquitous computing envisages everyday objects as being augmented with computation and communication capabilities. Date back to the 1970s, the rudiments of sensor network was composed of sensor control units interconnected through peer to peer transmission. Recent advances in embedded computing system have led to the emergence of the second generation sensor network which has the comprehensive process capability to achieve multiple information signals. Back around the end of the last Century, an intelligent sensor network system based on fieldbus technology was presented. (1) With the popularization of multifunctional sensors and the utilization of wireless connect technology, the wireless sensor network gradually developed. A wireless sensor network is a wireless network consisting of spatially distributed autonomous devices using sensors to cooperatively monitor physical or environmental conditions, such as temperature, sound, vibration, pressure, motion or pollutants, at different locations.(2)(3) As originally motivated uses by military(4), Wireless Sensor Network have traditionally been approached as independent research area. So far wireless sensor network has placed emphasis on the deployment of sensors, protocol stack, the synchronization algorithm and the routing algorithm in order to maximize the lifetime of the network(5), and relatively little attention has been given to the integration of computing and communication technology.

Wireless sensor network is destined to see widespread adoption in large-scale commercial applications, but are limited to, certain aspects such as technology, yet to be adequately resolved. Over the past few years, however, a substantial collection of wireless sensor network has been put into operation. Among those applications, perhaps some perform conform to the planning, but a majority might encounter some particular barriers to the widespread deployment of sensor networks, including:

1) Communication Problem. When utilizing wireless sensor network to implement regular communication, signal disturbed by certain barrier or other electronic signals, might be influenced, therefore it is essential to provide a solution to communicate safely and effectively.

2) Cost Considerations. Each wireless sensor network is made of plenty of small sensors, and these sensors are currently too expensive for many applications and most massive rollouts, so in this case cost will restrict development. It needs to take technical improvements and volume orders, such as those expected from Wal-Mart Stores Inc. and its

suppliers, to drive down pricing.

3) Energy Supply Problem. There is a need for energy supplies which could last for a long time. At present, some principal solutions includes the use of high-energy batteries, reduce sensor power, energy scavenging and energy efficient management besides. (6)

4) Efficient Wireless Sensor Network Structure. Each sensor node in the wireless network need to perform the functions of sensing, processing and communicating as the following figure 2.1 Architecture of a sensor node(7),

Hence a reasonable deployment of wireless sensor network could utilize the resources to its maximum. Besides, building a reliable wireless network to ensure network security probably based on a meshed topology, to transport data from sensors to server.

To achieve significant market adoption, wireless sensor network applications must overcome the present challenges which are addressed. In the meantime, developments lead traditional distributed sensor network to next generation wireless sensor network, and it is certainly a reflection of its far-reaching impacts on mankind.

Dipankar Raychaudhuri, director of WINLAB and professor of electrical and computer engineering at Rutgers University, North Brunswick, considered the five great changes happened in our daily life, which are:

Marching toward the ideal society, consumers could find the products and services through PDA while walking. Furthermore, they could directly purchase the expected products in the shop without the help of sales assistants.

Intelligent transportation system monitors factors that are at odds with each other in order to reduce traffic congestion and improve safety. And it could provide us with feedback on system's collision avoidance analysis. The most satisfaction is to assist people find their cars in the crowded parking lot.

Airport Transportation Security Administration ensures accessible boarding for passengers and retrieves data using devices called RFID tags to quickly get the lost luggage back, and even checks to see if there are special entrances or any explosive residue.

With respect to new smart house technology for elderly and disabled people, Smart House will play a very important role for in the future.

Office clerk in Smart Office could fast find the document and books in seconds, and they also could maintain the important log file based on location and dates.

Many developed countries such as America attach great importance to the development of wireless sensor network. Recently, the Boston University is leading the charge, forming a sensor network consortium to bring top academic, industry and venture-capital members together, expecting to promote sensor network industry growth. BusinessWeek Magazine predicted wireless sensor networks as one of the fourth new technology in the future, and MIT's Technology Review ranked it among 10 emerging technologies that most likely to change the way we live. (8)

In the following years, significant information and communication technology research and development will no doubt be needed to realize the potential of sensor networks. In addition, we could also express a bold forecast that the future view of wireless sensor network will become ubiquitous. Building on past success, early wireless sensor network have been used for various application areas, such as environmental and agriculture monitoring (9) (10), industry control (11), military operations (12) and medical care (13). Let us examine some of the emerging research trends in the sensor networks regime that are informed by experience with these deployments.

Multiple Applications. An important trend is the increased development of multiple applications in wireless sensor network. With the advances in Wireless Sensor Network, identical sensor network is headed for supporting multiple applications rather than single application. Since wireless sensor network is composed of large numbers of heterogeneous nodes, plenty of sensor data with different sensing attributes are emerged. For example, deploying a large-scale sensor network in a complex building, the wireless sensor network could provide quality services such as temperature and humidity sensors provide not only monitor temperature and humidity in different parts of the building at different times, but surpass conventional standards by also providing the foundation of air conditioning; movement detection sensor detect the distribution of all the workers inside the building in order to provide foundation of a distributed building air conditioning control; video sensor could ensure the security of the whole building. These sensors can be self-deployed in a purely decentralized and distributed monitoring area, or integrated different sensing functions into a single sensor. Rely on the different functions of sensor nodes, the variety of sensor data might not be the same, and even the speed of sensor data distribution due to the satisfactory of requirements of different service quality.

Heterogeneity. In heterogeneous sensor networks, typically, large numbers of inexpensive sensor nodes perform sensing, whereas a minority of expensive sensor nodes provides data filtering, fusion and transport. (14)The advantage of heterogeneity architecture is potential to increase network lifetime and reliability without significantly increasing the cost. It consists of three distinct types, computational heterogeneity, link heterogeneity and energy heterogeneity.

In a heterogeneous architecture, some nodes such as backhaul links have long-distance highly reliable links, some have unlimited energy resources or more capabilities the more demanding tasks, and the others have added computational power. For instance, resource-rich nodes can be better suited for localization, digital signal processing and long-term storage, nodes with more energy reserves for hierarchical coordination, whereas short-ranging sensing can be undertaken by the smaller nodes.

Another advantage of heterogeneity is some of the nodes could perform more complex tasks during the operation of the network. For example, vision provides an important, orthogonal sensing modality to traditional sensing applications but requires greater systems complexity. Cypress, which is the commercial sampling of a high-sensitivity, high-speed SXGA (Super Extended Graphics Array) resolution CMOS image sensor with color, offers a triggered and pipelined synchronous shutter with a high frame rate and windowing capability for undistorted images and fast readout. (15)

2.2 Wireless Sensor Network Applications

It is envisioned that large-scale, distributed sensor networks will eventually cover and instrument the entire world. They will continuously monitor and collect information on diverse phenomena, including endangered species, soil and air contaminants, patients, and man-made environment. The applications of wireless sensor network technology have been classified into four main categories: environmental monitoring, health care, security, and additional applications. (16) We will illustrate some application cases from different domains briefly to demonstrate the most widespread used of this field:

1) Environmental and habitat monitoring. Nowadays mankind attempts to highlight the environmental issues and concerns that have significant affect on all of us, therefore the required data collection becomes more and more important, as well as the amounts of the data. However, the emergence of wireless sensor networks provide convenience for those random research data, and also avoid, minimize or reduce unnecessary environmental damage by traditional methods of data collection. For example, in order to monitor the shy seabird's nest activity, researchers from University of California, Berkeley, and the Intel Research Berkeley laboratory installed a network of more than 20 miniaturized sensors, or motes which could beam back raw data about the conditions in the burrows and the island's microclimate to the Internet, on nearby Great Duck Island, and now they are able to monitor a popular breeding site in real time through the Internet while just sitting comfortably in front of their computers.(17)

Wireless sensor network could not only monitor the migration of migratory birds and insects, research on the effects of environmental changes on crop, but also monitor the basic components of ocean, air and soil, etc. For instance, MoistureMap, which is a system for sustainable land and water management, has been developed for Australia. To provide soil moisture information in different time periods, the system combine weather, climate and land surface model predictions with soil moisture data from satellite sensors.(18)Besides, wireless sensor network could apply to precision agriculture, monitoring pests within a crop cycle, soil acidity and fertilizer concentration.

2) Medical diagnostics and health care. Wireless sensor network technology has been explored to a range of medical applications. Researchers could make good use of wireless sensor network to implement remote medical monitoring. For example, deploying seventeen distributed sensor nodes in every room within a building; each sensor node contains five sensors: temperature, humidity, light, infrared and sound sensors, some of them even has ultrasonic sensors. Based on the data collected by these sensors, monitor interface in real-time will display the performance through people. Through the integration of information that obtained from multiple sensors, we could accurately identify the act of people, who is monitored, such as cooking, sleeping, watching television, taking a shower, etc, so that we could exactly determine the elderly' s physical health conditions. The smart medical home is an experimental deployment of wireless sensor network example in medical care (19) as shown in Figure 2.2 The Smart Medical Home Research Laboratory.

The researchers from University of Rochester built this intelligent medical room, using dust to measure patients' important symptoms, such as blood pressure, pulse rate and breathe, sleeping pose and 24 hours performance. The utilization of wireless communications not only efficiently transfers necessary information from each sensor networks, but also reduces the heavy burdens placed on carers. No wonder Eric Dishman, the director of Intel's proactive health research, said the wireless sensor networks are an extremely promising area for home health technology development. (20)

3) Military surveillance and industry security. Due to its intensive nature, distributed wireless sensor networks are suitable to apply to hazardous battlefield with the purpose of conducting reconnaissance, monitoring military strength, equipment and material. An example of network-centric warfare includes the cooperative engagement capability, a system that consists of multiple radars collecting data on air targets. (21) The U.S. Defense Advanced Research Projects Agency (DARPA) sponsored large amounts of money to assist the research of smart dust. The concept of the "Smart Dust" involved the use of loads of tiny wireless microelectromechanical sensors that could be spread over a large battlefield area, monitoring enemy movements and detecting everything from light to vibrations in a covert manner. (22)

Besides, wireless sensor networks enables security in some dangerous industry environments such as mine and nuclear power station. These wireless sensor networks could identify important information, like workers working in the field, what are they doing, and their safety guarantee. Deploying relevant wireless sensor nodes in each vent within the factory could monitor waste water discharged into water body and waste gas released into the atmosphere, collect, analysis and report of hydrometric sample data. Flammable, explosive and poisonous materials have provided a wide range of potential risks for workers working in mine and petrochemical industry, the high cost of monitoring is prohibitive. The widespread uses of wireless sensor networks benefit a few practitioners and also increase reactive speed and accuracy in dangerous situation.

2.3 Wireless Sensor Network Characteristics

As we mentioned before, wireless sensor networks could represent the common features as ad-hoc networks such us mobility and energy power limitation, and moreover, it is further characterized by the following features:

1) Large-scale network. Spatial and temporal scale concerns the sampling interval, the extent of overall system coverage, and the relative number of sensor nodes to input stimuli, and it is an important determinant of system design. (23) To be able to acquire accurate information, the combination of fine granularity sensing and large coverage area implies thousands of sensors, or even more, deploying in monitoring area. The spatial data attained from view-angles of different granularities contains larger signal-to-noise ratio (SNR) which is significant in the acquisition of high-quality digital images and applications requiring accurate light measurements. (24) In addition, using distribution management system methods to execute complex and large numbers of data could increase monitoring accuracy and decrease accuracy requirement of each nodes. The existence of the redundant node can improve the lifetime of the whole wireless sensor network and provides the system with strong capacity of fault tolerance. A high density of sensor nodes enables increase monitoring coverage and provides chances to eliminate caves or fade zone.

2) Self-organizing network. Under ordinary circumstances, sensor nodes will be placed in certain remote area without existing infrastructure. The geographic location of each node may not be possible to determine in advance, even the relationship between two physical neighbor nodes. For example, large numbers of sensor nodes are usually scattered in the spacious virgin forest or some places unreachable or dangerous for mankind. The communicating sensor nodes are abstracted into an easily controllable network infrastructure. That is, when triggered, nodes have the ability to deploy to locally self-configure among them to automatically interconnect to form a network. (25)

The lifetime of wireless sensor networks is an important issue. It is because some sensor nodes might run out of energy as a result of energy consumption or environmental factors. The wireless sensor networks are considered as a complex system, the fact that single node might fail will be ignored as long as the overall is fulfilled finally.(26) Yet new sensor nodes will be supplemented to network in order to make up invalid nodes and increase monitoring accuracy. Thus, dynamically increase or decrease the number of sensor nodes in wireless sensor network will also lead to the dynamic change of topology structure, which could prolong the networks' lifetime and greatly improve their performance.

3) Multi-hop routing. Since the communication distance between nodes is limited, usually in a maximum range of a few hundred meters, node could just communicate with its nearest neighbor. If majority of these nodes is expected to communicate with nodes outside of the radio frequency coverage, the intermediate node will represent its routing capacity, as the figure 2.3 The case of multi-hop routing below.

Node A can communicate with node B, and node B can communicate with node C. However, node A can not communicate with node C because of the range of radio frequency.(27) Suppose the implement of multi-hop routing in network is reliable on gateway and router, then typical multi-hop wireless sensor network architecture is formed by ordinary network nodes without any routing equipments. Thus, with routing protocols, each node plays a role as both the source node and destination node.

4) Dynamic network. Due to the presentation of the network capacity results under the node mobility**,** Wireless sensor network is a dynamic network. Some sensor nodes might quit the network as a result of energy consumption or other factors; whereas new sensor nodes will be supplemented to network, which depend upon the network requirements. Therefore, the topology architecture in wireless sensor network might be changed according to the following factors:

- Environmental factor or energy consumption, which leads to sensor nodes failure or invalidation;
- The elements in network, such as wireless sensors, awareness objects and observer, might be mobility;
- New sensor nodes joining the network;
- Reliable networks.

5) Data-centric network. Tasks and communications form a task network which performs monitoring tasks in wireless sensor network. Variability in system task determines the extent to which we can optimize the system for a single mode of operation. By no means can sensor nodes be separated from sensor network. Conventional sensor networks name every node with an identifier, the unification of node names depend on telecommunication network protocol design.

Because of the differential random deployment of sensor nodes, the relationship between sensors and identifiers is completely dynamic; there is no positive connection between node identifier and their current geographical location. Once in-network data processing is in place, we have to develop programming abstractions that allow users to program the entire sensor work rather than individual sensor nodes. (28) The idea of querying or transmitting clues based on data itself is much closer to natural language communication habits. That is why we always say that wireless sensor network is a network which is data-centric. For example, target tracking is an important application in wireless sensor network. The targets might appear anywhere in the network. However, users are concerned about nothing but location and time in which a target, often a spot, could appear. They don't particularly care which nodes that track the target.

6) Application-specific network. Mankind apperceives the objective world depending on multiple sensors, and even acquiring tremendous quantity of information in a physical world. For different applications we consider sensors is related to different quantity of information, when developing sensor systems, it should provide variety of requirements to meet the actual demands.

As we know, the differences in application context may lead to different sensor network requirements, and it differs greatly in hardware platform, software system and network protocols. According to it, sensor network is not like Internet that have uniform communication protocol platform. Due to the lack of the uniform protocol standard of sensor network, there is no universal architecture suitable for all types of different sensor networks.(28) Though there is still a lot of common problems existed in different sensor network applications, especially developing more effective target-specific sensor systems. But clearly directed against each exact application in sensor network design when researching sensor network technology remains a distinct feature that be different from conventional networks.

Wireless sensor networks are particularly well adapted for use in hazardous environment or some places unreachable for mankind. An outdoor, open wireless sensor network might be intentionally destroyed by irrelevant personnel or animals. Due to the environmental limitation of present monitoring area and significant amount of sensor nodes, manual configuration is not feasible. Furthermore, communication confidentiality and security in wireless sensor network are extremely necessary. Consequently, soft hardware in wireless sensor network has to possess the capacity of robustness and fault tolerance.

CHAPTER III: LITERATURE RIVIEW (ii) Data Visualization

Abstract

Data visualization is the study of the visual representation of data, defined as information which has been abstracted in some schematic form. This chapter introduces fundamental concepts and problems approached in the data visualization. The applications of data visualization technology, which are from different areas briefly to demonstrate the most succeeded in specific field, are presented.

3.1 Data Visualization: Introduction to Critical Problems, Goals and Challenges

In his early days, Hans Rosling, who is a professor of International Health at Karolinska Institute and Director of the Gapminder Foundation(29), made a searching enquiry to discover the imprint of starvation in Africa, then he came back to teach in Swedish university. Once in his global healthy lecture to top Swedish undergraduate students, he was sort of to expect them to know everything about the world. And then he gave them a pretest that which country, as he illustrated, has the highest child mortality in five pairs of different countries. However, the correct answer fill rate is far less than 50%. The result made Rosling fell that they did not correctly answer not because of their ignorance but deeply and firmly rooted erroneous preconceived ideas. Rosling asked his students how they view the world today, and their answer is it was still we and them, "we" means the western world which the people have long life and small family, and "them" refer s to the third world, they even thought the people from the third world, however, do not fill the traditional living standards and have a very short life span of the people. Having gone through that experience, Rosling has infinite faith in that the truth is not the same as what the students convinced. Since this, he realized there is really a need to communicate because the data and what happening in the world the child in every country could very well aware. Thus Rosling decided to using data to describe problems, as he considered, information could be interpreted from data, and data visualization is the most important step in data analysis.

When you go out for a walk, your vision system would immediately recognize various objects such as vehicle, buildings, human beings, trees and pets, etc. All these above have a coherent and meaningful organization scheme. Your brain attempts to overcome the problems associated with boundary, movement and distance, organize them in the form of multidimensional entirety to the effect that we could memorize their characters. The continuous process looks unnecessary but subconscious. Data visualization is powerful not just because human awareness is controlled by visual cortex but the rapid information transfer process. Besides displaying large amounts of information, data visualization could accelerate recognization of hidden wealth of data.

In the past few years, people used many different words to describe graphic representations of data, but the overall aim is always to visualize the information in the data and so the term "data visualization" has been emerged as a new

specialism within the field of computer graphics. (30)(31) Now data visualization is the study of transforming data into some kind of visual representation. By means of graphical approach, data visualization could clearly and effectively communicate information. Yet it does not mean to achieve functions we have to visualize the data in a very dry and boring manner or make the graphs gorgeous but looks extremely complicated. Aesthetic form and functional needs have to go hand in hand for the sake of conception communication. Intuitively conveying important aspects and characters could lead to further observation of discrete and complex datasets.

Data visualization technology consists of the following basic concepts:

- Spatial data, a multidimensional information space which is made up of n-dimensional attributes and m elements;
- Data development, which covers the algorithm and tools for quantitative computation and deduction;
- Data analysis, slice or dice profile data, thereby could observe data from multi-angle.

With the popularization of network technology and electronic commerce, the decision making will depend on the implicit discipline found from large amounts of finance, communication and business data. In order to accommodate the recent development to hardware platform, operating system and network communication, visual software products get up to speed with those high-throughput technologies developments quickly, of which with AVS/Express developer edition, IDL(including VIP, ION) and PV-WAVE as their representatives. Take an example of AVS/Express developer edition; it provides multi-platform, component-based software development environment with interactive visualization and graphics features. (32)

How to analyze and explore large amounts of complicated and multidimensional data? The answer is to provide a visual environment like human eyes which is known to be more intuitive, interactive and quick-witted. Therefore the principal features of data visualization technologies are as follows:

1) Interactivity. Users could be more convenient to manage and develop data in a manner that is both interactive and enjoyable.

2) Multi-dimensions. It could allow users to view multi-attributes or variables that represent data on objects or events. According to the value of each dimension, the data could be classified, sequenced, integrated and displayed.

3) Visualization. A visualization technique for different kinds of data represent it as images, curves, two-dimensional graphics images, three-dimensional objects and animations, as well as for visual data analysis in examining data patterns and correlation. People's visual performance played a significant role in scientific discoveries, and this view has borne out by the history of evolution. Generally focused on aspects of visualization, the emergence of a new key technology is the preface to a great scientific discovery. The wonderful scientific effects of telescope and microscope in Astronomy and development of biology is the best proof of this. Our field of vision has been enlarged and extended far beyond our present ability via those tools. To the present day, there were many elements of truth in it. People's visual performance has the capacity to analyze the behavior of large amounts of abstract data. New data development tools could greatly extend our vision. A people's creativity not only depends on their logical thinking but also lies on their thinking in terms of images. Only visual representation of a mass of data into concrete terms can arouse people's thinking in terms of images. On the face of it, all of the data are jumbled up. But once you could find out the principle behind it, it will provide a basis for scientific discovery, engineering development, medical diagnosis and business decision. In addition, the generation of predictive models and the capacity to integrate multiple information resources are important to the development of system, and such data, knowledge and models are dependency relationship. Thus it is elementary to improve the understanding of their concepts. Data refer to a collection of facts, and information is useful data sorted from multiple resources, but it is not identical with knowledge, because not like knowledge, information can not reflect the internal relation between data. With regard to knowledge, there is no single agreed definition of it recently, nor any prospect of one(33), and someone presented a proposal that intended to separate it into two sections. One is the so-called tacit knowledge which can not be described as language and text, the other which is called explicit knowledge is completely opposite to it. Currently, information is one kind of explicit knowledge; it can be articulated, codified and readily transmitted to others. Looking ahead, based on the significant breakthrough in brain science, human beings will successfully develop a bio-computer that resembles human brains. It will consequently usher in a golden age in artificial intelligence. But even in that time, information can not fully express all the explicit knowledge. Only when focused on graphs and images to display numerical data and information, there is a possibility to set the stage for knowledge acquisition. In brief, data visualization could greatly accelerate data processing speed so as to make effective use of tremendous amounts of data that generated in every second. What's more, data visualization could implement image communication between people; thereby people could observe implicit phenomena from data and pave a way for discovering and understanding scientific laws. Besides, data visualization could implement guidance and control for computing and programming process.

Computer has been widely used in scientific computing and data processing for nearly 50 years. (34) But it have been a

long time that data can be run to completion in a batch processing mode which is in contrast to interactive manipulation. Batch processing could not lead the intervention in computing process, and it has to passively wait for sets of output data files. And hand operation is the only way in which large numbers of output data manipulated. In this way, a user does neither get a visual global concept of relational data in time, nor be likely to lose vast quantities of information. In recent years, the data from communication equipment, such as super computer, communications satellite, advanced medical imaging equipment and geological prospecting, are growing with each passing day. Thus effectively visualize data constitutes increasingly the most urgent problem. On the other hand, with rapidly advancing increases in computing speed, and the constant expansion of memory capacity, network functions exist to continuously enhance and implementing many important pattern generation and image processing algorithm via hardware, there can be a possibility to visually display large amounts of data and information, as well as carry out interactive manipulation.

Let us take an example to illustrate the great significance of the development of visualization technology. Human beings have a long enough aspiration of recognizing human body structure. But it is only 1970s, with the emergence of computed tomography (CT), magnetic resonance imaging (MRI) and visualization technologies; the aspiration has become a reality. Under the direction of the US National Library of Medicine's (NLM) Board of Regents in 1989, the long term biological information repository project - Visual Human Project (VHP) came into effect. (35) The University of Colorado Health Sciences Center created a dataset of complete human male and female cadavers in anatomical modes. The researchers scanned a human male and a human female cadaver from the sole of the foot to the crown of the head in CT and MRI. The acquisitions of the anatomical cross-section images are at 1mm intervals and totally there are 1878 cross-sections. The anatomical cross-section images which are obtained from the female cadaver are at 0.33mm intervals but obtaining 5189 cross-section images that comprise the female dataset. After filling blue latex and wrapping in gelatin to the cadaver, the cadaver should be frozen as soon as possible. Similarly, to acquire the anatomical cross sectional images in the same interval as before, which contain a higher resolution of 2048×1216, the data produced are 56GB in all. (36) The emergence of Visible Human Project datasets announce the signing that digital three-dimensional reconstructed image and virtual reality technology are widely used for medical purposes.

In recent years, the question of information visualization has been raised. Generally speaking, visualization in scientific computation refers to spatial data visualization, but information visualization concern large-scale collections of non-numerical information which is non-spatial data. With the advanced society informatization and the popularization of web application, there existed a gigantic source of information. There is an urgent need to deal with the data storage, transmit, retrieval and classification, and realizing the close correlation and development tendency are an exception which is necessary to take into account most. As a matter of fact, a great many of important information are hidden behind the exploding data. People expect to analyze that information in a higher level as to make good use of the available data. The existing database system could efficiently implement certain functions such as inserting new data into existing data structure, querying existing data by end-users, but the only drawback is that it can not discover the existed data connection and regulation, as well it can not forecast the prospective trend in the development of in accordance with existing data. On the other hand, artificial intelligence has made significant progress since its birth in 1956. (37) Machine learning is a main focus these days. It is a technology that simulate of human-like aspects of learning via computers.(38) As our understanding of some mature algorithms continue to mature, neural networks and genetic algorithm have proven to be powerful and general technique for machine learning.(39) To store and retrieve data via database management system, and analyzing and mining the knowledge behind large amounts of data in the forms of machine learning, their combination result in the generation of Knowledge Discovery in Databases (KDD). Actually, knowledge discovery in databases including interdisciplinary topics in a variety of application fields such us machine learning, pattern recognition, statistics, intelligent database, knowledge acquisition, data visualization, high-performance computing and expert system.(40) And knowledge discovery in databases could widely use in area of information management, process control, query optimization, scientific research, decision support and data self-maintenance.

Data mining is the core technology of Knowledge discovery in databases, in which knowledge discovery actually takes place. It is an iterative process that aims at extracting previously unknown and hidden patterns from large numbers of incomplete, noisy, blear, random data. (41) People considered the original raw data as a source of knowledge, just like mining of minerals. The original raw data either could be fit structural equations models like data in relational database, or it could be semi-structured data such as text, graph, image data and even different configuration data distributed in network. The standard analytic methods for data mining could be either mathematical or non-mathematical, and it might as well be deductive or inductive. Data mining allow us to discover various kinds of data including extential forms of knowledge that reflect associative property of a group of things which are all of the same general type, characteristic-based knowledge that reflect every respect to the character of objects, knowledge that reflect different attributes between different objects, benefit-related knowledge that reflect dependent or associated relationship between one object and another, predictive knowledge that infer data in the future in accordance with present history and current data, and knowledge that reveal abnormal phenomena that object deviated. In order to discover the above different

kinds of knowledge, we have to adopt multiple knowledge discovery tools. Furthermore, we must develop visualization methods for knowledge discovery for the sake of better understanding the process and result of knowledge discovery, as well as human-computer interaction in the knowledge discovery process. And falling back on visualization technology while attempts to understand the correlation and development tendency between data. Information visualization not only display multi-dimensional non-spatial data via images, leading users to get a deeper understanding of the meaning of data, it also point the way to data retrieving using visual graphs and accelerate retrieval rate. In visualization in scientific computing, displayed objects refer to different kinds of spatial data like scalar, vector and tensor, and the research focus on how to veritably and quickly display three-dimensional datasets. In recent information visualization, the displayed objects are mainly multi-dimensional scalar quantities; therefore, the key to the study is design and choose specific display modes so that it is convenient for users to understand enormous multi-dimensional data and their mutual relationship, and more emphasis on the problem of psychology and human-computer interaction.

Information visualization has a bright future for application in the field of commerce, finance and communication. On the one hand, the field of communication focuses on developing much more sophisticated and advanced network model for the sake of assistance of prospective planning process. But on the other hand, more complex transmission and exchange equipment provide greater degree of freedom and flexibility for current network reconfiguration, therefore, original raw data that operated in a single network element continuously increase. The optimization of entire network operation require necessarily employ the entire information source effectively, furthermore, it also need dynamic data exchange to exchange information and ideas between different conventional fields such as market, network plan and day-to-day management. Of course, the effective area of coverage of the physical network contains a wide range of fields such as sound, data and imaging services, and each of them has their own data management requirements. Besides, modern computer networks are specifically exempted from national boundaries, and it is an international organization covered many countries and carriers. Thus both its potential data size and complexity level increase progressively at a greater order of magnitude. Take the case of BT, one of the world's leading providers of communications solutions and services, its network bring information visualization technology into exercise. The network has more than six thousand switching devices and nearly twenty-five million client threads. As a result, it produces network state and control data megabyte per minute. In BT's network, running condition associated with local route which is connected to a digital switch, at an average of sixty thousand per five minutes, should report to central operations unit. And then central operations unit monitor and control these data in real time. By means of measurement of large amounts of operational parameter, the network produces more than two thousands megabyte data every day. The graphical output vividly describes the geographical distribution of chosen operational parameter and the animation you might be interested in within a specific time interval. Color bar pattern could be used to represent the maximum, minimum and average value of each local concentration parameter. Visualization is reflected a wide variety of interests in non-spatial data such us the applications in financial target or turnover statistics. A great many of visualization tools and technologies which are initially used in engineering and scientific applications could transfer rapidly to the fields of finance and statistics. The key to success of visualization applications is having the capacity of providing users with interactive research data and revealing the trend, circulation and pattern that difficult to repeal through other methods. A typical example of non-spatial data coverage application is network statistics, which each pattern is made up of plenty of attributes, such as the character, switch, and major distinct or physiographic division of single network element. (42)

In addition, using the Cityscape as a visualization tool is a potential useful technology in this respect as well. It is basically a generalization of three-dimensional bar charts. (43) The position in a scalar field represents blocks or buildings within a uniform grid. Visualization could describe statistical information which divided one year into twelve months and then using twelve geographical zones to represent them. BT Group has been employed cityscape application to offer investigation in statistics service and ride quality of transportation system by the month and area. These applications could apply to financial information very easily, such as income stock character for each region and specified period, or VisualMine based on geography and income to display total quantity in currency circulation, gross income and operating cash flows. (44) Take the case of bank of Italy. They employ the application which is developed by Artificial Intelligence Software Ltd, Italy to monitor unlawful activity through banking systems. Due to the real-time resolution of increasingly obvious "data overload", information visualization will make a profound impact in the fields of commerce, finance and communications. It can be seen from this that the increasingly data and information are useful, but the crux lies in abstract helpful knowledge as soon as possible.

3.2 Data Visualization Applications

At present, data visualization applications have been widely used in various fields such as physical science, engineering technology, finance, communication and business etc. Take a closer look on some data visualization application examples that succeeded in specific fields.

1) Medical science. Medical data visualization is currently one of the most active and vital research areas in the field of data visualization. Due to the development of modern noninvasive diagnostic technology (CT, MRI etc.) and the

progress in positron emission tomography (PET) technology, doctors could more easily obtain a set of two-dimensional cross-sections imaging of functional processes in the patients' body. Computer tomography (CT) technology breaks conventional sensitive film imaging mode, restructuring images of human organs and tissues via computer leads medical images moving towards from two-dimension to three-dimension era, and it enables the clinician to view and assess the human body from a functional biochemical perspective. PET combines nuclear technology and computer technology. Computer analysis reconstructs the images of tracer, called a positron-emitting radionuclide as well which is introduced into the body on a biologically active molecule, concentration in three-dimensional space within the body (45), it makes us possible to gain images of human metabolome and functions. On this basis, image fusion the images of diversified modes as mentioned above could accurately determine the pathogen's spatial location, size, geometry and spatial relationship between ambient biological tissue and it, thus efficiently diagnosing disease for patients in due course. A great deal of organizations have researched to translate and reconstruct the obtained two-dimensional cross-sectional images into three-dimensional images associated with human organs and tissues, including Advanced Diagnosis, Automation, and Control (ADAC) Laboratory at North State University (NCSU) (46), Medical Imaging Lab at Johns Hopkins University (47), Medicim, spin-off company of the Catholic University of Leuven (48), Technical University of Bialystok (49) etc. Now the software they developed have been widely used in a great many of hospitals. In addition, researchers in University of Washington utilize visualization software system and echocardiogram diagnostic technique to obtain three-dimensional images of human heart and provide proof for general inspection and diagnosis by means of monitor shape, size and movement of human heart. (50) Electron beam computed tomography (EBCT) substituted electron beam scanning for conventional X-ray tube and detector used in conjunction with mechanical scanning. As a result, scanning speed increased a hundred times, and clinician could indicate the presence of coronary atherosclerosis via clear images, it is a world-wide revolution in computed tomography technology. Cardiovascular Institute and Fuwai Hospital, Chinese Academy of Medical Sciences (CAMS) & Peking Union Medical College cardiovascular disease have been used EBCT three-dimensional image reconstruction technology in clinical diagnosis of aortic valve disease and display of blood vessel after Coronary Artery Bypass Graft (CABD).(51) Because of the high temporal resolution of EBCT angiography, it eliminates respiratory and motion artifact, and clarifies diagnosis of various aortic valve disease as well as reveals blood vessel anatomic structure of coronary artery bypass graft. Bringing to a conclusion with it, three-dimensional image reconstruction is propitious to integrally and visually display pathological changes and help clarify a diagnosis and provide operation guide. Therefore, EBCT is expected to replace conventional angiography in aortic valve disease diagnosis and postoperative blood vessel display of coronary artery bypass graft.

CHAPTER IIII: RESEARCH METHODOLOGY

Abstract

The process of visualize data are routinely to acquire and analyze vast amounts of data. This chapter focuses on introducing the process of visualization urban transportation data generated by wireless sensor network.

4.1 Research Design

The research plan will combine two disciplines, which are wireless sensor network and data visualization. Urban transportation monitoring system comprised Wireless Sensor Network (WSN) and assigned around the capabilities of autonomous nodes. Each node in the network could integrate specific sensing capabilities with communication, data processing and power supply. The system could round-the-clock monitoring at the main roads, 24 hours a day, including a series of phenomenon (e.g. overspeed, retrogradation, running a red light, parking prohibition, floating car data and Latency time). Those images, data and information are used to transmit back to the Monitoring Center. Obtained the complex data from monitoring center, using it to provide a meaningful solution to represent it to a visual form is another key part of the research plan, it requires insights from diverse fields: data acquisition, data analysis, data governance, data management, data mining, graphic design and information visualization.

Nowadays, the overwhelming majority of traffic map tools provide real-time traffic information, helping drivers make better decisions on choosing a correct traffic route on the basis of current traffic state. However, it is an unusual sight to view the full scenarios of vehicle flow statistic at traffic crossing, like vehicle flow rate on a time basis (year/month/day). It is the most regretful thing because it concerned with each citizen more than drivers.

A small quantity of existing map contained statistical information did not make data really and truly readable. For example, the website of Kansas Department of Transportation, America provides traffic and travel information as well as the road conditions map, they are all full and accurate data with beautiful design, and worth to consult, but the weakness or flaw existing in it is hard to understand. (52) Thus there is really a need to using a meaningful solution to represent data rather than generating a bar chart or table to output the information.

4.2 Research Methodology

As mentioned above, we must reconcile these fields as parts of a single process. The importance of computer science

could be understood by Graphic designers for visualization, by the means of being aware of the principles for the visual design behind data representation, statisticians could communicate their data more effectively.(53) In this chapter, we use separated processes that bridges the individual disciplines, and form a path to the final question.

4.2.1 Data acquisition

Obtained the data from monitoring center, in which the data acquisition system reflect the data from sensors located in main roads. In this part we will describe the deploy of wireless sensor network and demonstrate how large number of sensors can be integrated into Intelligent Transport System using Wireless Sensor Network to improve performance.

As a core technology for traffic surveillance and control, a Real-time Vehicle License Plate Recognition (VLPR) applies broad technical knowledge in multiple sub-systems. Intelligent multimedia network license plate recognition system could be widely used in vehicle safety audits, pay tolls to drive on a turnpike, parking management, etc.

Considered we deploy large numbers of sensors in urban main roads, we make a number of assumptions regarding the capabilities of them.

The sensors detect and snapshot by means of real-time trigger, as well as automatic sensing, accurately recognize and check the plate number no matter the vehicle is under steam or power-off. Verifying the snapshot image by using database document for comparison, sensors could report to the monitoring system when and where they found the intercept vehicle. The system adopt advanced fuzzy image process technique, identifying plate numbers that human eyes are hard to distinguish by means of dealing with images with low spatial resolution(too small characters on the plate), blur, low contrast, bad light conditions(shadow and strong light) and high distortion.

To enable the real-time vehicle license plate recognition process, we divided it into four separate sections, including plate localization, plate pretreatment, character segmentation and character recognition. In order to improve the recognition performance, an algorithm on character recognition was proposed which use a Support Vector Machine (SVM) to train character samples and obtain the rules. (54) The main approach, which is called 'one against one', applies SVMs for multi-class classification. A series of classifiers are applicable to each class, furthermore, the system keep nothing but the label of the most prevalent computed class for each case. The utilization of such an approach requires $k(k-1)/2$ classifiers, once all $k(k-1)/2$ classifiers are undertaken, the max-win strategy is followed.

The approach algorithm can be described as below.

Given n training data

$\Omega = \{(x_1, y_1), (x_2, y_2), \ldots, (x_m, y_n) | x_i \in R^n, (i = 1,2,\ldots,n)\}$, and $y_i \in \{i = 1,2,\ldots,k\}$,

where k is the number of classes. The classification function is as:

$$\begin{cases} \min \quad {}^1/_2 \| w^i_j \|^2 + C \sum \xi^i_j \\ s.t. \quad (w^i)^T \varnothing(x_i) + b^i >= 1 - \xi^i_j, \ if\, y_j = i, \\ \quad\quad (w^i)^T \varnothing(x_i) + b^i <= 1 - \xi^i_j, \ if\, y_j = i, \\ \quad\quad \xi^i_j >= 0, j = 1,\ldots,n \end{cases}$$

where $K(x, x_i) = \varnothing(x)^T \varnothing(x_i)$

In APRN, k contains 10 for digits and 26 for letters. The above formula shows the following 36 decision functions for all 36digis and letters:

$(w^1)^T \varnothing(x) + b^1$,

...

$(w^{36})^T \varnothing(x) + b^{36}$.

An x is classified to be the digit or letter a if its decision function gives the maximum value in the SVM for a, i.e.,

Class of $x \equiv \arg\max_{i=1,\ldots,36} ((w^i)^T \varnothing(x) + b^i$.

Assumed that the sensors combine the capacity of vehicle flow statistic at as well, like vehicle flow rate on a time basis (year/month/day). The principle of this real-time system is to install sensors onto the main traffic lane, drawing power from the city's infrastructure, and sensors adopt video trigger method to estimate the passing vehicle, and then transmit the digital video signals back to analyze. When discovering vehicle appear in monitoring area, the system startup vehicle flow rate detection module at once, once there is a car passing by, the arithmometer within the sensor automatic increase and make sure accomplish processing of vehicle flow rate detection, queue length, vehicle waiting time at a traffic lane, lane occupancy ratio, urban road information analysis and data retrieval in a short time.

Sensors are located throughout the crossroads in a consistent way in every district of the city. Some sensor locations are indicated as Figure 4-1. All of the observational sensing is built directly into the crossroads. Although the sensors are ubiquitous, they become part of the interior infrastructure.

We make the following assumption. The area of potential field is S, and the deployment position of sensor nodes satisfy uniform distribution model, as well as any two of the sensor nodes in the potential field does not locate in the same position. Furthermore, the sensing direction in [0, 2∏]of sensor nodes satisfy the uniform distribution model. Without regard to sensor nodes might be fall in edge area that leads to decrease the effective coverage (nodes that are unoccluded and within potential field are detected; nodes that are occluded or outside the range are undetected), because the monitoring area of each sensor nodes are aR^2, therefore the probability of monitoring whole potential field for each sensor node are $\alpha R^2/ S$. The initial probability p_0 formula of potential field which is covered by N sensor nodes as follows:

$$p_0 = 1 - (1 - aR^2/ S)^N$$

By the above formula, when the network coverage in the potential field reach at least p_0, the formula of deployment scale of sensor nodes are

$$N \geqq \ln(1 - p_0)/(\ln(S - aR^2) - \ln S)$$

when network coverage are respectively p_0 and $p_0 + \triangle p$, the deployment scale of sensor nodes are respectively $\ln(1 - p_0)/ \tau$, $\ln(1 - (p_0 + \triangle p))/ \tau$, where $\tau = \ln(S - aR^2) - \ln S$. Therefore, the difference number of sensor nodes $\triangle N$ is

$$\triangle N = \ln((1 - (p_0 + \triangle p)/ (1 - p_0)) / \tau$$

If the area of potential field, radius of sensing coverage and sensing included angle are all fixed, τ is a constant. By this time, when p_0 are a certain number, $\triangle N$ increase along with the increase of $\triangle p$; when Δp is a certain number, ΔN increase along with the increase of p_0, and the increasing rate become bigger. As a result, if increasing the coverage rate Δp, we should deploy ΔN sensor nodes(when p_0 is a big value, which is greater than *80%*, increasing Δp by *1%* will lead ΔN increase ten or even hundred times).

In wireless sensor network, each sensor nodes located in the main road constitute a self-organizing multi-hop ad hoc mesh network infrastructure, terminal sensor nodes used for special traffic information acquisition and each neighboring nodes together compose star network to communicate, and ultimate data converge toward gateway nodes. Gateway nodes could be installed in the traffic signal controller as a module at crossroads, transmitting the collected data back to monitoring center via proprietary network of signal controller for processing purpose.

Data acquisition could be either complicated (obtaining data from large systems) or very simple (reading from a text file). In this particular case, data derived from sensors which contain various capacities, and it will update in an extremely short period. A copy of the vehicle flow rate list can be found on the IMD website, as it contains information of Madrid streets, it lists street statistics in alphabetical order, and measures data from each street. The listing is a freely available file, one for each of the code, a tiny portion of which is shown below in Figure 4-2. (55)

4.2.2 Data analysis

Data analysis is a process of precise and detailed studying and summarizing data to achieve a desired result of abstract useful information and come to a conclusion. Data analysis is directly bound up with data mining, but basically data mining tends to concern larger data sets, with less emphasis on reasoning. In the field of statistics, data analysis is divided into two basic forms of statistics, known as exploratory data analysis (or descriptive statistics) and confirmatory data analysis. (56) Exploratory data analysis tends to discover new features from data, whereas confirmatory data analysis emphasizes on existing hypothesis or falsification.

After acquiring data from monitoring center, we need to tag each part of the data with its intended use. For each line in the data file, we divide it into separate parts; in this case, it must be confine to each tag character. Therefore, each individual part of data will be converted into useful information format. The layout of each line of the vehicle flow rate data as has shown in the Figure 4-3 below, which we need to understand each of the prominent quantitative relationships and discover what we want.

With intent to handle in a conversion program later, we format each field as a data type:

Float. In computer programming, floating point numbers is representation of decimal fraction or more commonly, binary point. It could be places anywhere relative to the significant digits of the number. Here, the streets are assigned float data type, because the street name might be a large number of characters which requires tremendous memory space. But if we assign unique number to different streets, the name will be short for floating point.

String. Considered as a kind of data type in computer programming, it always used for represents an ordered sequence of characters. In this case, the scope is assigned string data type. Because the scope themselves are all composed of characters without any numbers. If there is number 0 existed in the beginning of a specific field like *0ARGANZUELA*, it

would be stored as *ARGANZUELA* rather than *0ARGANZUELA*.

Index. Index is an associated pointer that mapping data to a location in another table of data. An index points to the associated table which could help you locate information faster than if there is no index. Here, the index maps numbered codes to the specific districts. The numbered code might be two or three bits which requires less memory space than the full name of the districts.

Integer. Integer data type is used to represent some finite subset of the mathematical integers. They are numbers without a fractional or decimal points.

After formatting each field as an individual data type, the data are completely tagged. Therefore, it would be more useful to manipulate or represent in some ways.

4.2.3 Data mining

Data mining, which is called knowledge discovery in database as well, is an extraordinary process that abstract effective, novel, potential useful and understandable module from large amounts of data.(57) In brief, data mining offers potential for extracting or mining knowledge from a great deal of data.

This step involves classification, estimation, prediction, affinity grouping or association rules, clustering and description. In this case, we simplify the handling process. The program must calculate the average of vehicle float rate during a specific time interval, such as per hour, per day or per week etc. Therefore, the data could be represented on a screen at a proper scale. But in most cases, the whole procedure would be far more complicated rather than simplex operation.

4.2.4 Data modeling

Data modeling is a process to structure a data model so it can be used easily by databases. The modeling process is shown as Figure 4-4. (58)

A physical data model is developed based on performance considerations for the application which is developed, perhaps in the context of technical environment. The physical data model generally constitute of tables, columns keys and triggers.

This step will determine the form of data representation. Some data sets are shown as line graphs, and some are presented as tabular charts. Different data sets might be represented in different forms. Here, each crossroad has the coverage and vehicle flow rate, so the codes can be mapped as a two-dimensional plot, with the average value for the coverage and vehicle flow rate used for the overall scale in each dimension. In our model, data presentation includes nodes where represent particular concepts or elements of the traffic condition.

This step makes me consider the forms of representation and making a most important decision in the project. It is extremely significant because it will affect what data I acquire and what particular pieces I should abstract.

Here, the system is composed mainly of two individual components which are the front end and background processing. Google maps APIs and AJAX together constitute the front end.

Google Maps API allows developers to integrate Google Maps into their websites with their own data points. It is reasonably possible to embed the full Google maps into external sites via Google Maps API. The advantage of Google maps is that it allows the maps to support as many detail levels as the satellite photography warrants. It allows us to retrieve the route information between arbitrary points on the map. Furthermore, to convert the string based location information of a sensor into estimated discrete latitude and longitude positions on the surface of the globe, it provides us some build-in JavaScript to carry out geocoding, and ready-to-use mapping information will be offered by its servers based on the search terms.

It allows users to interact with the layout by typing the specific name of the streets. In addition, users could make use of the “zoom in “or “zoom out” feature so that draws them closer to each subsequent digit, displaying more details around the area.

Based on the Google map, when we begin to visualize the data, we will probably have more in our project rather than just a map. Adding a small number of interactions could help display more attractive. Using the mouse, which is a kind of performance that interacts with the map, you might find yourself struggling to locate the pixel position of the various map objects on the screen. (59)

We should also take into account where we need to trigger events. In this case, when users zoom in and finally mouse clicks the specific crossroad, it will default display dense spot which the coverage depends on the value of the vehicle flow rate. In addition, we should also run into situations of other mouse-related events, such as mouse drag which the cursor did not touch the location, but we will indicate to the user the exact geographical position in means of two-dimensional representation.

CHAPTER V: CONCLUSION

Integrate mapping and information have been a new trend in the computing development. It allows users to search the information they expect, and display with high-quality pictures and written explanations, even those development tendency and business model that traditional table and graphs cannot represent.

Due to large amounts of factors we should consider in the deployment of wireless sensor network, the real system might be more complicated than what we expect, we will encounter lots of problems such as where we should deploy the sensor nodes, what capacity the sensor should have, the cost and the energy of the sensor nodes, what data we acquire from the database, how to improve the data analysis process, and the exact technology to represent the data, etc. Thus, we should research further to extend the goals and themes explored in this dissertation.

Based on the current applications widely used in the world, the combination of these two research fields will make fresh achievements in the coming future.

Acknowledgements

First and foremost, I would like to thank Marie Redmond for her guidance during my MSc period at the Department of Computer Science. (I know that she does not like to be called a 'supervisor' or anything or anybody, so I will refrain from doing so.) She created the freedom for me to do want I thought was best, while giving me ample opportunities to make the most out for my Trinity year. Her view – that focusing on teaching theory rather than on applications – was providing me solid academic foundation in Computer Science.

In addition, I would like to thank Linda Doyle for her suggestion of my dissertation topic selection and also for discussing various practical and interesting aspects of the problem in hand. Her extensive learning was inspiring me during my first encounters with dissertation writing.

Many people helped me during my scientific explorations. I feel privileged to thank the following researchers for both their insightful comments and the enjoyable discussions I had with them: Dr. Glenn Strong (Trinity College Dublin, Ireland), Prof. Edwin Hancock (University of York, UK), Dr. Andrew Vande Moere (University of Sydney, Australia), Dr. John Dingliana (Trinity College Dublin, Ireland), and Dr. Patrick Hiller (National University of Ireland, Galway).

Finally, my parents and friends are thanked for their love, understanding and friendship.

References

3rd Annual Conference on Arteriosclerosis, Thrombosis and Vascular Biology, at http://atvb.ahajournals.org/cgi/reprint/22/5/878-a.pdf?ck=nck

A. Dunkels, T. Voigt, J. Alonso, H. Ritter, and J. Schiller. (2004). Connecting Wireless Sensornets with TCP/IP Networks, in Proceeding of the 2nd International Conference on Wired/Wireless Internet Communications, February, 2004.

ADAC Laboratories to Provide Leading Pinnacle 3Radiation Therapy Planning Systems to The Johns Hopkins Hospital, Business Wire, 1999.

Alipio Jorge, Luis Torgo, Pavel Brazdil, Rui Camacho, Joao Gama. (2005). *Knowledge discovery in databases* – PKDD 2005: 9th European Conference on Principles and Practice of Knowledge Discovery in Databases, Porto, Portugal, October 3-7, 2005: proceedings, Birkhauser, 2005.

Ana-Bela(c)N Garca-A-Hernando, Ana-Belen Garcia-Hernando, Josa(c)-Fernan Marta-Nez-Ortega, Juan-Manuel La3pez-Navarro, Aggeliki Prayati, Luis Redondo-La3pex, *Problem Solving for Wireless Sensor Networks*, Springer, 208, p.177.

Antony Unwin, Martin Theus, Heike Hofmann. (2006). *Graphics of Large Datasets: Visualizing a Million*, Springer, 2006, p.4.

AVS/Express Agreement, at http://www.eduserv.org.uk/chest/agreements/software/existing/avs/overview.aspx

Ben Fry, *Visualizing data*, O'Reilly, 2008, p.5.

CCD Signal-To-Noise Ratio, at http://www.microscopyu.com/tutorials/java/digitalimaging/signaltonoise/

Computational Biomagnetics, at http://www.ee.washington.edu/research/compbe/

Cypress: Image sensors have snapshot shutter capability, at http://www.eetimes.eu/products/displays/212000600

Edgar H. Callaway, *Wireless Sensor Networks: Architectures and Protocols*, CRC Press, 2003, p.21

Falko Dressler. (2007). *Self-Organization in Sensor and Actor Networks,* John Wiley and Sons, 2007, p.96.

Francisco Sandoval, Alberto Prieto, Joan Cabestany, Manuel Grana. (2007). *Computational and Ambient Intelligence*: 9th International Work-Conference on Artificial Neural Networks, IWANN 2007, San Sebastian, Spain, June 20-22,

2007: Proceedings, Springer, 2007, p.891.

Frits H. Post, Gregory M. Nielson, Georges-Pierre Bonneau. (2003). *Data visualization: the state of the art,* Springer, 2003, p.ix.

Graham Wills, Daniel Keim. (1999). IEEE Computer Society, IEEE Computer Society Technical Committee on Visualization and Graphics, *1999 IEEE Symposium on Information Visualization(InfoVis '99)*: Proceedings, October 24-29, 1999, San Francisco, California, IEEE Computer Society, 1999, p.93.

Guang-Zhong Yang, Magdi Yacoub. (2006). *Body sensor networks, Birkhauser*, 2006, p.1.

Hans Rosling, at http://en.wikipedia.org/wiki/Hans_Rosling

Heinz U.Lemke. (2000). *CARS 2000: Computer Assisted Radiology and Surgery*: proceeding of the 14th international congress and exhibition, San Francisco, June 28-July 1, 2000, Elsevier, 2000, p.11.

Heng Tao Shen. (2006). *Advanced Web and Network Technologies, and Applications: APWeb 2006 International Workshops: XRA, IWSN, MEGA, and ICSE, Harbin, China, January 16-18, 2006: Proceedings*, Birkhauser, 2006, p.281.

Holger Karl, Andreas Willig, and Adam Wolisz. (2004). *Wireless Sensor Networks: First European Workshop, EWSN 2004, Berlin, Germany, January 19-21, 2004: Proceedings*, Springer, 2004, p.356.

IEEE 802.11 Layers, at http://www.cs.utexas.edu/~ypraveen/surveys/wlan_security/node3.html

Intel showcases innovative wireless sensor networks for in-home health care solutions, at http://www.intel.com/pressroom/archive/releases/2004/20040316corp.htm

Isaac Bankman. (2000). *Handbook of Medical Imaging: Processing and Analysis Management*, Elsevier Science & Technology Books, October 2000.

Jadwiga Indulska, Jianhua Ma, Laurence Tianruo Yang, Theo Ungerer and Jiannong Cao. (2007). *Ubiquitous Intelligence and Computing: 4th International Conference, UIC 2007, Hong Kong, China, July 11-13, 2007: Proceedings*, Springer, 2007, p.589.

Jie Wu. (2006). *Handbook on theoretical and algorithmic aspects of sensors, ad hoc wireless, and peer-to-peer networks*, CRC Press, 2006, p.370.

John Robert Anderson, Ryszard Stanislaw Michalski, Jerzy W. Bala, Gheorghe Tecuci, Jaime Guillermo Carbonell, (1994). *Machine Learning: a multi-strategy approach,* Morgan Kaufmann, 1994, p.405.

KANSAS Department of Transportation, at http://www.ksdot.org/

Kazem Sohraby, Daniel Minoli, Taieb F Znati. (2007). *Wireless Sensor Networks: Technology, Protocols, and Applications*, Wiley-Interscience, 2007, p.27.

Khan, A. and Jenkins, L. (2008). *Undersea wireless sensor network for ocean pollution prevention*, Communication System Software and Middleware and Workshops, 2008.

Knowledge, at http://en.wikipedia.org/wiki/Knowledge

Maneesha Singh. (2007). *Process in Pattern Recognition*, Springer, 2007, p.153.

Markus Kunze. (2000). *Non-smooth dynamical systems*, Springer, 2000, p.48.

Medicim, Medical Image Computing, the Catholic University of Leuven, at http://www.medicim.com/en/products

Michael Purvis, Jeffrey Sambells, Cameron Turner. (2006). *Beginning Google Maps Applications with PHP and Ajax: From Novice to Professional*, Apress, 2006, p.210.

Mohammad Llyas and Lmad Mahgoub, (2004). *Handbook of Sensor Network: Compact Wireless and Wired Sensing Systems*, CRC Press, 2004, 15-3.

Nirupama Bulusu, Sanjay Jha. (2005). *Wireless Sensor Networks,* Artech House, 2005, p.5, p.14.

Nitaigour Premchand Mahalik. (2003). *Fieldbus Technology: Industrial Network Standards for Real-Time Distributed Control*, Springer, 2003, p.152.

Nitaigour Premchand Mahalik. (2006). *Sensor Networks and Configuration: Fundamentals, Standards, Platforms, and Applications*, Springer, 2006, p.439.

Paul E. Ceruzzi. (2003). *A history of modern computing*, MIT Press, 2003, p.118.

Paul Martin, Patrick Bateson. (1993). *Measuring Behaviour: An Introductory Guide*, Cambridge University Press, 1993, p.126.

Peter Perner, Rudiger W. Brause, Hermann-Georg Holzhutter. (2003). *Medical Data Analysis*: 4th International

Symposium, ISMDA 2003, Berlin, Germany, October 2002: Proceedings, Springer, 2003, p.15.

Positron emission tomography, at http://en.wikipedia.org/wiki/Positron_emission_tomography

Robert Greenberger, Sandra Giddens. (2007). *Careers in Artificial Intelligence*, The Rosen Publishing Group, 2007, p.6.

Römer, Kay and Friedemann Mattern. (December 2004). "The design Space of Wireless Sensor Networks". *IEEE Wireless Communications* **11**(6):54-61.

Sankarasubramaniam, Y., Akyildiz, I.F., Su, W., Cayirci, E.. (2002). *Wireless Sensor Networks: A Survey*. Computer Networks. 393-422(2002).

Sholom M.Weiss, Nitin Indurkhya. *(1998). Predictive data mining: a practical guide*, Morgan Kaufmann, 1998, p.1.

Smart Medical Home Research Laboratory, at http://www.centerforfuturehealth.com/smart_home/

Special Report 10 Emerging Technologies 2008, Technology Review (n.d.). Retrieved from http://www.technologyreview.com/specialreports/specialreport.aspx?id=25/

Street data in different districts in Madrid 2006, at http://www.madridmovilidad.es/imd/resumen_data3.asp

The data modeling process, at http://en.wikipedia.org/wiki/Data_visualization#Data_mining

The Visible Human Project, at http://www.nlm.nih.gov/research/visible/visible_human.html

Thomas Haenselmann(2006-04-05). *Sensornetworks*. GFDL Wireless Sensor Network textbook.

VisualMine, at http://www.iunet.it/ais/vis1.htm

Walker J., Barrett D., Gurney R., Kalma J., Kerr Y., Kim E. and LeMarshall J., MoistureMap: *A soil moisture monitoring, prediction and reporting system for sustainable land and water management.*

Walter R. J. Baets. (2005). *Knowledge management and management learning: extending the horizons of knowledge-based management*, Springer, 2005, p.118.

Wireless Sensors Help Biologists Monitor Seabird in Maine, at http://www.universityofcalifornia.edu/news/article/4602

Yang Xiao, Yi Pan and Jie Li. (2006). *Ad hoc and sensor networks*, Nova Publishers, 2006, p.71.

Yarvis M., Kushalnagar N., Singh H., Rangarajan A., Liu Y., Singh S.. (2005). *Exploiting heterogeneity in sensor networks, INFOCOM 2005.24th Annual Joint Conference of the IEEE Computer and Communications Societies:Proceedings*, 2005.

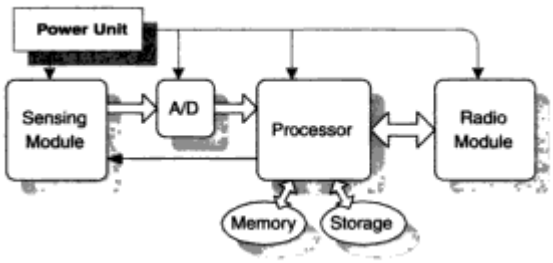

Figure 2.1 Architecture of a sensor node

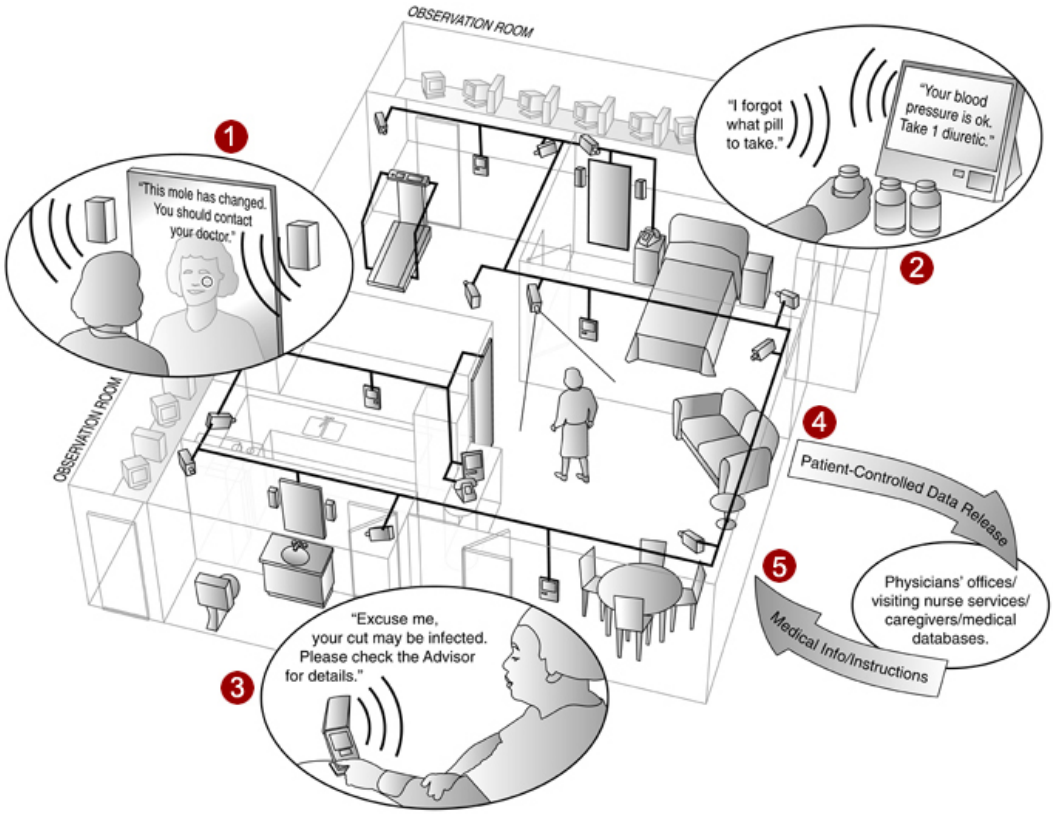

Figure 2.2 The Smart Medical Home Research Laboratory

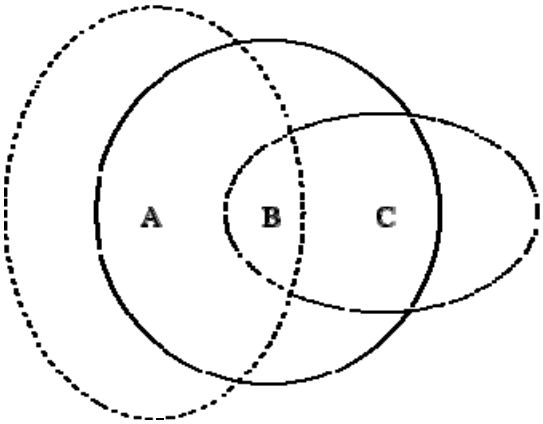

Figure 2.3 The case of multi-hop routing

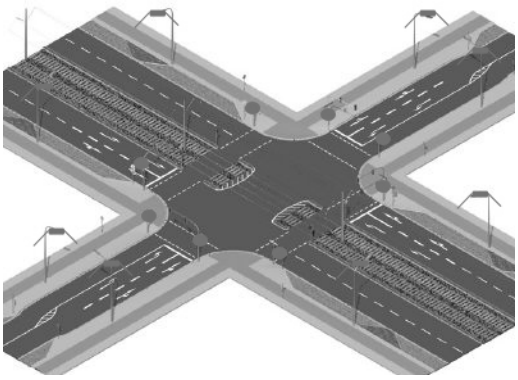

Figure 4.1 Sensor Deployment in crossroads

Número de:		Ambito	Ubicación		Datos		% de Participación	
Calles	Tramos		Zona	Distrito	Long.(Kms.)	VHS*Kms/día	Long.(Kms.)	VHS*Kms/día
	293	CENTRO		01	60.125	1.001.990	4.28%	
182	187	ARGANZUELA		02	60.555	1.535.763	4.31%	2.35%
97	157	RETIRO		03	47.550	1.536.893	3.38%	3.60%
70	278	SALAMANCA		04	76.330	1.821.063	5.43%	3.60%
88	369	CHAMARTIN		05	98.450	2.690.666	7.01%	4.27%
139	190	TETUAN		06	52.005	952.337	3.70%	6.31%
77	238	CHAMBERI		07	57.920	1.202.655	4.12%	2.23%
91	234	FUENCARRAL-EL PARDO	T	08	107.725	3.724.936	7.67%	2.82%
121	308	MONCLOA-ARAVACA		09	135.535	4.621.570	9.65%	8.73%
161	191	LATINA	O	10	81.850	2.305.262	5.83%	10.83%
101	199	CARABANCHEL		11	80.040	2.218.253	5.70%	5.40%
102	145	USERA	D	12	57.590	1.781.982	4.10%	5.20%
72	211	PUENTE VALLECAS		13	82.805	2.831.968	5.89%	4.18%
112	86	MORATALAZ		14	38.550	1.351.794	2.74%	6.64%
51	286	CIUDAD LINEAL	A	15	92.930	2.552.697	6.61%	3.17%
132	177	HORTALEZA		16	68.320	2.272.405	4.86%	5.98%
105	87	VILLAVERDE	S	17	48.280	1.575.617	3.44%	5.33%
58	42	VILLA DE VALLECAS		18	18.665	703.670	1.33%	3.69%
28	39	VICALVARO		19	20.740	907.087	1.48%	1.65%
27	177	SAN BLAS		20	77.480	2.963.870	5.51%	2.13%
92	63	BARAJAS		21	41.660	2.116.323	2.96%	6.95%
39	3.957	CONJUNTO			1.405.105	42.668.801	100.00%	4.96%
1.945								100.00%

Figure 4.2 Vehicle flow rate in the format provided by Department of Security and Mobility, Spain

182	187	ARGANZUELA	02	60.555	1.535.763	4.31%	2.35%
float TAB	String TAB	String TAB	Index TAB	float TAB	Float TAB	float TAB	float TAB

Figure 4.3 Structure of acquired data

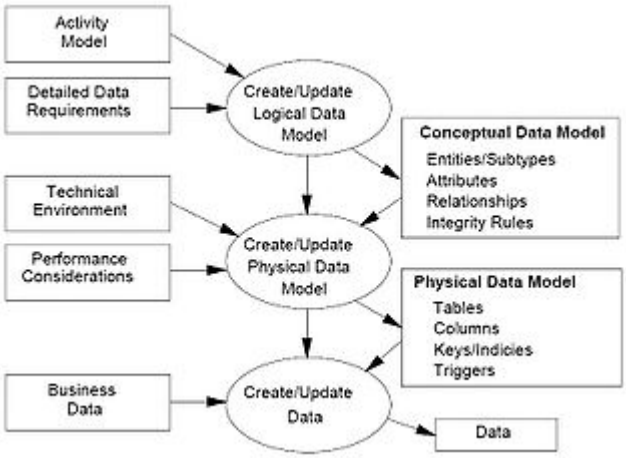

Figure 4.4 The data modeling process

Modern Applied Science

www.ccsenet.org/journal.html

Vol. 3, No. 6

June 2009

Spatial Sound Reproduction Based on HRTF Auto-Selection Algorithm

Cheng Zhang, Ke'an Chen & Chao Xing

College of Marine, Northwestern Polytechnical University

Xi'an 710072, China

E-mail: zhangcheng001@mail.nwpu.edu.cn

Abstract

The desired beam pattern of the array can be achieved by applying specific array weighting in the eigenbeam space derived from the plane wave decomposition. Head related transfer function (HRTF) data are selected automatically from the KEMAR HRTF measurements database of MIT media lab without the message of the direction of the incoming sound wave. The HRTF for the sound wave direction are derived by combining the directivity of the eigenbeam beamforming and the algebraic expression of HRTF. Computer simulations demonstrate that the HRTF approximation derived from this paper are similar to those of the measurements by MIT media lab in certain frequency band. The higher the order of the eigenbeam used in eigenbeam beamforming, the more similar of the derived HRTF data with those of the measurements. Listening experiments are conducted to evaluate the efficiency of the proposed HRTF auto-selection algorithm subjectively. The results indicate that the audio localization precision for virtual sounds using approximated HRTF is consistent with those of the measured HRTF, which verifies the validity of the proposed algorithm.

Keywords: Planewave decomposition, Eigenbeam beamforming, HRTF, Virtual audition

1. Introduction

Virtual audition has been wildly used in virtual reality, robotics, communication, tele-conferencing, entertainment, and training simulations, etc.. The presentation of binaural signals over headphones is a convenient way for recreating the original auditory scene for a listener. There are two kinds of methods to get binaural signals. One is the traditional binaural technology. It records sound signals using miniature microphones placed at the entrance to the ear canals of a listener or a dummy head. Then replaying these signals via headphones will reproduce the original auditory experience, evoking the auditory perception of a source located at a point in the space surrounding the listener. The other method is based on signal processing technology which gets binaural signals through computer combination. It reproduces the processed sound through head-related transfer function (HRTF) filter (Moller, 1995; Xie, 2008), which has been wildly implemented in practice as it can be realized easily. The direction of the actual or virtual sound source must be known in advance. Then binaural signals can be derived by filtering the sound signal using HRTF data for the sound direction. Reproducing the binaural signals through a pair of headphones can create the three-dimension sound in human auditory perception (Bai, 2004; Savioja, 1999). Array signal processing can improve the signal-to-noise ratio (SNR) and eliminate the influence of the noise and the interferer (validly, 2001). As a result, with the same sound intensity, the distance of the processed sound source is much further using array signal processing technology than listening to the sound signal directly. Furthermore, the sound image of the former in listener's auditory perception is much clear than the latter with the same distance between the sound source place and the listening place. It has great significance to combine the array signal processing technology with human audition system in sound source localization and identification applications as human audition has great ability of sound localization and identification. In practice, the incoming direction of the sound signal is often unknown, and it may be appeared in any direction in three dimensional space blended with a lot of interferer and noise especially in battlefield environment. Thus, in order to reproduce the space sound through HRTF filter, the direction of the sound signal must be known in advance. In present literature, the direction of the incoming sound must be estimated using array signal processing technology, which may increase the computing load and can not be implemented in practice conveniently.

This work deals with the HRTF auto-selection algorithm without the message of the direction of the incoming sound wave. Firstly, the soundfield is decomposed to the eigen-beam space using the planewave decomposition theory based on the array model of a uniform circular array (UCA) mounted around a rigid sphere. Special array beam patterns are derived through eigenbeam beamforming processing using distinct array weighting function. Through filtering the

HRTF measurements data for all the directions by the beam directivity of eigenbeam beamforming, the HRTF approximation are derived without the message of the direction of the sound source based on the HRTF algebraic expression. Then, virtue sound is achieved using the HRTF approximation data. Simulations and subjective experiments are carried out to investigate the validity of the proposed method lastly.

2. Eigenbeam beamforming

Applying the soundfield decomposition theory, the soundfield around the array can be decomposed to the eigenbeam space. Then, the sound signal can be further processed using array signal processing technology in the eigenbeam space (Rafaely, 2004; Teutsch, 2006).

Assume a UCA with radius R_0 mounted around a rigid sphere with radius R, and a unit magnitude impinging plane wave comes from the direction of (θ_0, φ_0). The equation describing the resulting sound pressure at (r, ϑ, φ) around the array in spherical coordinates is (Meyer, 2001)

$$P(r,\vartheta,\varphi)=\sum_{n=0}^{\infty}(2n+1)(-j)^n[j_n(kr)-\frac{j_n^{'}(kR_0)}{h_n^{'}(kR_0)}h_n(kr)]\sum_{q=-n}^{n}\frac{(n-|q|)!}{(n+|q|)!}P_n^{|q|}(\cos\vartheta)P_n^{|q|}(\cos\vartheta_0)e^{-jq(\varphi-\varphi_0)} \quad (1)$$

where k is the wave number, $k=2\pi/\lambda$, λ is the wave length of the plane wave, $j_n(\cdot)$ is the nth-order spherical Bessel function of the first kind, $h_n(\cdot)$ is the nth-order spherical Hankel function, $j_n^{'}(\cdot)$ and $h_n^{'}(\cdot)$ denotes the derivative of the nth-order spherical Bessel function and the nth-order spherical Hankel function with respect to the argument respectively, $P_n^q(\cdot)$ is the Legendre function of order n and degree q. The time dependency is omitted in the equation.

For simplicity, the theoretical construct of a continuous circular aperture and a unit magnitude plane wave impinging from $\vartheta_0=\pi/2$ are concerned firstly. Assuming the continuous circular aperture is located on the equator of the rigid sphere, i.e. $\vartheta=\pi/2$, the sound pressure at the position of the continuous circular aperture is described by $r=R$. Then, Eq. (1) becomes

$$P(R,\vartheta,\varphi)=\sum_{n=0}^{\infty}(2n+1)(-j)^n[j_n(kR)-\frac{j_n^{'}(kR_0)}{h_n^{'}(kR_0)}h_n(kR)]\sum_{q=-n}^{n}\frac{(n-|q|)!}{(n+|q|)!}\times P_n^{|q|}(\cos\vartheta)P_n^{|q|}(\cos\vartheta_0)e^{-jq(\varphi-\varphi_0)} \quad (2)$$

$P(R,\vartheta,\varphi)$ can be seen as the acoustical transfer function from the source point (ϑ_0,φ_0) to the sensor location (R,ϑ,φ). Assume the aperture weighting function is $\omega(\varphi,f)$, and since $\omega(\varphi,f)$ has to be 2π periodic, it can be expanded in a Fourier series

$$\omega(\varphi,f)=\sum_{p=-\infty}^{\infty}a_p(f)e^{jp\varphi} \quad (3)$$

For simplicity, assume further $a_p(f)=1$, then the pth eigenbeam caused by the pth term of the aperture weighting function can be represented as

$$P_p=\frac{1}{2\pi}\int_0^{2\pi}P(R,\vartheta,\varphi)\omega(\varphi,f)\mathrm{d}\varphi \quad (4)$$

Using Eq. (2) and Eq. (3), we can get

$$\begin{aligned}P_p=&\frac{1}{2\pi}\int_0^{2\pi}\sum_{n=0}^{\infty}(2n+1)(-j)^n[j_n(kR)-\frac{j_n^{'}(kR_0)}{h_n^{'}(kR_0)}h_n(kR)]\sum_{q=-n}^{n}\frac{(n-|q|)!}{(n+|q|)!}\\&\times P_n^{|q|}(\cos\vartheta)P_n^{|q|}(\cos\vartheta_0)e^{-jq(\varphi-\varphi_0)}e^{jp\varphi}\mathrm{d}\varphi\end{aligned} \quad (5)$$

From Eq. (5), we can finally get (Meyer, 2001)

$$P_p=b_p e^{jp\varphi_0} \quad (6)$$

where

$$b_p=\sum_{n=p}^{\infty}(2n+1)(-j)^n[j_n(kR)-\frac{j_n^{'}(kR_0)}{h_n^{'}(kR_0)}h_n(kR)]\frac{(n-|p|)!}{(n+|p|)!}P_n^{|p|}(\cos\vartheta)P_n^{|p|}(\cos\vartheta_0) \quad (7)$$

P_p can be seen as the p th order eigen-beam derived from the decomposed soundfield.

Array received signals can be processed in eigenbeam space by applying eigenbeam beamforming technology based on the planewave decomposition theory. In order to eliminate the frequency influence in the eigenbeam, assume

the *p*th order weighting coefficient as

$$w_p(\varphi) = \frac{1}{b_p} e^{jp\varphi} \tag{8}$$

Then, the *p*th order array output is

$$y_p = \frac{1}{2\pi} \int_0^{2\pi} P(R, \vartheta, \varphi) w_p(\varphi) \mathrm{d}\varphi = e^{jp\varphi_0} \tag{9}$$

Considering a square integrable function on the unite circular, this function can be expressed as the summation of Fourier series

$$f(\varphi) = \sum_{p=-\infty}^{\infty} F_p e^{jp\varphi} \tag{10}$$

The coefficients of Fourier series is defined as

$$F_p = \frac{1}{2\pi} \int_0^{2\pi} f(\varphi) e^{-jp\varphi} d\varphi \tag{11}$$

Assuming an ideal beam pattern $F(\varphi, \varphi_k)$ looking at the direction φ_k , it can be expressed as a delta function

$$F(\varphi, \varphi_k) = \delta(\varphi - \varphi_k) \tag{12}$$

It can also be expanded into a summation of the Fourier series

$$F(\varphi, \varphi_k) = \frac{1}{2\pi} \sum_{p=-\infty}^{\infty} e^{-jp(\varphi - \varphi_k)} \tag{13}$$

From the above analyses, the aperture weighting function to achieve this beam pattern is

$$w(\varphi, \varphi_k) = \frac{1}{2\pi} \sum_{p=-\infty}^{\infty} \frac{1}{b_p} e^{jp(\varphi - \varphi_k)} \tag{14}$$

Sampling the continuous circular array using a UCA result in the same expressions as Eq. (6) when the number of the elements of UCA satisfies $M \geq 2N$ .The highest order of the eigen-beams N is satisfied by $N \leq [kR]$, $[\cdot]$ stands for the biggest integer (Mathews, 1994). Then the array weighting function is

$$w(\varphi_s, \varphi_k) = \frac{1}{2\pi} \sum_{p=-N}^{N} \frac{1}{b_p} e^{jp(\varphi_s - \varphi_k)} \tag{15}$$

where φ_s denotes the elements place. The beam pattern can be expressed as

$$F_N(\varphi, \varphi_k) = \frac{1}{2\pi} \sum_{p=-N}^{N} e^{-jp(\varphi - \varphi_k)} \tag{16}$$

The array output is

$$y_{\mathrm{EB}} = \frac{1}{2\pi} \sum_{p=-N}^{N} e^{-jp(\varphi - \varphi_k)} \tag{17}$$

So far, the array beam output pointing to the signal direction φ_k is achieved using the array weighting function defined in Eq. (15). This beamforming technology using eigenbeams derived from the soundfield decomposition process is called as eigenbeam beamforming (EBF). The array received sound signals can be further processed using the directivity of the EBF.

The delay-and-sum beamforming (DSBF) technology can also be applied to the array with baffles in eigenbeam space. All processed microphone outputs can have the same phase by compensating for the delays due to a single plane wave.

A widely used performance measure of array is the directivity factor (DI), which evaluates the improved directivity of the array compared to an omnidirectional microphone (Brandstein, 2001). It can be defined as the logarithm expression of the ratio of the array output in look direction and the array output integrated over all directions. So, the DI of the EBF array can be expressed as

$$\begin{aligned}\mathrm{DI}_{\mathrm{EB}} &= 10\lg\left(\left|y_{\mathrm{EB}}(\varphi_k)\right|^2 \Big/ \frac{1}{2\pi}\int_0^{2\pi}\left|y_{\mathrm{EB}}(\phi)\right|^2 d\phi\right) \\ &= 10\lg\left(\left|\frac{1}{2\pi}\sum_{p=-N}^{N} e^{-jp(\varphi-\varphi_k)}\right|^2 \Big/ \frac{1}{2\pi}\int_0^{2\pi}\left|\frac{1}{2\pi}\sum_{p=-N}^{N} e^{-jp(\varphi-\phi)}\right|^2 d\phi\right) \\ &= 10\lg\left(\left|\sum_{p=-N}^{N} 1\right|^2 \Big/ \sum_{p=-N}^{N}\left|1\right|^2\right) = 10\lg(2N+1)\end{aligned} \tag{18}$$

It's clearly from Eq. (18) that the DI of the EBF array is independent on the frequency.

For DSBF array, assume the pressure on the array is $e^{i\boldsymbol{k}_0\boldsymbol{r}}$ due to a plane wave comes from the direction φ_0, where $\boldsymbol{k}_0$ is the wave vector represents the plane wave arrival direction, and $\boldsymbol{r} = (z = 0, \theta = \pi/2, \varphi)$ denotes the microphone positions. Then the output of the DSBF array can be written as

$$y_{\mathrm{DS}} = \frac{1}{2\pi}\int_0^{2\pi} e^{i\boldsymbol{k}_0\boldsymbol{r}} e^{-i\boldsymbol{k}_l\boldsymbol{r}} d\varphi \tag{19}$$

where $\boldsymbol{k}_l$ denotes the wave vector of the array look direction φ_l. The pressure signal can be expressed as the summation of the Fourier series, and the coefficients of the Fourier series can be written as (Rafaely 2004; Teutsch, 2006)

$$P_p = b_p e^{jp\varphi_0} \tag{20}$$

With Eq. (10) and Eq. (20), the DSBF array output becomes

$$\begin{aligned} y_{\mathrm{DS}} &= \frac{1}{2\pi}\int_0^{2\pi}\sum_{p=-N}^{N} P_p e^{jp\varphi}\sum_{p'=-N}^{N} P_{p'}^{*} e^{-jp'\varphi} d\varphi = \frac{1}{2\pi}\int_0^{2\pi}\sum_{p=-N}^{N} b_p e^{jp\varphi_0} e^{jp\varphi}\sum_{p'=-N}^{N} b_{p'}^{*} e^{-jp'\varphi_l} e^{-jp'\varphi} d\varphi \\ &= \sum_{p=-N}^{N}\left|b_p\right|^2 e^{jp\varphi_0} e^{-jp\varphi_l} = \sum_{p=-N}^{N}\left|b_p\right|^2 e^{-jp(\varphi_l-\varphi_0)} \end{aligned} \tag{21}$$

Using the same analysis with the EBF array, the DI of the DSBF array can be written as

$$\mathrm{DI}_{\mathrm{DS}} = 10\lg\left(\left|\sum_{p=-N}^{N}\left|b_p\right|^2\right|^2 \Big/ \sum_{p=-N}^{N}\left|b_p\right|^4\right) \tag{22}$$

The DI of the EBF array is compared with that of the DSBF array for different frequencies in Fig.1. It's shown that the DI of the EBF array remains constant throughout the frequency band, which is a benefit for processing low frequency and broad band signals. The DSBF array has approximately the same DI with the EBF array only at higher frequencies. As frequency lowered, the DI of the DSBF array is also reduced until it becomes omidirectional , i.e., DI=0. Figure 2 shows the beam patterns of the EBF array and the DSBF array with kR =2 and 12 respectively. It's obvious from this figure that the beam patterns of the EBF array have frequency-independent characteristic, and the directivity of the DSBF array is very weak at low frequencies ($kR = 2$) as the values of b_p in this case are much smaller. It increases gradually as the frequency increase. Approximately the same directivity are derived for the DSBF array and the EBF array at high frequencies ($kR = 12$) as the values of b_p are almost equal for different eigen-beams.

3. HRTF auto-selection

As sound propagates from a distant source to the eardrums of a human listener, it is acoustically transformed by interactions with the head, torso, and pinna. This transformation can be modeled as a linear filter. The transfer function is called the head related transfer function (HRTF). HRTF describe the spectral filtering and contain all the information on the sound transmission from a given source position to the ear canals of a human subject including the interaural time difference (ITD), the interaural level difference (ILD), and spectral characteristics. The inverse Fourier transform of a HRTF is termed the head-related impulse response (HRIR) (Xie, 2008). HRTF are used in binaural virtual auditory displays for the synthesis of a sound source with spacial characteristics. The direction of the sound or the virtual sound must be known in advance in order to select the HRTF data for the sound direction. However, the direction of the sound is often unknown and there are a lot of interferers and noise companied with the target sound as described in introduction. So array signal processing technology is needed to estimate the DOA of the sound wave and cancel the influence of the interferers and noise. In order to reduce the DSP computing load, a new method must be investigated to derive the HRTF data for the desired direction without the message of the sound wave direction. We combine the directivity of the beamforming and the algebraic of the HRTF to achieve this goal. Only the eigenbeam beamforming is concerned in the following as it has better performance at low frequencies and for broad band signals.

Assume the sound wave comes from the point (r, ϑ, φ), then the HRTF can be expressed as (Duraiswami, 2004)

$$h(\vartheta,\varphi)=\sum_{n=0}^{\infty}\sum_{p=-n}^{n}\alpha_{nm}h_n(kr)Y_n^m(\vartheta,\varphi) \tag{23}$$

where α_{nm} are the fitting coefficients which be determined using the discrete HRTF measurements. $Y_n^m(\vartheta,\varphi)$ is the spherical harmonics of order n and degree m. Here the incoming planewave paralleling to the array is concerned only for simplicity, i.e., only the HRTF in the array plane is discussed. Then, $\vartheta=\pi/2$, and the following expression is derived by expanded the spherical harmonics

$$h(\varphi)=\sum_{n=0}^{\infty}\sum_{m=-n}^{n}\alpha_{nm}h_n(kr)\sqrt{\frac{2n+1}{4\pi}\frac{(n-m)!}{(n+m)!}}P_n^m(0)e^{jm\varphi} \tag{24}$$

Assume the sound wave comes from the direction φ_k, we need to select the HRTF for the direction φ_k to combine the virtual sound. In order to achieve this goal, we use the delta function (ideal beam pattern) to select the HRTF data. Using Eq. (12), we can get

$$\int_0^{2\pi}h(\varphi)F(\varphi,\varphi_k)d\varphi=\int_0^{2\pi}h(\varphi)\delta(\varphi-\varphi_k)d\varphi=h(\varphi_k) \tag{25}$$

From Eq. (13), we can also derive

$$\begin{aligned}\int_0^{2\pi}h(\varphi)F(\varphi,\varphi_k)d\varphi&=\int_0^{2\pi}\sum_{n=0}^{\infty}\sum_{m=-n}^{n}\alpha_{nm}h_n(kr)\sqrt{\frac{2n+1}{4\pi}\frac{(n-m)!}{(n+m)!}}P_n^m(0)e^{jm\varphi}\times\frac{1}{2\pi}\sum_{p=-\infty}^{\infty}e^{-jp(\varphi-\varphi_k)}d\varphi\\&=\sum_{n=0}^{\infty}\sum_{m=-n}^{n}\alpha_{nm}h_n(kr)\sqrt{\frac{2n+1}{4\pi}\frac{(n-m)!}{(n+m)!}}P_n^m(0)e^{jm\varphi_k}\\&=h(\varphi_k)\end{aligned} \tag{26}$$

In practice, HRTF are measured only at finite points at the array plane. Assume the highest order of the eigenbeam derived from the soundfield decomposition is N, and the number of measurements points is M, which are uniformly distributed around the circle. Then

$$h(\varphi_l)=\sum_{n=0}^{\infty}\sum_{m=-n}^{n}\alpha_{nm}h_n(kr)\sqrt{\frac{2n+1}{4\pi}\frac{(n-m)!}{(n+m)!}}P_n^m(0)e^{jm\varphi_l}\ ,\ \ l=1,2,\cdots,M \tag{27}$$

Equation (27) can be expand into two groups as

$$\begin{aligned}h(\varphi_l)&=\sum_{n=0}^{N}\sum_{m=-n}^{n}\alpha_{nm}h_n(kr)\sqrt{\frac{2n+1}{4\pi}\frac{(n-m)!}{(n+m)!}}P_n^m(0)e^{jm\varphi_l}\\&\quad+\sum_{n=N+1}^{\infty}\sum_{m=-n}^{n}\alpha_{nm}h_n(kr)\sqrt{\frac{2n+1}{4\pi}\frac{(n-m)!}{(n+m)!}}P_n^m(0)e^{jm\varphi_l}\\&=h_N(\varphi_l)+h_{N+1}(\varphi_l)\end{aligned} \tag{28}$$

Rewrite Eq. (26) as a summation form

$$\begin{aligned}\sum_{l=1}^{M}h(\varphi_l)F_N(\varphi_l,\varphi_k)&=\sum_{l=1}^{M}[h_N(\varphi_l)+h_{N+1}(\varphi_l)]\times\frac{1}{2\pi}\sum_{p=-N}^{N}e^{-jp(\varphi_l-\varphi_k)}\\&=\sum_{l=1}^{M}[\sum_{n=0}^{N}\sum_{m=-n}^{n}\alpha_{nm}h_n(kr)\sqrt{\frac{2n+1}{4\pi}\frac{(n-m)!}{(n+m)!}}P_n^m(0)e^{jm\varphi_l}\\&\quad+\sum_{n=N+1}^{\infty}\sum_{m=-n}^{n}\alpha_{nm}h_n(kr)\sqrt{\frac{2n+1}{4\pi}\frac{(n-m)!}{(n+m)!}}P_n^m(0)e^{jm\varphi_l}]\times\frac{1}{2\pi}\sum_{p=-N}^{N}e^{-jp(\varphi_l-\varphi_k)}\\&=\frac{M}{2\pi}\sum_{n=0}^{N}\sum_{m=-n}^{n}\alpha_{nm}h_n(kr)\sqrt{\frac{2n+1}{4\pi}\frac{(n-m)!}{(n+m)!}}P_n^m(0)e^{jm\varphi_k}+\varepsilon\\&=\frac{M}{2\pi}h_N(\varphi_k)+\varepsilon\end{aligned} \tag{29}$$

where ε are residual errors due to the sampling operation. The orthonormality property of the discrete Fourier transform is used in Eq. (29). Assuming an impinging wavefield is decomposed to eigenbeams up to a finite order *N*, the residual errors can be omitted in Eq. (29) when $M\geq 2N$ is satisfied (Mathews, 1994). Then

$$\sum_{l=1}^{M}h(\varphi_l)F_N(\varphi_l,\varphi_k)=\frac{M}{2\pi}h_N(\varphi_k) \tag{30}$$

The HRTF approximation for the direction φ_k can be achieved by multiplying a constant $2\pi/M$ to the summation in Eq. (30). It is obviously that the quality of the HRTF selection is determined by the highest order of the eigenbeams derived

from the soundfield decomposition.

The beam pattern looking at the sound incoming direction is arrived using EBF technology described above, and the HRTF auto-selection is achieved by filtering the HRTF measurements using the output of this beam pattern without the message of the incoming sound direction.

4. Virtual sound combination

The virtual audition space can be created by filtering the sound wave signal with appropriate HRTF data and replaying it through a pair of stereo headphone. The principal of the virtual sound combination using the HRTF data is calculating the convolution of the appropriate pair of HRIR with the sound signal (Xie, 2008). Here $h_l(n)$ and $h_r(n)$ denote the left and right ear HRIR respectively, and $x(n)$ denotes the input signal series. Then, the outputs after HRIR filtering are

$$y_r = h_r(n) * x(n) \tag{31}$$

$$y_l = h_l(n) * x(n) \tag{32}$$

Thus, the direction of the sound wave must be known in advance in order to select the appropriate HRIR. Using the method proposed in this paper, the virtual sound can be combined without the knowledge of the direction of the sound wave through filtering the HRTF measurements using the beam output of the EBF to yield the binaural signals for a pair of stereo headphone. Figure 3 shows the diagram of the proposed procedure of virtual sound combination.

5. Simulation analysis

In simulations, a UCA of 24 omnidirectional microphones with radius R =0.093m is mounted around a rigid sphere with radius R_0 =0.085m. Therefore, the maximum order of the eigen-beams derived from the soundfield decomposition is N=12. The HRTF auto-selection algorithm proposed in this paper is used to get the HRTF for the sound direction. Figure 4 and 5 show the HRTF approximation and the KEMAR HRTF measurements of MIT (MIT Media Lab, 1994) of the left and right ear for the direction of 35°, where the dotted line denotes the approximation data, and the solid line denotes the KEMAR measurements. The order of the eigenbeams used in the eigenbeam beamforming is 6. It can be seen that there is a good approximation for frequencies until about 3.5kHz. The order of the eigenbeams used in Fig. 6 and 7 is 12. There is a good approximation for frequencies until about 7.5kHz. It can be concluded that the HRTF auto-selection algorithm proposed in this paper is valid and can be used to synthesize virtual sound. Furthermore, the higher the order of the eigenbeams used in the EBF, the more similar of the approximation with the measurements at a given broad frequency band.

6. Experiments

There are traditionally two kinds of evaluation methods to evaluate the validity of the HRTF approximation. The first one is the objective evaluation, which compares the consistency of the amplitude and phase responses in the whole frequency band. The other one is the subjective evaluation, which compares the consistency of listeners' auditory perception caused by the virtual sound with those of the real sound. In order to verify the validity of the proposed method, a subjective listening experiment was conducted. The listening test involved 12 human subjects whose age range from 22 to 34 years, and all of them have normal hearing.

The experiment was conducted in an anechoic chamber to minimize unwanted reflections. The sound used in the experiment was 5s music sound, bandpass filtered between 50Hz and 6kHz. In the experiment, 9 positions, ranging from -60° to 60° with 15° intervals, were pre-selected to position the source, which were at the same height with the head of the listeners and the arrays. The right side of the listener's head was defined as positive angle, and the left side of the listener's head was defined as negative angle. The distance between the microphone array and the source was 2 m. Binaural signals were combined using the measured HRTF data and the approximation data respectively. The number of eigenbeams used in HRTF approximation was 12. The binaural signals were send to a pair of stereo headphones to reproduce the space sound. In order to have the proper listening perception, the listeners received extensive training with the real sound prior to the actual data collection. During the experiment, the listeners judged the directions of the virtual sound played in the headphones and recorded the directions. The sound was played stochastically at the 9 positions. Stochastic analysis was conducted to the experimental data. Figure 8 and 9 show the result of the subjective localization experiment. The judgment angle is plotted as a function of the target angle. The size of each symbol represents the percentage of judgments from each target-angle that fall within each judgment-angle. The positive-slope diagonal is also plotted in the panel. If the judgment angle was identical to the target angle, then all points would fall along this line. It shows that the perceived angles of the source are in very good agreement with the presented angles of the source since most data points fall on the diagonal of the plot. Another view of these data is shown in Fig. 10, which indicate the statistic of the localization errors in a bar chart. It can be seen in this result that the mean localization errors using the HRTF approximation data are very similar to the measured data. The largest localization error is 13.75°, less than one test interval. It can be concluded that the validity of the proposed method is verified by the subjective listening experiments.

7. Conclusion

In the application of virtual audition technology to the sound source localization and identification in the battlefield, the sound wave direction must be estimated in advance in order to select the proper HRTF to combine the binaural signals as this message is often unknown. Replaying the binaural signals through a pair of stereo headphones can reproduce the space sound in the listener's sensation. Traditional virtual sound combination technology need estimate the DOA of the sound wave which will increase the computing load of the system. An HRTF auto-selection algorithm is proposed in this paper using the directivity of EBF and the algebraic expression of the HRTF. Moreover, the EBF technology used in this paper has higher directivity than DSBF technology at low frequencies. Computer simulations demonstrate that there are good consistency between the HRTF approximation and the measurements under certain frequency band. Subjective listening experiment results indicate that the subjects are capable of localizing the presented source direction within an average error of 13.75°, which are consistent with the results using the measured HRTF data. Thus, the HRTF auto-selection algorithm proposed in this paper provides a resolution for the virtual sound applications with unknown sound wave directions.

References

Bai, M. R., & Lin, C. P. (2004). Microphone array signal processing with application in three- dimensional spatial hearing. *J. Acoust. Soc. Am*., 117(4): 2112-2121.

Brandstein, M., & Ward, D. (2001). Microphone Arrays: Signal Processing Techniques and Applications. New York: Springer-Verlag.

Duraiswami, R., Zotkin, D., & Gumerov, N. (2004). Interpolation and range extrapolation of HRTFs. *IEEE ICASSP*, IV: 45-48.

Mathews, C. P. & Zoltowski, M. D. (1994). Eigen-structure techniques for 2D angle estimation with uniform circular arrays. *IEEE Trans. Signal Process*., 42(9): 2395-2407.

Meyer, J. (2001). Beamforming for a circular microphone array mounted on spherically shaped objects. *J. Acoust. Soc. Am.*, 109(1): 185-193.

MIT Media Lab, (1994) HRTF measurements of a KEMAR dummy-head microphone. [Online] Available: http://sound.media. mit.edu./ resources/KEMAR.html (May 18, 1994).

Moller, H., Soerensen, M. F., Hammershoei, D., & Jensen C. B. (1995). Head-related transfer functions of human subjects. *J. Audio Engineer. Soc.*, 43(5): 300–321.

Rafaely, B. (2004). Plane-wave decomposition of the sound field on a sphere by spherical convolution. *J. Acoust. Soc. Am*., 116(4): 2149-2157.

Savioja, L., Huopaniemi, J., Lokki, T., & Vaananen, R. (1999). Creating interactive virtual acoustic environments. *J. Audio Engineer. Soc.*, 47(9): 675-705.

Teutsch, H., Kellermann, W. (2006). Acoustic source detection and localization based on wavefield decomposition using circular microphone arrays. *J. Acoust. Soc. Am*. 120(5): 2724-2736.

Xie, B. S. (2008). *Head-related transfer function and virtual audition* . Beijing: National defence industry press.

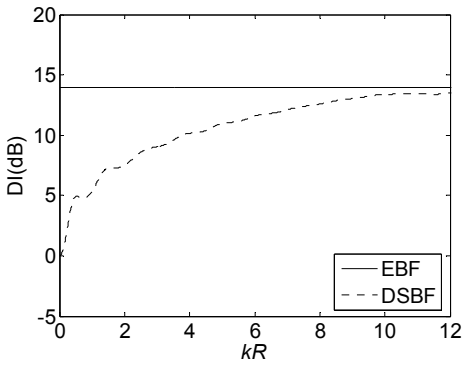

Figure 1. DI of the EBF and DSBF array.

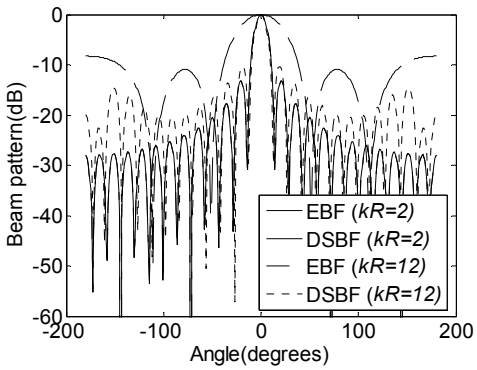

Figure 2. Beam pattern of the EBF and DSBF array.

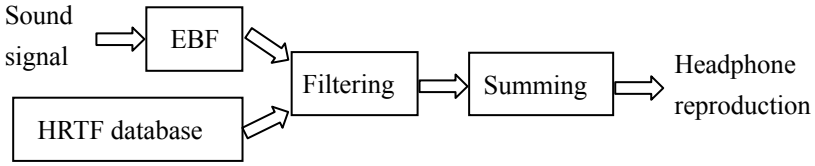

Figure 3. the diagram of virtual sound combination based on HRTF auto-selection

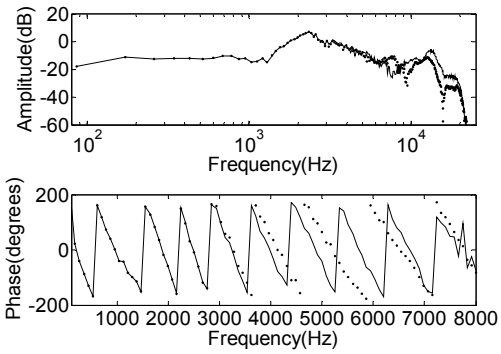

Figure 4. Left ear HRTF (*N*=6).

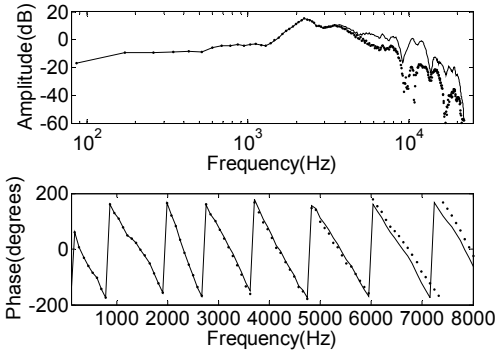

Figure 5. Right ear HRTF (*N*=6).

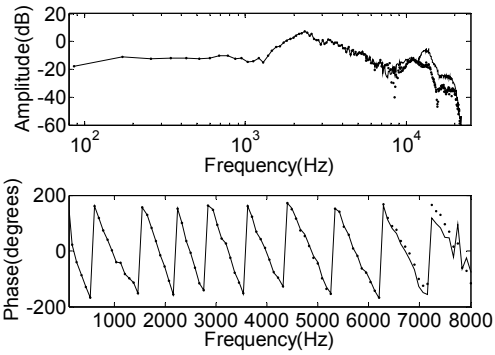

Figure 6. Left ear HRTF (*N*=12).

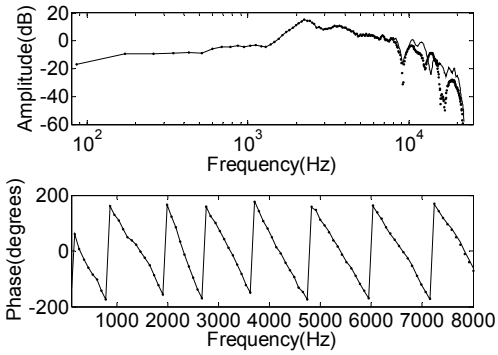

Figure 7. Right ear HRTF (*N*=12).

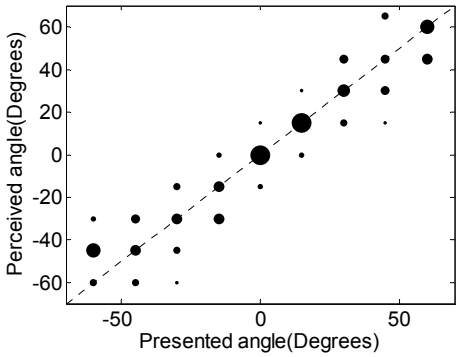

Figure 8. The results of the subjective listening experiment using approximated HRTF

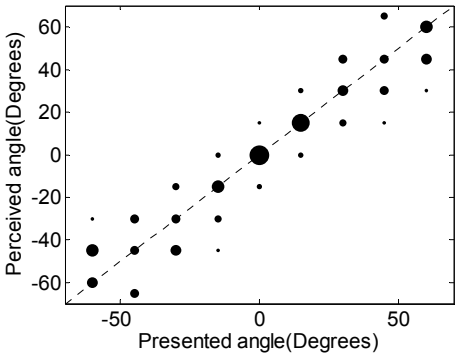

Figure 9. The results of the subjective listening experiment using measured HRTF

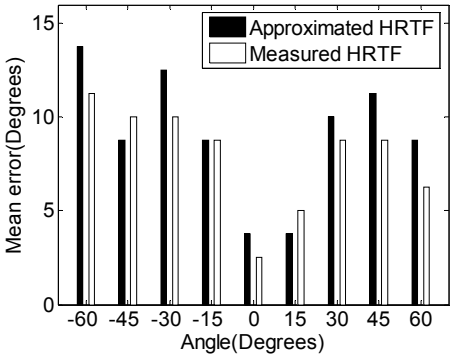

Figure 10. The localization errors for the presented angles

Modern Applied Science

www.ccsenet.org/journal.html

Vol. 3, No. 6

June 2009

Implementation of Energy Management Structure for Street Lighting Systems

C.Maheswari (Corrosponding author)
Lecturer, Department of Mechatronics Engineering
Kongu Engineering College, Perundurai
Erode – 638 052, India
E-mail: maheswarimts@yahoo.co.in

R.Jeyanthi (Corrosponding author)
Lecturer, Department of Mechatronics Engineering
Kongu Engineering College,Perundurai
Erode – 638 052, India
E-mail: jeyanthi.ramasamy@gmail.com

Dr.K.Krishnamurthy
Professor & Head, Department of Mechatronics Engineering
Kongu Engineering College, Perundurai
Erode – 638 052, India
E-mail: krishmech@kongu.ac.in

M.Sivakumar
Senior Lecturer, Department of Mechatronics Engineering
Kongu Engineering College, Perundurai
Erode – 638 052, India
E-mail: amsivakumar@yahoo.co.in

The research is financed by Real Tech Systems, TBI@Kongu Engineering College, perundurai, India.

Abstract

This work aims to develop an Energy efficient and low cost solution for street lighting system using Global System for Mobile communication [GSM] and General Packet Radio Service [GPRS]. GSM and GPRS are used to establish a communication between the streetlights and the Central Monitoring Station [CMS] at the operator side. The whole setup provides the remote operator to turn off the lights when not required, regulate the voltage supplied to the streetlights and prepare daily reports on glowing hours. Power shut downs also can be intimated to the remote CMS operator through GSM and GPRS communication setup. The energy meter placed at the lighting system sends the readings to the remote CMS in the form of short message [SMS]. From the data collected at CMS, energy report is prepared using visual basic programming.

Keywords: Energy saving, GSM, GPRS, Embedded system, SMS

1. Introduction

Now day's street lighting systems are the indispensable part of the town's infrastructure. Maintenance and control of the lighting systems and the production price of electricity by itself are the major expenses to the town's streetlight

operation budgets (1). There are thousands of streets connected in a common line, so it is very tedious work to maintain and control. Dark roads deter people and well its surroundings attract people. The generated electricity is improved by new technologies; demand for using electricity is increasing drastically. Hence energy savings is an important phenomenon to be considered while designing new equipment. In order to overcome this problem the street lighting controls are provided from a central control station using GPRS (2). Energy savings combined with reduced maintenance costs are prime benefits of remote energy tracking and control system. Energy savings through ON/OFF control, reduced maintenance costs by immediate reporting on defects and by monitoring glowing hours are possible. This paper mainly focuses on remote monitoring and control of streetlights. Monitoring panel and energy report are designed using Visual Basic [VB] system design.

2. Methodology

The functional block shown in the figure 1 describes the concept of remote monitoring and control of streetlights.

The system consists of two parts:

1) CMS server side

2) Client side

2.1 CMS Server Side

CMS server illustrated in figure 2 provides the control commands. These commands are processed by GPRS modem and sent to operate the loads [street lights] at client side remotely.

2.2 Client Side

Client system control is shown in figure 3. Power supply unit steps down the 230V supply and rectifies it to power the micro controller. Crystal Oscillator unit provides the clock to the controller. LCD display setup is attached with the control unit to display the current status of the relays and voltage supplied to the streetlights. Communication between client and CMS server is setup through GSM/GPRS mobile communication. Commands given by the remote CMS operator are received and processed by the micro controller at the client side. Controller issues the commands to operate the relay i.e. to turn the lights off when not required and to regulate the voltage supplied to the lights. Energy meter measures the energy consumed and sends the readings to the controller (6). Opto isolator protects the controller from external disturbances. Through GPRS and GSM communication readings are sent to the remote CMS operator. Two port serial communications is setup between the controller and GPRS modem using RS 232 network interface.

2.2.1 Relay unit

The block diagram of voltage regulator unit shown in figure 4 describes the voltage regulation done at the client side (4). Micro controller controls the main relay and tap changing relays according to the command sent by the CMS operator or timer set by the client. The relay connected with the secondary of the transformer is used to select the required voltage. The voltage above the rated value is controlled and maintained.

The secondary of the tap changing transformer with relay unit is shown in figure 5 tapped by 0V, 180V, 220V, and 230Vand 240V output. The Relays R1, R2, R3, R4 and R5 operate corresponding to the command set by the micro controller.

R-Main in the figure 5 indicates that the ON status of the main relay. R1 indicates the on condition of the first tap changer relay and continues the same for R2, R3, R4 etc. If R1 gets turned off; no supply will be connected to the load. Hence load is in OFF condition. In case of relay R1 and R2 gets turned on; 180V of input supply will be connected to the load. Likewise all the relays are operated based on the signal given by the controller.

The table 1 shows that the Glowing hours and relay status according to the time slot set by the programmer. During evening times (18.00hrs to 21.00hrs) maximum supply is connected with the load. During night times (21.00hrs to 6.00hrs) voltage is regulated step by step according to the relay status.

3. Remote Monitoring At The CMS Server Side

Monitoring and control panel is designed using VB on the CMS operator side. The control panel enables the current status of the load, which is being used. The programmer collects the information in terms of base KWH, load KWH, Relay status etc. Data are sent as SMS from the client side using GSM modem (8).

3.1 SMS Server

The System and the GSM module are serially connected via CMS (7). (Shown in figure 1). Oxygen software is used to enable communication between the mobile phone and the system. Oxygen phone manager is the software tool for managing the content and settings of a mobile phone from the personal computer. It can read, edit, store, load and rewrite the phonebook, import data from Microsoft Access.

To initialize Oxygen Mobile ActiveX Control component, serial communication port address and Connection Mode

properties of the system are to be set. Details of clients (area number, location of the street lights, SIM number of the client, glowing hours and current reading) are acquired and stored in a database. This database is created using Microsoft access (shown in figure 9). Using VB the front end is developed and the database is accessed.

The SMS server first checks the area number, location and other details (shown in figure 6). The SMS server first sends the request to the controller at the client side. The energy meter sends the meter reading to SMS server via micro controller. Then the SMS server authenticates the reading by checking with the SIM number from the database. From the readings, total amount of the units consumed, total glowing hours are calculated and updated in the database.

4. Monitoring Panel System Design

Figure 8 shows that the monitoring panel of the remote operator. The list of comment boxes indicated the current status of the controller mode.

MONITORING PANEL: displays current status of relays

SC NO: Indicates serial number of the current panel, which is monitored by the controller.

SIM NO: SIM Card number

ADD SERVICE: New connection establishment

VOLTAGE CONTROL: This panel indicates the current status of relays ON/OFF

KILO WATTS: Base /Actual input power in Kilo Watts (KW)

KWH: Base /Actual input power in KW/hour

LOAD KW: Load power in KW

SET TIME SLOT: Set time period for relay control

ENERGY REPORT: Gives details about the total load power consumed in Kilo watts hour.

GET DAY READING: Gives the information about total load power consumed/ Day

4.1 Energy Report

The amount of energy consumed by the load and percentage of energy saved is calculated using the following equations 1 and 2.

Percentage of energy saving = current reading/ maximum reading *100 ---------- (1)

(or)

Percentage of energy saving = {(current reading / Maximum reading) *(maximum on time/ minimum on time)}*100 ---------- (2)

Where, Current Reading = LOAD KWh, Maximum Reading = Total KWh of previous day

Figure 9 shows the readings for 12 hours before enabling the relay unit at the client side and total power consumed is indicated as BASE KW. Figure 10 shows the readings for 12 hours after enabling the relay unit and total energy consumed is indicated as LOAD KW. From these two readings, the total energy consumed is reduced after enabling the relay unit.

5. RESULTS AND DISSCUSSION

Results are taken based on the assumption, that there are N numbers of Loads like florescent lamps, Sodium lamps and Motors etc connected with the client. Where N=0, 1, 2….

Figure 10 shows the data of energy consumption before enabling the relay unit and after enabling the relay unit. Before enabling the setup, the lighting system consumes 3.8 BASE KW for 12 hours (13.06.2007). After enabling the relays the same system consumes 1.52 KW for 12 hours (14.06.2007). From the two readings percentage of energy savings is calculated using equation 3

Energy Savings in percentage = (Total Units / BASE KWH) * 100 ---------- (3)

= (1.52 / 3.8) * 100

= 40%

The energy report also shows the information of total energy savings in percentage. The percentage of energy saving may vary between 33 and 40 according to the input supply fluctuations. 1000MW of electricity produces 7.5 million tons of CO_2 [at production], this solution contributes to save tons of CO_2 by reducing electricity consumption. The street light failure identification within hours can help in reducing a considerable percentage of average lamp downtime. Can be used to collect data's such as pollution ratio, air composition, humidity, temperature, traffic and noise levels.

References

Akashi.Y, Neches.J. (2004). "Detect ability and acceptability of luminance reduction for load shedding", *Journal of illuminating engineering society* Vol. 33, pp 3-13.

Albert Treytl, Thilo Sauter and Gert Bumiller. (2003). "Real-time energy management over power-line and Internet" *Journal of mobile communication*, Vol. 13 pp.132-140.

Bernard J. Bennington and Charles R. Bartel. (2001). 'Wireless Andrew: "Building a high speed, campus- wide wireless data network", Mobilenetwork and application, Vol.6, pp. 9-22.

L.R. Nair, B.T.Maharaj. (2002). University of Pretoria, Department of Electrical and Theodore S. Rappaport, "Wire Communication-Principle and Practice", Second Edition, pp 236-335.

Minosi A, Martinola A., Mamkan .S, Balzarini .F, Kostadinov A.N., and Prevostini M. (2003). 'Intelligent, Low power and Low-cost. Measurement System for Energy Consumption", IEEE transaction in mobile network ,Vol.20, pp 27-29.

Sivakumar.M and C.Maheswari. (2007). "Embeddded System Based Automatic Energy Saver for Street Lights", Conference proceedings, Deccan College of Engineering, Hyderabad, pp 8-9.

Yao-Jung Wen, Jessica Granderson,Alice M. Agogino, (2006). "Towards embedded wireless – networked Intelligent day lighting systems for commercial buildings", IEEE, pp 326-331.

Zhixiong LIU, Guiming. (2005). "Embedded adaptive live video transmission system over GSM/CDMA Network", IEEE ICESS, pp 122-126.

Zhuli, Zhang Jingsen, Zerg Ming. (2005). "An Embedd system architecture for caustic signal capturing and orientation", Second international conference on embedded system, pp 12-19.

Table 1. Glowing hours Vs Relay status of street lights

Time slot (hours)	Voltage range (volts)	Relay status
18.00-21.00	221-240	R1 and R5
	>240	R1 and R5
21.00-23.00	201-220	R1 and R4
	221-240	R1 and R5
	>240	R1 and R5
23.00-06.00	181-200	R1 and R3
	201-220	R1 and R4
	221-240	R1 and R5
	>240	R1 and R5

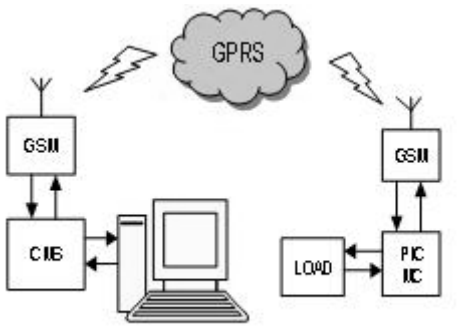

Figure 1. Functional block diagram of Remote Energy Monitoring System

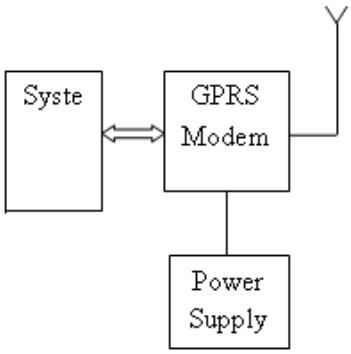

Figure 2. Functional Block of CMS Server

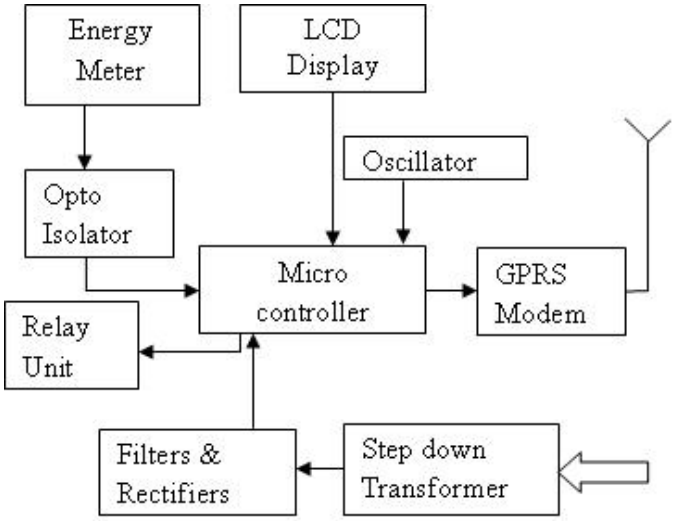

Figure 3. Functional Block of Client

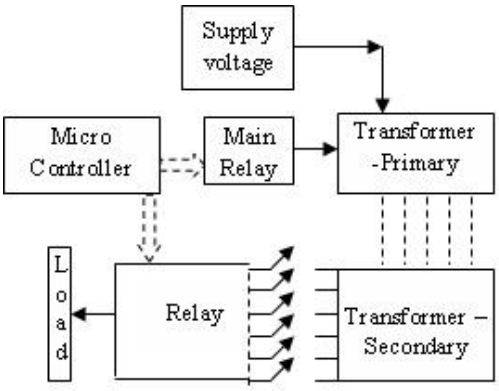

Figure 4. General block of Voltage Regulator Unit

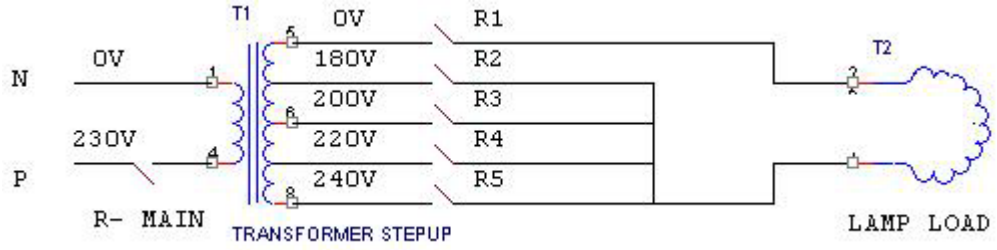

Figure 5. Tap Changing Transformer

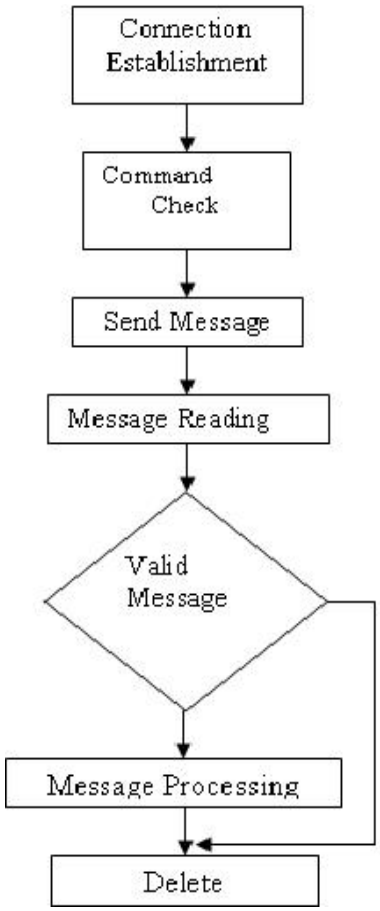

Figure 6. Flowchart for the SMS Server functio

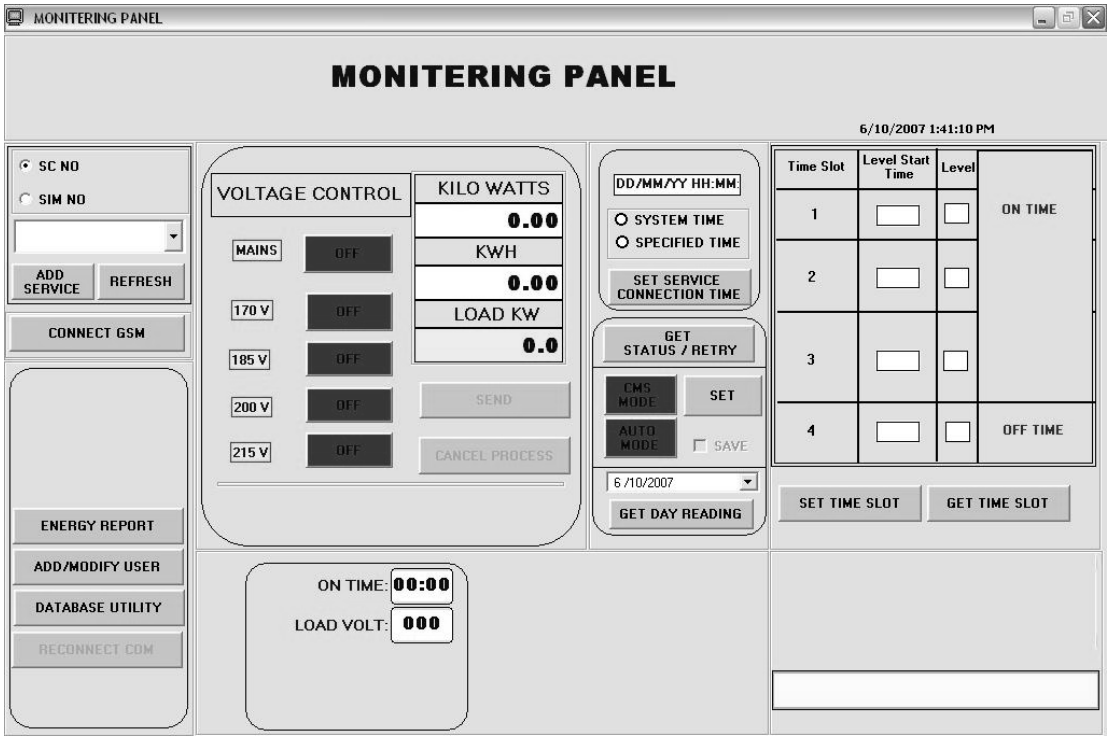

Figure 7. Monitoring Panel

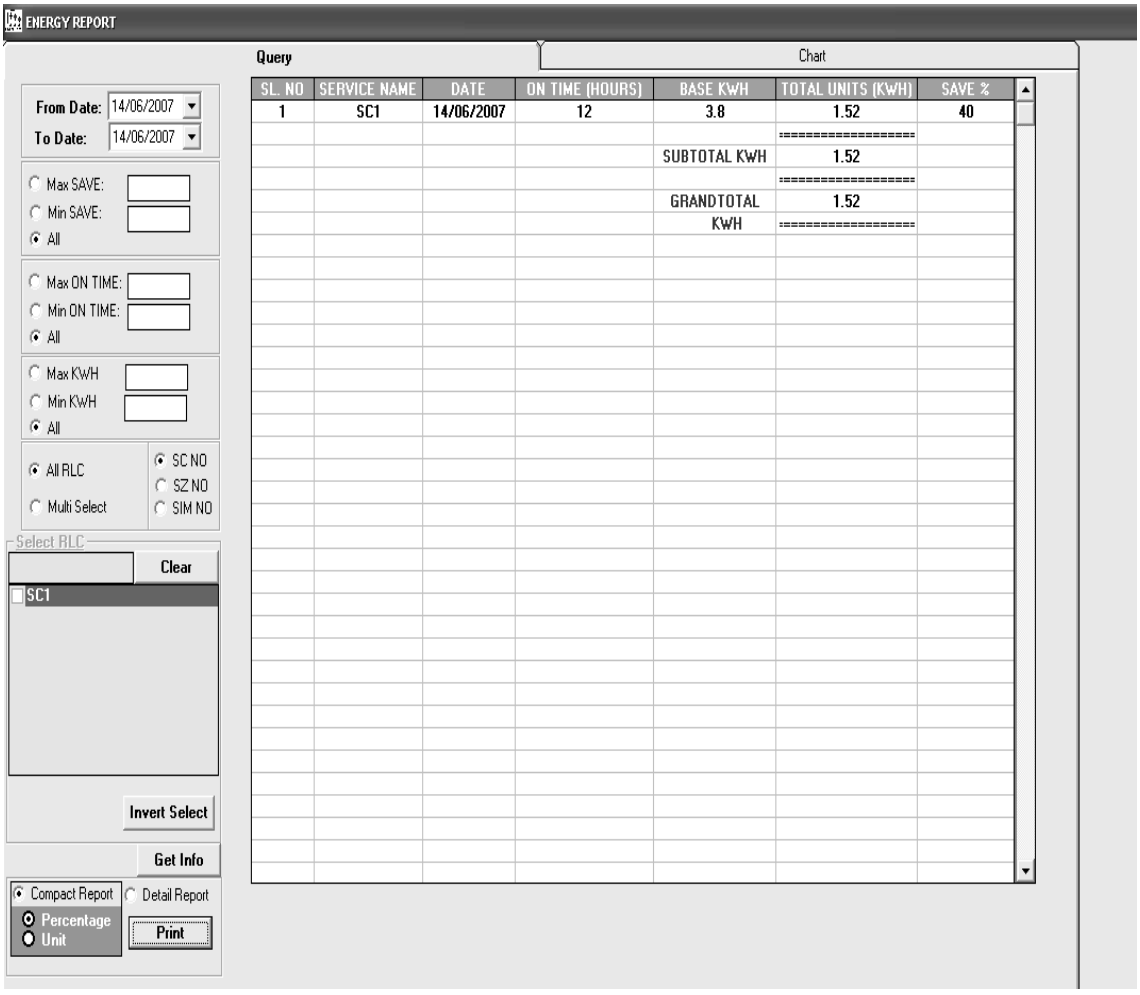

Figure 8. Energy report **(**displays energy savings for 12 hours)

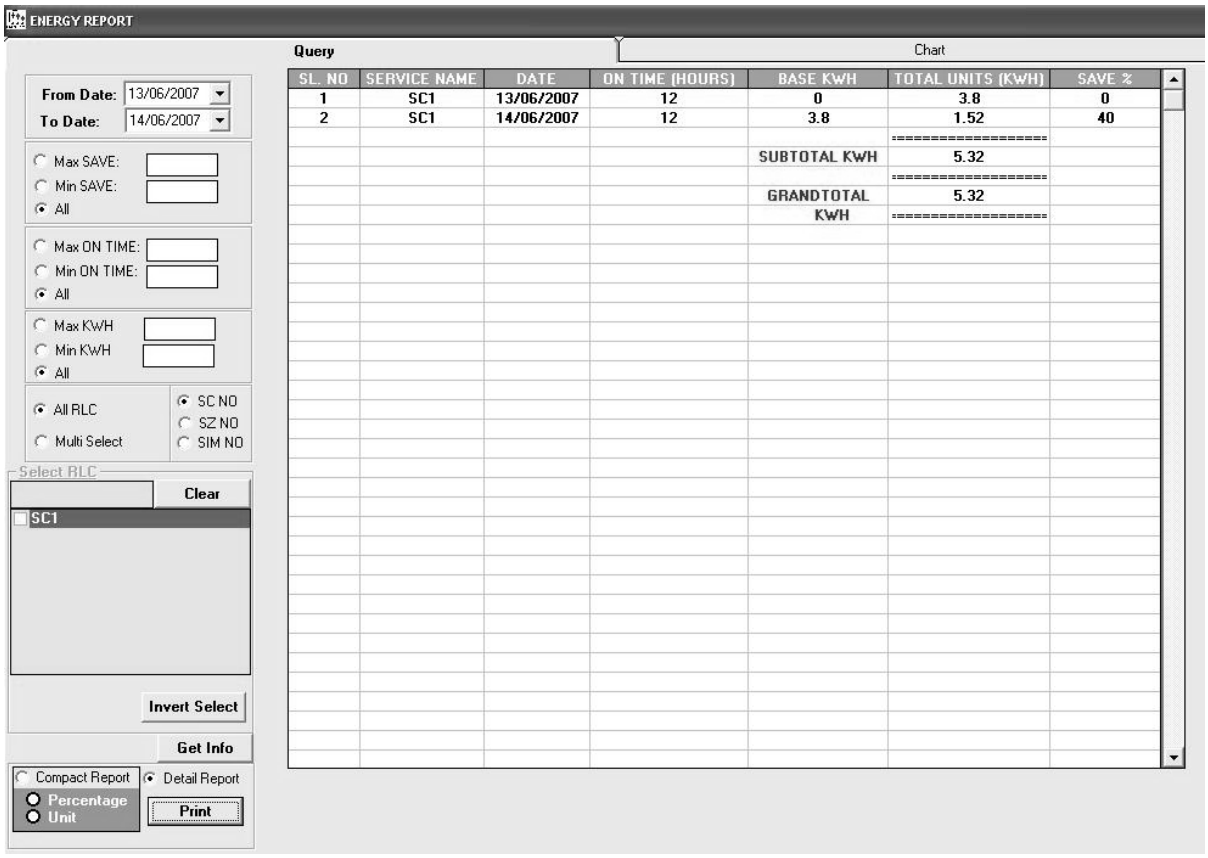

Figure 9. Energy report after enabling the relay unit for 12 hours

Modern Applied Science

www.ccsenet.org/journal.html

Vol. 3, No. 6

June 2009

Study on Economic, Rapid and Environmental Power Dispatch Based on Fuzzy Multi-objective Optimization

Lubing Xie, Songling Wang & Zhiquan Wu

School of Energy and Power Engineering, North China Electric Power University

No 619, Yong Hua North Street, Baoding, China

Tel: 86-312-752-2376 E-mail: rzpower2008@yahoo.com.cn

China National Water Resources & Electric Power Materials & Equipment Co, Ltd

Electric Researching Building, No 1, Di Zang An Alley, Fu Xing Men Street, Beijing, China

Tel: 86-10-5196-7603 E-mail: wuzhiquan@cweme.com

Abstract

Environmental awareness and the recent environmental protecting policies have extremely spurred many electric utilities to regulate their practices to account for the emission impacts. One way to accomplish this is by reformulating the traditional Economic Load Dispatch (ELD) module merely with a view to minimal coal consumption of fossil fired units. This paper presents a triple-objective ELD model which consists of the minimal coal consumption, the best time for the unit commitment response and the economic emission index. The rapid/economic/environmental dispatch problem is a multi-objective non-linear optimization problem with constraints. The fuzzy theory is adopted to convert the multi-objective problem into the single-objective problem. The problem is been tackled through dynamic programming algorithm and the approach is tested on a four-unit system to illustrate the analysis process in present analysis. Results simulated through MATLAB show that the approach has great potential in handling multi-objective optimization problem.

Keywords: Economic dispatch, Fuzzy method, Dynamic programming

1. Introduction

Recent years, many researchers stress on the economic statistics of the load optimal dispatching. The mathematical decision makings based on the economic index ensures the economical efficiency whereas ignores the rapid response on the varying loads. The committed generators in a power network operating at absolute minimum cost can no longer be the only criterion for dispatching electric power due to the increasing concern about the environmental protection. The generation of electricity from fossil fuel releases several contaminants, such as sulfur dioxide, nitrogen oxide and carbon dioxide into the atmosphere. Nowadays, environment constraints have topped the list of utility management concerns (Xuebin Li, 2009, pp.789-795).

The approach of minimizing the fuel cost and rapid response for the varying loads has been discussed in some dissertations. The disadvantage about this approach is that the introduced method of weighted makes it possible that the complicate computation and multiple subjective factors which causes the ambiguous optimum solutions. Economic/environmental/rapid dispatch is a multi-objective problem with conflicting objectives because pollution minimization is conflicting with minimum cost of generation. Various techniques have been proposed to solve this problem. Nanda et al (Nanda, 1988, pp.26-32).was one of the first approaches to solve the Economic/environmental dispatch problem considering multi-objective optimization using linear and non-linear goal programming techniques . An ε -constrained technique was used by Yokoyama et al (R.Yokoyama, 1988, pp.317-324).

One approach to solve the triple-objective (rapid response, economic, environmental) is presented in this paper. The mathematical optimal model is constructed through fuzzy multi-objective theory which leads to a feasible and objective counter measure. The separate goal concords with the integrate ones. The idea behind the fuzzy optimal model is to find the junction of the satisfaction with the consideration of every individual goal. Finally, the problem is solved with conventional optimal methods and the advantage is shown in this paper.

2. Problem description

Multi-objective programming is used to solve the minimax problem for the multiple numerical objective functions simultaneously with the condition of the engaged constraints. In many realistic problems, several goals must be simultaneously satisfied to obtain an optimal solution .However, sometimes these multiple objectives, which must be

simultaneously satisfied, conflict. The multiple-objective optimization method is the common approach to solve this type of problem. The conventional multi-objective problem (MOP) is formulated as follows:

$$\left.\begin{array}{c} opt\ \mathrm{f(x)}=[f_1(x)=z_1, f(x)=z_2 \ldots . f_p(x)=z_p]^T \\ subject\ to\ x \in \Omega \\ s.t\quad \mathrm{g}_i(x) \geq 0 \\ \mathrm{h}_j(x)=0 \end{array}\right\} \tag{1}$$

Where solution x is a vector of discrete decision variables, Ω is the finite set of feasible solutions. The image of a solution x∈Ω is the point z=f(x) in the objective space. Where $g_i(x)$ and $h_j(x)$ is the nonlinear and linear constraints. The solutions that are non-dominated within the entire search space are denoted as Pareto-optimal solutions and constitute the Pareto-optimal set or Pareto-optimal frontier.

It is difficult to handle with that the discrete goal is conflict with each other. Accordingly, the multi-objective problem sometimes transformed into single-objective problem. The method of weighted is widely used during the reforming process which depends on the selection of the subjective factors and the settlement of the dimensionless variables besides. The fuzzy theory is introduced in this paper so as to figure out this type of knotty challenges.

2.1 Fuzzy mathematical model

$$\left.\begin{array}{c} x=[x_1, x_2, \ldots x_n]^T \in \Omega \\ \min\ f(x,\omega) \\ s.t\quad g_u(x,\omega) \subset G_u \qquad u=1,2,\ldots,m \\ \omega=[\omega_1, \omega_2, \ldots \omega_k]^T \in \Omega \end{array}\right\} \tag{2}$$

Where x is the designed variable vector, ω is the fuzzy parameter vector, Ω is the fuzzy domain. Every single objective function is converted to a forged objective function which is represented by the membership function denoted by ufi(x)The membership function is one to one correspondence with the goal function, Where ufi(x)∈[0,1] represents the satisfying degree with the individual goal. λ is selected as the minimum value which is served as the auxiliary variable. If the mean value is found, it can be defined as the total satisfying degree among the forged membership functions.

2.2 MOP fulfilling Steps

Hence the basic ideology and detail resolving steps for the MOP is shown as follows:

(1) Resolving the constraint maximum and minimum value (M and m)of the sub-objective function.

(2) Fuzzy processing every sub-objective function

$$u_{f_i}(x)=\left(\frac{M-f_i(x)}{M-m}\right)^q \tag{3}$$

(3) Construct the fuzzy decision-making

$$D(X)=\bigcap_{i=1}^{n} f(x) \tag{4}$$

$$u_D(X)=\min\{u_{f_i}(x),\ldots,u_{f_n}(x)\} \tag{5}$$

(4) Resolving the optimum solution and get the maximum value for the membership function.

$$u_D(X^*)=\max\min\left[u_{f_i}(x),\ldots u_{f_n}(x)\right] \tag{6}$$

(5) So by making use of the mathematical manipulation, the MOP problem is transferred into the SOP(single objective problem), it can be mathematically stated as follows:

$$\left.\begin{array}{c} \max\ \lambda \\ s.t.\ u_{f_i}(x) \geq \lambda,\ i=1,2,\ldots n \\ 0 \leq \lambda \leq 1 \\ g_i(x) \leq 0,\ j=1,2,\ldots n \\ X=\left[x_1, x_2, \ldots x_n, \lambda\right]^T \end{array}\right\} \tag{7}$$

3. Mathematical model for the MOP

3.1 Economic dispatch

The proposed approach can accommodate non-quadratic (high order) fuel cost and multiple emission of differentiable nature objective function. The classical economic dispatch problem of finding the optimal combination of power generation which minimizes the total fuel cost while satisfying the total demand, it can be shown as follows(C.Palanichamy, 2008, pp.1129-1137):

$$F_T = \sum_{i=1}^{n} (a_i p_{Gi}^2 + b_i p_{Gi} + c_i) \quad \$/h \tag{8}$$

Where: F_T total fuel cost ($/h); P_{Gi}: generation of unit i (MW),a_i, b_i, c_i: fuel cost coefficient of unit i; and n: number of generation units. The economic dispatch problem is optimized subject to:

(i) Power balance constraint: the total power generated must supply total load demand and transmission loss.

$$\sum_{i=1}^{n} p_{Gi} = P_D + P_L \quad MW \tag{9}$$

Where P_D: total load demand (MW) and P_L: total transmission loss (MW)

(ii) Unit capacity constraint: the power generated P_{Gi} by each generator is constrained between its minimum and maximum limits, i.e

$$P_{Gi\ \min} \le p_{Gi} \le p_{Gi\ \max}$$

Where P_{Gimin}: minimum generation limit, and P_{Gimax}: maximum generation limit

3.2 Emission dispatch

The emission dispatch problem is defined as the following optimization problem, subject to the power balance and unit capacity constraints. Sulfur dioxide and nitrogen oxide emissions have taken into account, but carbon dioxide is ignored in this paper.

$$E_T = \sum_{i=1}^{n} (d_i p_{Gi}^2 + e_i p_{Gi} + f_i) \ \text{kg/h} \tag{10}$$

Where E_T: total emission (kg/h); P_{Gi}: generation of unit i(MW); di,ei,fi: emission coefficient of unit i: and n number of generating units.

3.3 Time dispatch

Considering the quick variable-load for the unit generation, the concept of the temporal summation of the quick variable-load for multiple units is introduced in this paper. If the load increment of the unit generation is given, the load should be changed as fast as possible so as to accomplish the mission of peak regulation, subject to the rate of variable-load for unit generation constraints, can be mathematically stated as follows (Peiyan Feng, 2007, pp.11-15):

$$Q_T = \min \Delta T = \min \sum_{i=1}^{n} (\Delta p_i / V_i) \quad 0 \le V_i \le V_{i\ \max} \tag{11}$$

3.4 Fuzzy processing of the sub-objective function

It is troublesome to determine the membership function of the fuzzy parameter during the working process. Thus, dualistic contrast composition and fuzzy statistical method is adopted generally (Panos Y. Papalambros, 2000, pp.20-25). If the data is efficiency, a approximate membership function which represent the transformation process from the may be used. Considering the Energy Saving & Emission Reduction, the lower semi-trapezoid curve represents the membership function. While the upper semi-trapezoid curve represents the membership function because the variable-load time is in inverse proportion to the load rate. The membership function is shown as follows separately.

$$u_{f1} = \begin{cases} 1 & F \le F_{\min} \\ \dfrac{F_{\max} - F}{F_{\max} - F_{\min}} & F_{\min} < F < F_{\max} \\ 0 & F \ge F_{\max} \end{cases} \tag{12}$$

$$u_{f2} = \begin{cases} 1 & E \le E_{\min} \\ \dfrac{E_{\max} - E}{E_{\max} - E_{\min}} & E_{\min} < E < E_{\max} \\ 0 & E \ge E_{\max} \end{cases} \tag{13}$$

$$u_{f3}=\begin{cases}0 & V\le V_{\min}\\ \dfrac{V-V_{\max}}{V_{\max}-V_{\min}} & V_{\min}<V<V_{\max}\\ 1 & V>V_{\max}\end{cases} \tag{14}$$

3.5 Model of fuzzy multi-objective problem

According the fuzzy theory, the corresponding solution of the maximum λ value is the optimal solution for the MOP.

$$\lambda=\min\left\{u_{f1}(x),u_{f2}(x),u_{f3}(x)\right\} \tag{15}$$

$$\max\lambda=\max\min\left\{u_{f1}(x),u_{f2}(x),u_{f3}(x)\right\} \tag{16}$$

The model can be mathematically stated as follows:

$$\left.\begin{array}{c}\max\lambda\\ \lambda\le u_{f1}(x)\\ \lambda\le u_{f2}(x)\\ \lambda\le u_{f3}(x)\\ s.t.\ \ p=\sum_{i=1}^{n}p_i\\ p_{\min}\le p_i\le p_{\max}\\ 0\le V_i\le V_{i\max}\\ 0\le\lambda\le 1\end{array}\right\} \tag{17}$$

4. Introduction of the dynamic programming algorithm

Dynamic programming algorithm used in the optimal solution of a certain nature (Liang tong, Li, 2003, pp.9-11). In such matters, there may be many feasible solutions. Each solution corresponds to a point; we hope to find a solution with the optimal value. Dynamic programming algorithm with sub-rule method is similar to the basic idea is to solve the problem to be broken down into several sub-questions, the first sub-problem solving, and then from the sub-problem of the solution in the solution of the original problem. With different sub-rule method is suitable to use dynamic programming to solve the problem, the decomposition of sub-questions have been often mutually independent. If sub-rule method is used to solve such problem, the problem is decomposed to be a subset of number, some sub-questions were double-counting of a lot of times. If we can save a sub-problem resolved the answer, and again when necessary to identify the answer has been obtained, so many double-counting could have been avoided. We can use a table to record all of the sub-solution answers to these questions. Regardless of the sub-problem used, as long as it was calculated that the results will populate the table. This is the basic idea of dynamic programming method. Specific dynamic programming algorithm shows a diversity of practice, but they have the same format to fill in a form

5. Case study

The four-generating unit system is used in this paper to demonstrate the dynamic programming approach. The fuel cost and emission coefficient of four generating is shown in table 1.

Simulation results:

The initial load of the four-units is 200MW, 220MW, 380MW and 360MW respectively. According to the different type of compound modes, 1 unit, 2 units, 3 units and 4 units complete the mission peak separately from the four units. Due to the space limitation, only two types of compound modes is discussed in this paper. The analytical results can be illustrated through bar graphics as Figurer1-6.

6. Conclusion

(1) The fuzzy decision making method is as easy as linear weighted method on constructing a single objective function. Hence, the programming approach of single objective problem may be naturally adopted on the MOP.

(2) The multi-objective design method is simple and practical. It is a recommend way to resolve the MOP which the coal consumption, emission and variable-load time is mutually conflict. Therefore, a utopia solution is easy to obtain amongst the tradeoff ones.

(3) According to the analysis of simulation result, the coal consumption of MOP is higher than the SOP. Whereas the variable-load time gets a sharp decrease. Meanwhile, exhausted pollutants get a gratifying decrease. Generally speaking,

the fuzzy multi-objective method is more satisfactory the single-objective method accounting for the coal consumption.

References

C.Palanichamy & N.Sundar Babu. (2008). Analytical solution for combined and emissions dispatch. *Journal of Electric Power System Research*, 78, 1129-1137.

J.Nanda, D. P. Khotari, & K.S. Lingamurthy. (1988). Economic–emission load dispatch through goal programming techniques. *Journal of IEEE Trans Energy Convers*, 3(1), 26-32.

Liangtong, Li, Shaorong, Zhu, Jianbing, Qian & Changjiang, Chen. (2003). Optimal dispatching based on dynamic programming. *Journal of Yunnan Electric Power*. Vol.31, No.2, 9-11.

Panos Y. Papalambros, & D.J.Wilde. (2000). *Principles of optimal design*. (2nd ed.). Cambrige University Press, (modeling and computation).

Peiyan, Feng & Yanqiao, Chen. (2007). Study on load optimal dispatching based on fuzzy multi-objective optimization. *Journal of Electric Power Science and Engineering*, Vol.23, No.4, (11-15).

R.Yokoyama,S.H., & Bae,T.Morita.(1988). Multi-objective optimal generation dispatch based on probability security criteria. *Journal of IEEE Trans Power Syst*, 3(1), 317-324.

Xuebin, Li. (2009). Study of multi-objective optimization and multi-attribute decision-making for economic and environmental power dispatch. *Journal of Electric Power System Research*, 789-795.

Table 1. Fuel cost coefficients and emission coefficient (SO_2,NO_X)

$Generator_i$	a_i	b_i	c_i	d_i	e_i	f_i	p_{min}	p_{max}	$\mathbf{v_i}$
G_1	0.003689	-2.26605	655.3730	0.00607	-2.28070	539.9171	180	350	5
G_2	0.00048	-0.40192	397.0223	-0.0508	28.59314	-3107.297	180	300	8
G_3	-0.00008	0.01882	338.7645	0.0058	-5.08329	1585.924	300	625	10
$\mathbf{G_4}$	0.000126	-0.131228	357.1300	-0.0121	14.89956	-3363.239	305	600	15

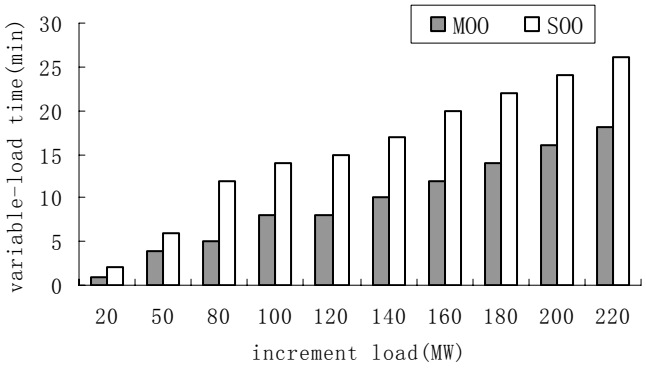

Figure 1. Variable-load Time Contrast Simulation Results of One from Four Modes

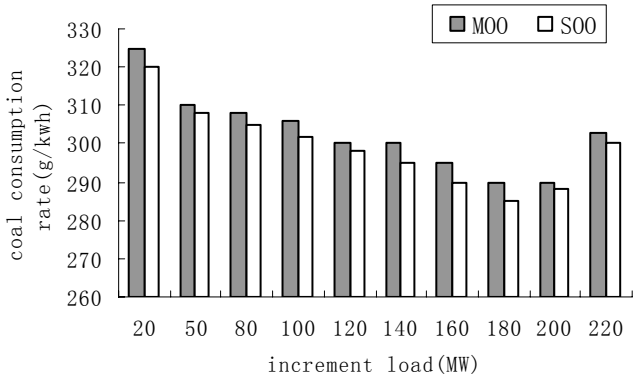

Figure 2. Coal Consumption Rate Contrast Simulation Results of One from Four Modes

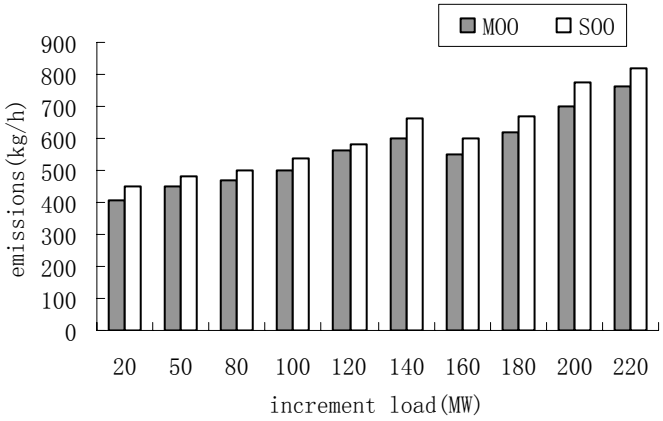

Figure 3. Emission Contrast Simulation Results of One from Four Modes

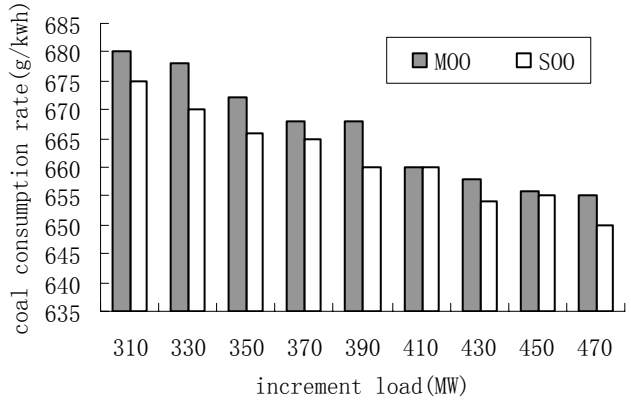

Figure 4. Coal Consumption Rate Contrast Simulation Results of Two from Four Modes

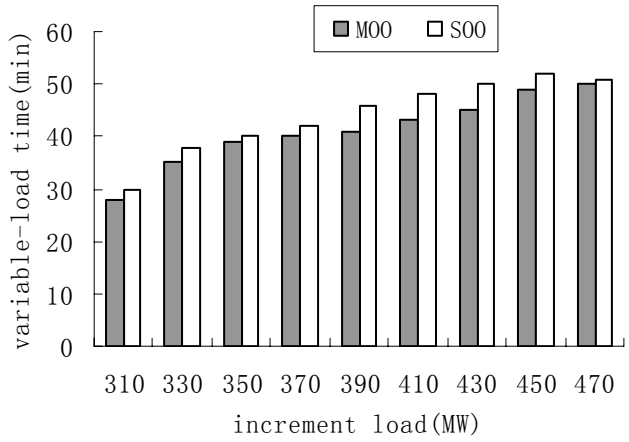

Figure 5. Variable-load Time Contrast Simulation Results of Two from Four Modes

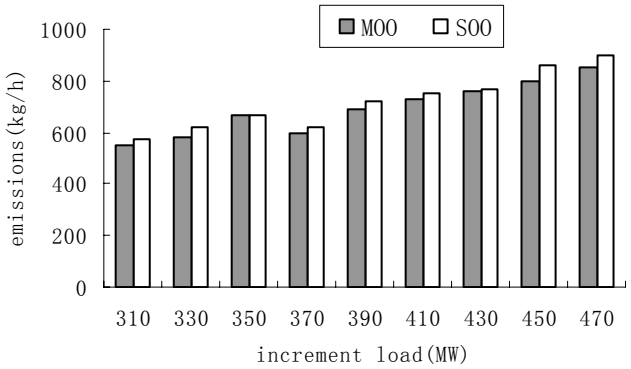

Figure 6. Emission Contrast Simulation Results of Two from Four Modes

Modern Applied Science

www.ccsenet.org/journal.html

Vol. 3, No. 6

June 2009

The Effect of Radial Swirl Generator on Reducing Emissions from Bio-Fuel Burner System

Mohamad Shaiful Ashrul Ishak

School of Manufacturing Engineering, Universiti Malaysia Perlis

PO Box 77, Pejabat Pos Besar, 01000 Kangar, Perlis, Malaysia

Tel: 60-4-985-1778 E-mail: mshaiful@unimap.edu.my

Mohammad Nazri Mohd Jaafar (Corresponding author)

Department of Aeronautical Engineering, Faculty of Mechanical Engineering

Universiti Teknologi Malaysia, 81310 Skudai, Johor Malaysia

Tel: 60-7-553-4851 E-mail: nazri@fkm.utm.my

Yehia A. Eldrainy

Department of Aeronautical Engineering, Faculty of Mechanical Engineering

Universiti Teknologi Malaysia, 81310 Skudai, Johor Malaysia

Tel: 60-7-553-5843 E-mail: yeldrainy@yahoo.com

Abstract

A liquid bio-fuel burner system with various radial air swirlers attached to combustion chamber of 280 mm inside diameter and 1000 mm length has been investigated. All tests were conducted using crude palm oil as fuel. A radial flow air swirler with curved blades having 50 mm outlet diameter was inserted at the inlet plane of the combustor to produce swirling flow. Fuel was injected at the back plate of the swirler outlet using central fuel injector with single fuel nozzle pointing axially outwards. The swirler vane angles and equivalence ratios were varied. Tests were carried out using four different air swirlers having 45°, 50°, 60°and 70° vane angles. NOx emissions reduction of about 12 percent was obtained at swirl number of 1.911 as compared to 0.780 at the same equivalence ratio of 0.83. In addition, emission of carbon monoxide decreased as the swirl number increased. The results shows that a proper design of air swirler has a great effect on mixing process and hence the combustion and emission.

Keywords: Swirler, Pressure drop, Swirl number, Combustion, NOx emission

1. Introduction

Burners are usually used in industrial applications such as starters for boilers, district heating and cooling and also for domestic central heating system. However, bio-fuel conventional burners, operating at or above stoichiometric air/fuel ratios, produce high flame temperatures that resulted in the production of nitrogen oxides, which is then emitted to the atmosphere (Craig, 1975). However, lowering NOx emission by reducing flame temperature will lead to reduced flame stability or increase in Carbon Monoxide (CO) emission (Khezzar, 1998). Therefore, a method must be found that will be able to reduce the time for peak temperature and will reduce the formation of NOx.

Basically there are two techniques of controlling NOx in burner applications: those that prevent the formation of nitric oxide (NO) and those that destroy NO from the products of combustion. The methods that prevent the formation of NO involved modifications to the conventional burner designs or operating condition. In this research, the burner will be designed to incorporate swirling flow to enhance turbulence and hence helps in mixing of fuel and air prior to ignition. Swirling flow induces a highly turbulent recirculation zone, which stabilises the flame resulting in better mixing and combustion (Gupta *et al*., 1998). It has been suggested that the large torroidal recirculation zone plays a major role in the flame stabilisation process by acting as a store for heat and chemically active species and, since it constitutes a well-mixed region, it serves to transport heat and mass to the fresh combustible mixture of air and fuel (Judd *et al*., 2000).

Beer and Chigier promoted the methods of inducing rotation in a stream of fluid and they can be divided into three principal categories:

- Tangential entry of the fluid stream, or of a part of it, into a cylindrical duct.
- The used of a guide vane in axial tube flow.
- Rotational of mechanical devices that impart swirling motion to the fluid passing through them. This includes rotating vanes or grids and rotating tubes.

They concluded that method (a) and (b) are generally used in practice but method (c) is sometimes applied for experimental investigation of swirling flow. Most conventional liquid fuel burners employ the axial-flow type swirler. These swirl vanes are usually flat for easy manufacturing process, but curved blade may give better performance in aerodynamic properties (Iannetti *et al*., 2001).

Swirling flow is a main flow produced by air swirled in gas turbine engine. Such flow is the combination of swirling and vortex breakdown. Swirling flow is widely used to stabilize the flame in combustion chamber. Its aerodynamic characteristics obtained through the merging of the swirl movement and free vortex phenomenon that collide in jet and turbulent flow. This swirl turbulent system could be divided into three groups and they are jet swirl turbulent with low swirl, high jet swirl with internal recirculation and jet turbulence in circulation zone. Each and every case exists due to the difference in density between jet flowing into the combustion chamber and jet flowing out into the atmosphere from the combustion chamber.

When air is tangentially introduced into the combustion chamber, it is forced to change its path, which contributes to the formation of swirling flow. The balance in force could be demonstrated by the movement of static pressure in the combustion chamber and can be calculated by measuring the distribution of the tangential velocity. Low pressure in the core center of the swirling flow is still retrieving the jet flow in the combustion chamber and thus, produces the not-so-good slope of axial pressure. Meanwhile at the optimum swirl angle, the swirl finds its own direction and as a result, swirl vortex is formed.

The recirculation region in free swirl flow is shown in Figure 1. Due to assumption that the flow is axially symmetrical, thus only half of the flow characteristics are discussed. The recirculation region is in the OACB curve. The point B is known as stagnation point. The flow outside of the OACB curve is the main flow, which drives the recirculation along the AB solid curve. The ultimate shear stress could happen at points near to point A, along the boundary of recirculation. The condition of zero axial velocity is represented by hidden curve AB. Every velocity component decreases in the direction of the tip. After the stagnation point, the reverse axial velocity will disappear far into tip; the peak of velocity profile will change towards the middle line as an effect of swirling decrease.

As the level of applied swirl increase, the velocity of the flow along the centerline decreases, until a level of swirl is reached at which the flow becomes stationary. As the swirl is increased further, a small bubble of internal recirculating fluid is formed. This, the vortex breakdown phenomenon, heralds the formation of large-scale recirculation zone that helps in stabilizing the flame. It has been suggested (Beer and Chigier, 1972) that the large torroidal recirculation zone plays a major role in the flame stabilization process by acting as a store for heat and chemically active species and, since it constitutes a well-mixed region; it serves to transport heat and mass to the fresh combustible mixture of air and fuel.

In high velocity combustion system, the fuel and air mixing requires high turbulence levels and these result from the combustor pressure loss (Escott, 1993). Whether this pressure loss is generated by a jet flow system or swirl system, the air inlet aerodynamics generate shear layer which create the turbulence. In a conventional swirl burner the turbulence energy is mostly generated close to the central toroidal recirculation zone and is not fully utilised in an efficient way. In order to achieve enhanced flame stabilisation and better control of mixing process, a swirler shroud consisting of an orifice plate at the outlet of swirler throat was introduced. The aim of this was to create the main pressure loss at the outlet phase rather than in the vane passage so that the swirler outlet shear layer turbulence was maximised to assist with fuel and air mixing. Orifice plate insertion also helps to prevent fuel from entraining into the corner recirculation zone that will create local rich zone thus generates lower NOx emission by eliminating locally rich region (Kim, 1995). Locally rich region tends to generate locally high NOx emission that contributes to overall high NOx emission. Smaller orifice plate's outlet does increase the velocity of the air and fuel at the swirler shroud thus reduce the risk of flashback. However, this velocity should not be to high as lift off could occur and cause blow off of combustion. The increase in velocity also would increase the Reynolds number, which increases the strength of turbulence effect and thus reduces the combustions residence time. Other than that, from the aerodynamic factor, air and fuel mixing rate increases as the pressure drop in the swirler outlet increases.

Syred and Beer showed that for tangential entry including radial vanes, the swirling flow may produce high efficiency for isothermal performance and low loss of pressure coefficient compared to that when using axial straight and profiled vane.

Al-Kabie, on the other hand, found a significant improvement in performance as well as NOx emissions when using radial swirler compared to the axial swirler due to the immediate contact of fuel with turbulent by swirled air as it leaves the fuel nozzle. Aerodynamic curved vanes allow the incoming axial flow force to turn gradually. This inhibits flow separation on the suction side of the vane. This mean that more complete turning and higher swirl and radial velocity component can be generated at the swirler mouth, with the added advantage of lower pressure loss.

Al-Kabie also investigated the discharge coefficient (CD) for the various radial swirlers. He showed that, by using the radial swirler, the discharge coefficients were low, approximately 0.6 compared with the zero angle blade, approximately 0.9. Poor CD is due to the vane angle and not just the 90º inlet and outlet blades. This led to a major consideration of the flow field inside the swirler vane passage as low CD implied that flow separation occurred in the passage in spite of the curved vane.

1.1 Swirl number

The swirl number is usually defined as the fluxes of angular and linear momentum (Beer and Chigier, 1972) and it is used for characterising the intensity of swirl in enclose and fully separated flows.

The parameter can be given as (Beer and Chigier, 1972)

$$S' = \frac{G_\phi}{G_\chi . r_o} \tag{1}$$

where G_ϕ is the axial flux of angular momentum:

$$G_\phi = 2\pi \int_0^\infty \rho U_x U_\theta r^2 dr \tag{2}$$

and G_x is the axial flux of momentum (axial thrust):

$$G_\chi = 2\pi \int_0^\infty \rho U_x^2 r dr + 2\pi \int_0^\infty p r dr \tag{3}$$

In the above, r_o is the outer radius of the swirler and U_x and U_θ are the axial and tangential component of velocity at radius r.

Since the pressure term in Equation (3) is difficult to calculate due to the fact that pressure varies with position in the swirling jet, the above definition for swirl number can be simplified by omitting this pressure term. Swirl number can be redefined as:

$$S = \frac{G_\theta}{G_x' r_o} \tag{4}$$

where

$$G_x' = 2\pi \int_0^\infty \rho U_x r dr \tag{5}$$

The swirl number should, if possible, be determined from measured values of velocity and static pressure profiles. However, this is frequently not possible due to the lack of detailed experimental results. Therefore, it has been shown (Beer and Chigier, 1972) that the swirl number may be satisfactorily calculated from geometry of most swirl generator.

2. Experimental set up

The drawing for radial air swirler is shown in Figure 2. Table 1 shows the various dimensions of radial air swirler used in the present work. The air swirlers are made from mild steel. They were manufactured in various angles to investigate the effect of pressure loss and combustion performance due to swirl number on the overall performance of the air swirler.

The general set-up for liquid bio-fuel burner tests is shown in Figure 3. The rig was placed horizontally on a movable trolley. The air is introduced into the liquid bio-fuel burner and flows axially before entering radial through the air swirler of 8 blades where the amount of air entering the combustor is controlled by the flame swirler minimum area. The rig is equipped with a central fuel injector. The inside diameter of the combustor is 280 mm and the length is 1000 mm. The combustor was cooled by convection from the ambient air. Industrial ring blower was used for air supply at below 0.5% pressure loss.

3. Results and discussions

3.1 Isothermal performance

In order to achieve better mixing between fuel and air in liquid bio-fuel burner, turbulence flow must be generated to promote mixing. Turbulence energy is created from the pressure energy dissipated downstream of the flame stabilizer. In the radial swirler with orifice insertion, turbulence can be generated by increasing the aerodynamic blockage or by increasing the pressure drop across the swirler.

The discharge coefficient for radial swirler were obtained by passing a metered air flow through the radial swirler and flame tube while monitoring the static pressure loss upstream of the radial swirler relative to the atmospheric pressure. The results for isothermal performance were plotted as a function of Reynolds number and presented in Figure 4.

From Figure 3, it can be seen generally that all discharge coefficients were approximately constant with variation in Reynolds number. Thus the value of discharge coefficient may be concluded to be independent of Reynolds number. In the case for S = 1.911or 70º vane angle swirler gave the highest CD around 0.68. The CD values were decreased with the decreasing in swirl number (S), with the lowest S = 0.780 having the CD value of around 0.58. This may be attributed to the fact that the excessive swirl was generated by the restriction on swirler exit width.

3.2 Combustion Performance

Figures 5 and 6 show the effect of increasing the swirl number on exhaust emissions from burner system. Tests on exhaust emission were carried out using four swirler vane angles of 45°, 50°, 60° and 70°.

Figure 5 shows vast reduction in oxides of nitrogen (NOx) emissions when the vane angle was increased from 45° to 70°. This was apparent for the whole range of operating equivalence ratios. Emissions level of below 35 ppm was obtained for all range of operating equivalent ratios. For swirl number of 1.911, NOx emissions reduction of about 12 percent was obtained at equivalence ratio of 0.83 compared to the swirl number of 0.780 at the same equivalence ratio. This proved that swirl does helps in mixing the bio-fuel and air prior to ignition and hence reduced NOx emissions. This situation occurs at certain swirler vane angle. However this was achieved at the expanse of increased in other emissions and reduction in combustion stability.

Figure 6 shows carbon monoxide emissions versus equivalence ratio for all swirl number. There was a 13 percent, 22 percent and 31 percent reduction in carbon monoxide (CO) emission for swirl number 0.978, 1.427 and 1.911 compared to swirl number of 0.780 at the equivalence ratio of 0.833. The concentration of carbon monoxide emission increases with increase in equivalence ratio. This was anticipated due to the fact that any measure of decreasing NOx will tend to increase CO since both emissions were on the different side of the balance (Al-Kabie, 1989). Nonetheless, the increase was quite high, which indicates that there is some fuel escaped unburned, which was the product of incomplete combustion.

4. Conclusion

An experimental investigation of swirl number effect on the NO_x and CO emissions of palm oil combustion has been conducted. Four radial swirlers with vane angles of 45°, 50°, 60°and 70° which are corresponding to 0.780, 0.978, 1.427 and 1.911 respectively was used in this investigation.

NOx emissions reduction of about 12 percent was obtained at equivalent ratio of 0.83 at swirl number of 1.911 as compared to 0.780 at the same equivalence ratio. Other emissions such as carbon monoxide decreased when using higher swirl number compared to that of the lower swirl number. This shows that the proper design of the swirler enhances the mixing process of the air and bio-fuel prior to ignition.

It can be also concluded that NOx emissions of less than 35 ppm were achievable over the whole range of equivalence ratios for all swirlers.

Acknowledgement

The authors would like to thank to Ministry of Science, Technology and Innovation (MOSTI) for supporting this research under Science Fund Grant Schemes (SF 9005- 00031) and (03-01-06-SF0043) as well as to School of Manufacturing Engineering, Universiti Malaysia Perlis and UTM for providing research facilities to undertake this work.

References

Al-Kabie, H.S., (1989). ‘Radial Swirler for Low Emissions Gas Turbine Combustion’, PhD. Thesis, Univ. of Leeds.

Beer, J.M. and N.A. Chigier, (1972). Combustion Aerodynamics. Applied Science Publishers Ltd.

Craig T. Bowman, (1975). ’Kinetics of Pollution Formation and Destruction in Combustion.’, Prog. Energy Combust. Sci. Vol. 1, pp 33-45, Pergamon Press.

Escott, N.H., (1993). “Ultra Low NOx Gas Turbine Combustion Chamber Design”, University of Leeds, Department of Fuel and Energy, PhD.

Gupta, A.K., Lewis, M.J., and Qi, S., (1998). “Effect of Swirl on Combustion Characteristics of Premixed Flames,” J. Eng. Gas Turbine and Power, Trans, ASME, 120, July, 488-494.

Iannetti, A., Tacina, R., Cai, J., and Jeng, S.-M., (2001). “Multi-Swirler Aerodynamics: CFD Predictions”, AIAA 2001-3575, 37th AIAA/ASME/SAE/ASEE Joint Propulsion Conference and Exhibit, Salt Palace, Salt Lake City, UT, USA, July 8-11, 2001.

Judd, K.P., Rusak, Z., and Hirsa, A., (2000). "Theoretical and Experimental Studies of Swirling Flows in Diverging Streamtubes," in: Advances in Fluid Mechanics III, edited by M. Rahman and C.A. Brebbia, WIT Press, 491-502.

Khezzar L., (1998). 'Velocity Measurement in the Near Field of a Radial Swirler.' Experimental Thermal and Fluid Science, Vol 16, pp 230-236, Elsevier Science Inc.

Kim, M.N., (1995). Design of Low NOx Gas Turbine Combustion Chamber. University Of Leeds, Dept. of Fuel & Energy, PhD.

Syred, N. and M. Beer, (1974). 'Combustion in Swirling Flow: A Review', Combustion and Flame. 23:143-201.

Table 1. Dimensions of Various Radial Air Swirler

Swirler angle / Parameter	45º	50º	60º	70º
Passage width, h (mm)	12	11.2	9.6	8.8
Swirl number, $S^{'}$	0.780	0.978	1.427	1.911
No. of vane, n	8			
Outlet diameter, do (mm)	98			
Inlet diameter, di (mm)	50			
Vane depth, L (mm)	25			

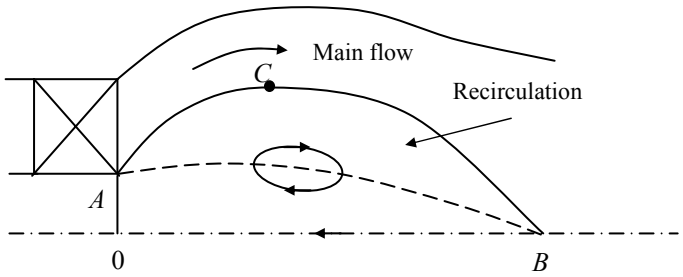

Figure 1. Recirculation zone in swirling flow

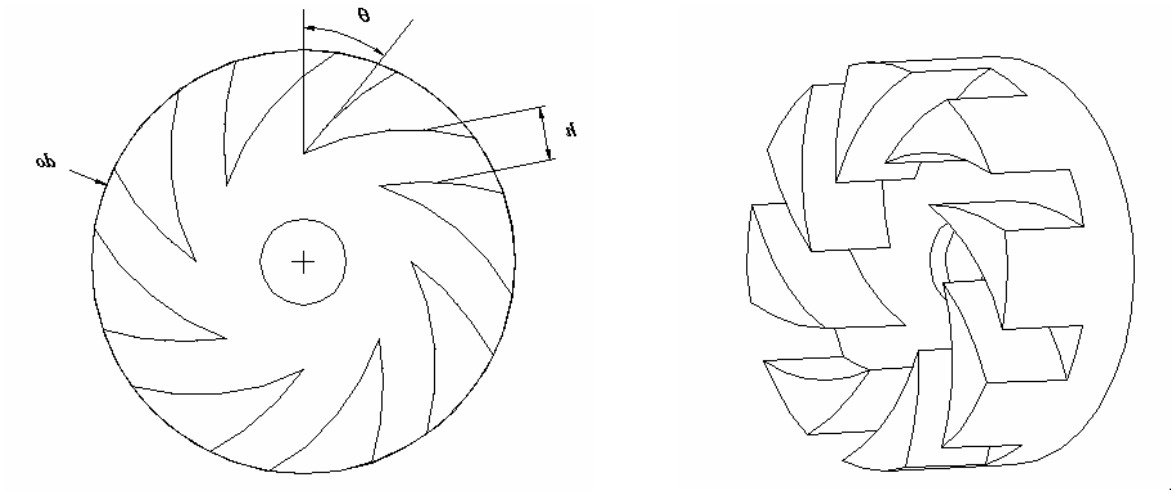

Figure 2. Schematic of Radial Air Swirler Design

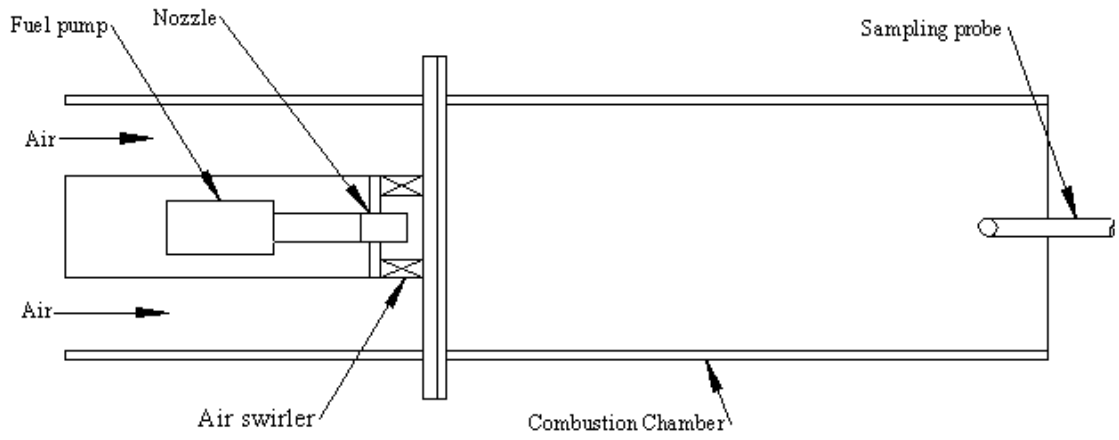

Figure 3. Schematic Diagram of the liquid bio-fuel burner experimental rig

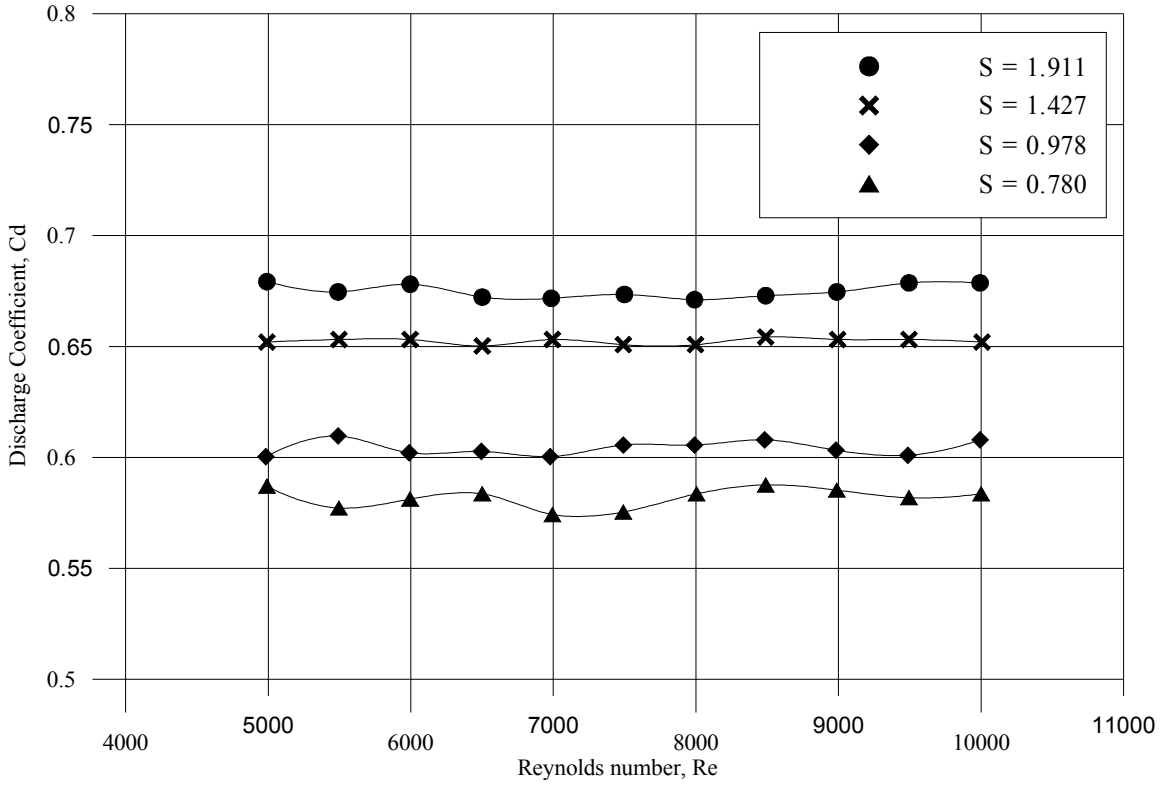

Figure 4. Discharge Coefficient vs. Reynolds Number for Various Swirl Numbers

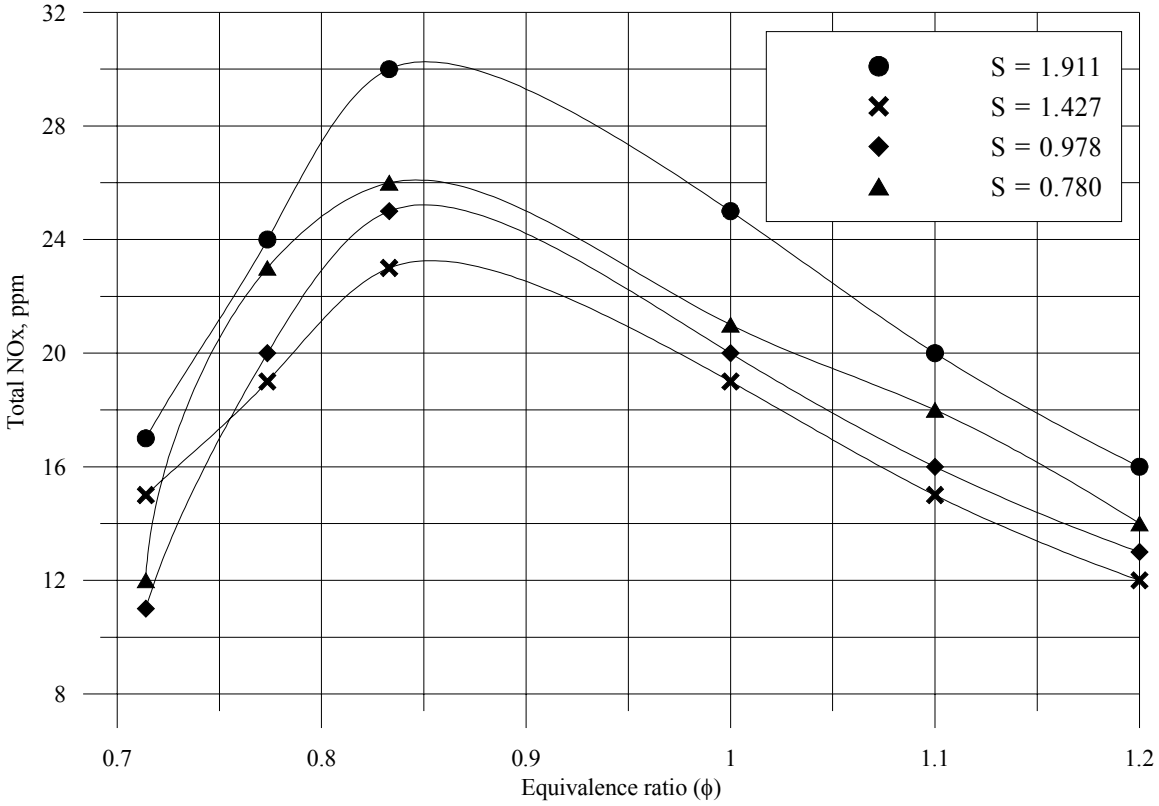

Figure 5. NO_X vs Equivalence Ratio for various swirl Number

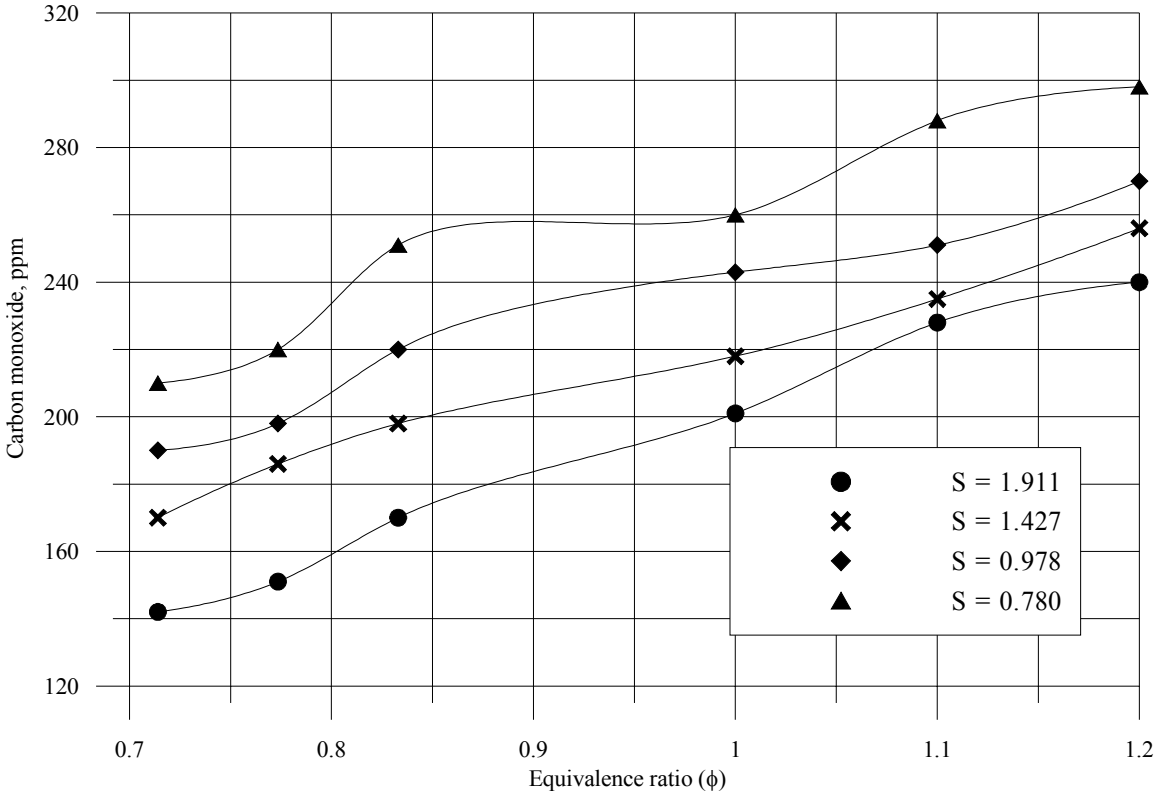

Figure 6. CO vs. Equivalence Ratio for various swirl number

Modern Applied Science

www.ccsenet.org/journal.html

Vol. 3, No. 6

June 2009

Study on Coating and Luminescence Mechanism of Hydrothermal Preparation of Mica-based Pearlescent Pigments

Daguang Li

School of materials science and engineering, Northwestern Polytechnical University

Xi'an 710072, China

Faculty of chemical engineering and light industry, Guangdong University of Technology

Guangzhou 510006, China

Tel: 86-20-3932-2235 E-mail: daguangl@gdut.edu.cn

Chao Yu

Faculty of chemical engineering and light industry, Guangdong University of Technology

Guangzhou 510006, China

Tel: 86-20-3932-2231 E-mail: hadiyuchao@163.com

Tiehu Li

School of materials science and engineering, Northwestern Polytechnical University

Xi'an 710072, China

Weiqing Fu, Wenjin Ji & Fenghua Zhao

Faculty of chemical engineering and light industry, Guangdong University of Technology

Guangzhou 510006, China

Abstract

Pearlescent pigment with the properties of high crystallinity, good dispersity, no agglomeration and smooth and crackless surface was prepared by hydrothermal method instead of calcination in the present paper. Through observation, rules of preparing high performance pearlescent pigment were obtained, described as follows: Increment of temperature and elongation of time during the period of hydrothermal reaction was beneficial to the crystallization of pearlescent pigment. Herein, coating and luminescence mechanism of pearlescent pigment was taken into further investigation.

Keywords: Mica-based pearlescent pigments, Hydrothermal synthesis, Coating mechanism, Luminescence mechanism

1. Introduction

Mica-based pearlescent pigment is a new kind of inorganic nonmetallic pigment with special effect which showing lustrous and iridescent due to angle-dependent optical effects deriving from alternating transparent layers with different reflection, refraction and transmission indices. It can reproduce graceful luster and colors which butterfly, shell, pearl, migratory fish and metals possess in nature. With many peculiarities which other pigments are provided with, such as pearlescent effect, metal-spark effect, perspective shot effect, color transferring effect, additional coloring effect, three dimensional effect and background contrast effect(Xu, 2005, PP. 23-26). Due to many excellent effects, mica-based pearlescent pigments are widely applied in a variety of industrial products, such as paints, ink, cosmetics, plastics, rubber and printed products(Sun, 2004, PP. 27-29).

In the producing process of mica-based pearlescent pigments, a critical point is crystallization treatment of pearlescent pigments. Currently, they are typically produced by the deposition of metal oxide layers on the substrate in aqueous suspension followed by a calcinations process(Xu, 2002, PP. 227~229, Young, 2008, PP. 213-218).The calcination of hydrous TiO_2 in order to eliminate surface absorbing water, capillary pores water and crystal water results in crystalline

TiO_2. As a matter of fact, agglomeration is an cardinal limiting factor in calcination. Particles of pearlescent pigment are prone to result in hard agglomeration and thus being caked, and thermal expansion coefficient between mica plate and TiO_2 thin layer is different, which have a notable influence on the dispersive property of pearlescent pigment and its optical effects.

It had been investigated that crystal materials were prepared using hydrothermal methods by geologists through simulating the natural mineralization since mid-19th century. Ever since 1905, functional materials have alternatively attracted many researchers' attention. It has been recently developed that nano-materials were prepared by hydrothermal methods(Li, 2007, PP. 1864-1868, Wang, 2007, PP. 225-230). Herein, crystal particles developed completely, granularity distributed uniformly with less agglomeration; material used was cheaper, and desirable stoichiometric composition materials could be obtained; particle size could be controlled during the process with lower production cost. Nano-powder prepared by hydrothermal methods need not calcination which could avoid the defects of agglomeration and introduced impurity.

Pearlescent pigments have been extensively applied, however, reports on the coating and luminescence mechanism were less available in the literature. In the present paper, pearlescent pigment was prepared by hydrothermal methods and the underlying coating and luminescence mechanism was also investigated.

2. Materials and methods

2.1 Preparation of mica-based pearlescent pigment

The synthetic (fluorophlogopite) mica used as the substrates for pearlescent pigment was purchased from Shantou, China. Mica powders were dissolved in certain volume of deionized water at the ratio of 1:n (n=10~30) and then transferred into 250ml 3 mouth flask. Solution pH value was adjusted to 1.0~2.4 with the addition of certain concentration of sulfuric acid solution. The batch was then heated in the acid solution under stirring for 30 mins. Then titanium solution with certain concentration as well as some deionized water was introduced into the agitated slurry. The slurry was stirred for 20 mins. After the completion of hydrolysis, the solids were filtered, washed with distilled water into neutral position and dried by air forced drying for 4 h or so at 70~110 °C.The resultant precursor was undertaken hydrothermal treatment. After filtering and drying, mica-based pearlescent pigment was obtained.

2.2 Testing and analysis

Scanning electron microscopy(SEM) images was obtained to observe the morphological aspects of fired samples by S-3400N-Ⅱ(kabushiki kaisha, Japan) with an accelerated voltage of 20KV; zeta potential was measured by Zetaprobe Software Operators Manval(Colloidal Dynamics, USA); X-ray diffraction(XRD) patterns were obtained on a XRF spectrometry(PGENERAL, Beijing) with Cu Ka radiation(40 KV, 200mA, λ=1.5406Å) and 2θ range of 20~70° and scan speed of 4°/min. According to X-ray diffraction rationale(Yang, 1989, PP. 184-189), within 2θ range, tangent was made at the lowest point, connected with the lowest point of characteristic diffraction peaks and thus amorphous scattering curve was depicted where the lower area was the integral intensity(Sa) of amorphous portion and the upper area was that (Sc) of crystalline portion.Crystallinity Xc was calculated by the following formula:

$$Xc = \frac{Sc}{Sc + 1.297Sa} \times 100\%$$

3. Results and discussions

3.1 Univariate analysis of hydrothermal reaction

Precursors of pearlescent pigment were dispersed into high-pressure reactor with deionized water and undertaken to hydrothermal reaction at certain temperature for certain time. These two factors were associated with crystallization of precursors and keeping integrity of coating membrane after dehydration process. Therefore, effects of time and temperature on the hydrothermal reaction should be investigated.

3.1.1 Effects of time

At the constant temperature of 240℃, hydrothermal reactions were performed for 4, 8 and 12h, respectively, using the same batch precursors of pearlescent pigment. Resultant powder was measured by XRD, and results were depicted with detail in Figure 1 and Table 1.

As seen from Figure 1 and Table 1, it was known that reaction time had a great influence on the crystallization of pigment, and crystallization increased with the increasing of time. Compared Figure 1 to the Joint Committee on Powder Diffraction Standards (JCPDS), crystal form of TiO_2 coating mica powders was anatase with a characteristic diffraction peak at 25.28° which corresponded to the crystal face(101) of TiO_2. Sample a was basically not crystallized. With the increasing of time, anatase TiO_2 diffraction peak of sample b and c at 25.28° became intensive and sharp, which indicated that the increment of reaction time was favorable to the crystallization of membrane coated by anatase TiO_2.

3.1.2 Effects of temperature

For the constant time of 12, hydrothermal reactions were performed at 180℃, 210℃ and 240℃, respectively, using the same batch precursors of pearlescent pigment. Resultant powder was measured by XRD, and results were depicted with detail in Figure 2 and Table 2.

As seen from Figure 2 and Table 2, it was known that crystallization increased with the increasing of reaction temperature.

3.2 Comparative analysis of hydrothermal synthesis and calcination

Results showed that hydrothermal process was simple and could obtain more excellent powder material than calcination without high temperature sintering.Powder material with the properties of high crystallinity, good dispersity and less agglomeration could be directly prepared by hydrothermal method.

As seen from Figure 3, it was obvious that there was agglomeration among pigments with calcination(Figure 3Ⅱ); pigments were well dispersed without any agglomeration(Figure 3Ⅰ). Furthermore, TiO_2 membrane layer crazed due to stress concentration during the period of calcination and was easy to shed(Figure 3 Ⅳ); Pigments by hydrothermal method could efficaciously avoid stress concentration, and thus resulted in good properties of smooth and compact surface without cracking and shedding(Figure 3 Ⅲ).

3.3 Coating mechanism of pearlescent pigments

Liquid phase deposition resulting in the precursors of mica-based pearlescent pigments belongs to the typical liquid-solid non homogeneous reaction. It is believed that mica substrate was first wetted by titanium solution, under the interaction of electrolyte solution and reaction temperature, mica flake with constant negative charge began to adsorb cationic complexes of $[Ti(H_2O)_6]^{4+}$ resulting from the first stage of hydrolysis of $TiCl_4$ solution, and formed a "double electrical layers" in the surface of mica flake. H^+ derived from H_2O group of $[Ti(H_2O)_6]^{4+}$ continuously transferred into solutions, gradually formed dimeric- or poly- complex ions of titanium, and then finally metatitanic acid particles which inhabited and developed in the surface of mica flake. Polynuclear complexes in the double electrical layers could develop any way along the solid surface. Due to the increasing of charges of polynuclear complex ions, their electrostatic attraction with the surface of mica flake increased correspondingly, which made them develop first along a certain part of the surface of mica flake and formed a "island-like coating" until coating the whole flake. Resultant complex ions develop further along the liquid surface, and thus completed the whole process of preparing titanium dioxide microcrystalline, namely a whole process of coating as follows: emergence--develop--converge--multi-layer coat(Gong, 2002, PP. 13-16).

According to the previous discussion of coating mechanism, surface electrokinetic potentials of mica flake and metatitanic acid particles at various pH values were measured, which were presented in Figure 5.

As seen from Figure 5, charges of mica flake and metatitanic acid particles varied at various pH values. Isoelectric point of metatitanic acid particles resulting from hydrolysis of $TiCl_4$ solution is 2.68 in water, when the pH values in reaction ranged from 1.0~2.3, due to great difference of heterocharge and intensive electrostatic attraction between mica flake and metatitanic acid particles, particles were proned to adsorb in the surface of mica flake when they collided with mica flake due to the stirring. When pH value was high in reaction system, both mica flake and metatitanic acid particles carried high negative charges. Electrostatic repulsion between them exceeded the adsorbability of particles, which kept the dispersion stability of reaction system and thus hampered the deposition of metatitanic acid particles in the surface of mica flake. Therefore, white turbidity happened usually during the process of reaction.

3.4 Luminescence mechanism of mica-based pearlescent pigment

Average particle size of crystal TiO_2 coating in the surface of mica flake was about 30~100nm. According to optical theory, when diameter of solid particle is smaller than half wavelength of visible light, it is transparent. Only transparent nano solid particles could completely reveal the light interference characteristic of films. When visible light(Ⅰ) exposed TiO_2 film at an incident angle, a part of light(Ⅱ) reflected, and other part of light permeate TiO_2 film to the surface of mica flake and reflected and transmitted iteratedly. In some certain condition, interference of parallel reflective lights (such as Ⅱ and Ⅲ) and parallel transmitted lights(Ⅳ and V) occurred, which introduced interference effect(Figure 7).

Single light transmitted by pearlescent pigment was strongly limited, only when the thickness of TiO_2 poly-crystal film attained the status of some light with certain wavelength resulting in constructive interference(Maile, 2005, PP. 150-163), and resultant single light was transmitted corresponding to the wavelength(color). Therefore, pearlescent pigment showed lustrous and iridescent due to angle-dependent optical effects deriving from alternating transparent layers with different reflection, refraction and transmission indices, which is the chromophoric essence of magical color pearlescent pigment. Such pigment showed different color based on the corresponding relation between the thickness of TiO_2 poly-crystal film and the wavelength of single light, and with the increasing of thickness, gradually showed silvery

white, golden yellow, red, purple, blue and green. Due to the limit of human eyes' discrimination, pigments with many transitional hue were produced during the process, which was approximately described here.

In the process of preparing pearlescent pigment, the thickness of film is the thinnest. Preparation of silver white pearlescent pigment need the simplest coating technology while its luminescence mechanism was the most complicated. Some researchers(Xu, 2005, PP. 23-26) speculated that it was composed of pigments which reflected a great deal of various color single light, and all these pigments reflecting different colors was distributed even. When the quantity of the single color pigment exceed 50% of the total pigments, pearlescent pigment showed our eyes not silver white but other colors.

We speculated that aforementioned reason was one of the cardinal factors resulting in silver white of pearlescent pigments, and the color transmitted was associated with the thickness of anatase TiO_2 film. Film of silver white was thinner than all other magic color pigments, and its average film thickness failed to attain the status of some light with certain wavelength resulting in constructive interference. Corresponding relation among the hue, wavelength, film thickness and optical thickness were listed in Table 3. According to optical constructive interference theory(Liang, 2008, P. 102) and the first colored pigment, golden yellow pearlescent pigment in the experiment, the thickness ranged from 53.9~58.8nm could transmit single colored light after calculating. Though average thickness failed to achieve the lowest condition of constructive interference, reflectivity of pigments increased enormously and the light intension we saw increased due to the high refractive index of TiO_2 poly-crystal film(2.55 of anatase TiO_2 and far higher than 1.58 of mica)(Chen, 2006, P. 30), which was an important reason that pearlescent pigment could show silver white luster. On the other hand, due to the irregularity of mica particle size, there was great difference among their specific surface area. In the deposition of meta-titanic acid, under the same reaction condition, TiO_2 poly-crystal film was coated irregularly in different mica flake and their optical thickness became more and more discrepant which made pigments tough to obtain pure single colored interference light. Consequently, few pigments with different colored light could be found when silver white pearlescent pigment was observed by ordinary microscope. Mixture of different wavelength light(different colored light) transmitted by pigments was beneficial to the formation of white light transmitted by pearlescent pigment from the global aspect. Taken together, silver white light derived from pearlescent pigment showed be investigated in two aspects.

4. Conclusions

Pearlescent pigment with the properties of high crystallinity, good dispersity, no agglomeration and smooth and crackless surface was prepared by hydrothermal method instead of calcination in the present paper. Rules of preparing high performance pearlescent pigment were obtained, described as follows: Increment of temperature and elongation of time during the period of hydrothermal reaction was beneficial to the crystallization of pearlescent pigment. Coating and luminescence mechanism of pearlescent pigment was further discussed based on our observations.

References

Chen, Z.H., & Liu, C.H. (2006). *Production and application of Titanium dioxides*. Beijing: Chemical Industry Press, 30.

Gong, X.Z. (2002). Study on the Mechanism of Mica-Titanium Pearl Pigment. *Industrial Minerals & Processing*, (6):13-16.

Li, G.P., & Luo, Y.J. (2007). Hydrothermal Preparation of ZnS Nanowires. *Chinese Journal of Inorganic Chemistry*, (11):1864-1868.

Liang, Q.T. (2008). *Physical Optics*. Beijing: Publishing House of Electronics Industry, 102.

Maile, F.J., Pfaff, G., & Reynders, P. (2005). Effect Pigments-Past, Present and Future. *Progress in Organic Coatings*, 54:150-163.

Sun, X.J., & Li , Z.J. (2004). Chromatics Art of Pearlescent Automobile Paint. *Modern Paint & Finishing*, (3):27-29.

Wang, Z.M., Li, Y.M., & Yang, X.J., et al. (2007). Hydrothermal Synthesis and Crystal Structure of Titanate Nanotubes. *Chinese Journal of Inorganic Chemistry*, (2):225-230.

Xu, K.Q., Dai, X.Y., & Chen, S.T. (2002). Synthesis of Rutile-Mica Pearlescent Pigment. *Fine Chemicals*, (4):227-229.

Xu, Y.Q. (2005). *Manufacture Processing and Application of Pearlescent Pigment*. Beijing: Chemical Industry Press, 23-26.

Yang, C.Z., Xie, D.C., & Chen, K.Z. (1989). *Phase Diffraction Analysis*. Metallurgical Industry Press, :184-189.

Young, C.R., Tae, G.K., & Guem, S.S., et al. (2008). Effect of Substrate on the Phase Transformation of TiO_2 in Pearlescent Pigment. *Journal of Industrial and Engineering Chemistry*, 14:213-218.

Table 1. Pigment's crystallization at various times

Sample	4 h(a)	8 h(b)	12h(c)
Xc(%)	——	72.3	74.4

Table 2. Pigment's crystallization at different temperature

Sample	180℃(d)	210℃(e)	240℃(f)
Xc(%)	50.3	75.1	86.7

Table 3. Corresponding relation among the hue, wavelength, film thickness and optical thickness

Hue	Wavelength (nm)	Film thickness(nm)	Optical thickness(nm)
Golden yellow	550~640	53.9~58.8	137.4~149.9
Red	640~780	58.8~76.5	149.9~195.1
Purple	380~450	111.8~132.4	195.1~337.6
Blue	450~480	132.4~141.2	337.6~360.1
Green	480~550	141.2~161.8	360.1~412.6

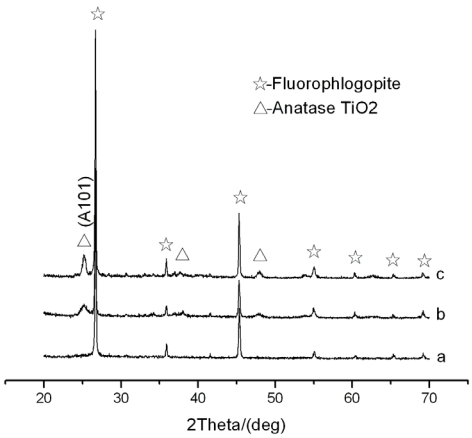

Figure 1. XRD patterns of pigment at various time: (a) 4h ; (b)8h; (c) 12h

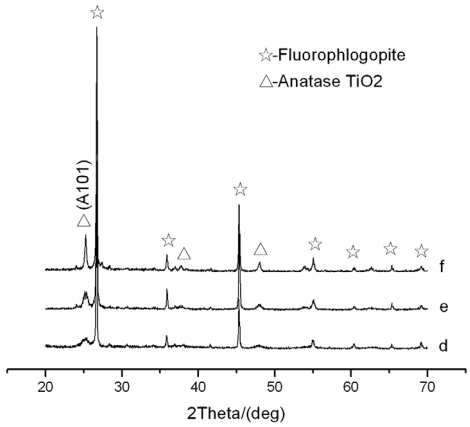

Figure 2. XRD patterns of pigment at different temperature: (d) 180℃; (e) 210℃; (f) 240℃

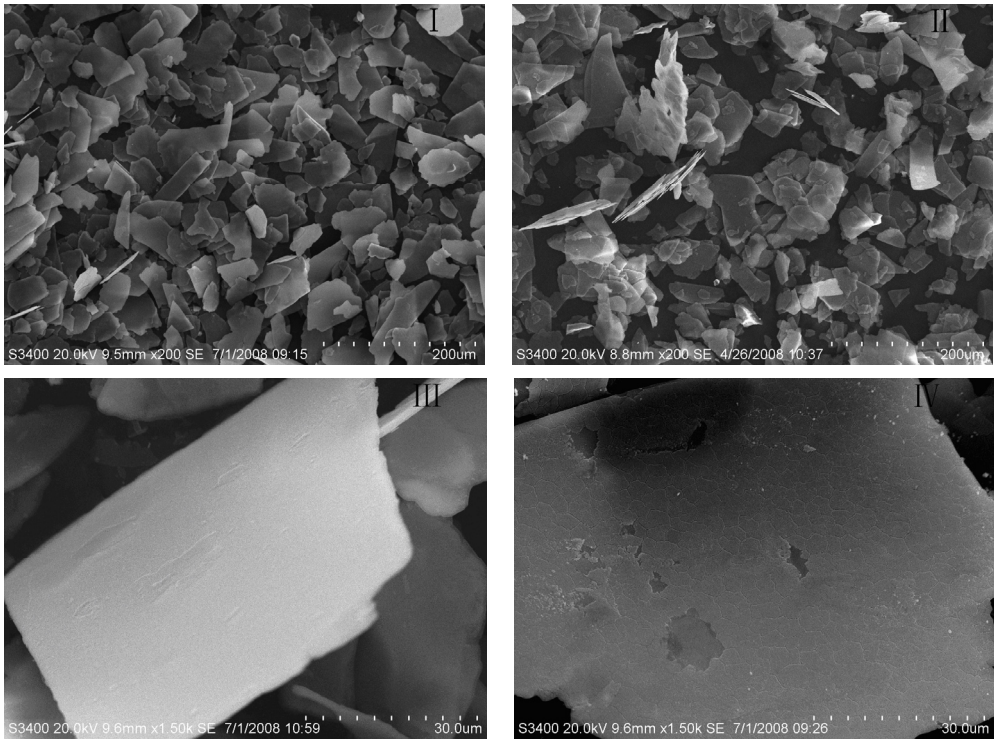

Figure 3. SEM images of pearlescent pigments

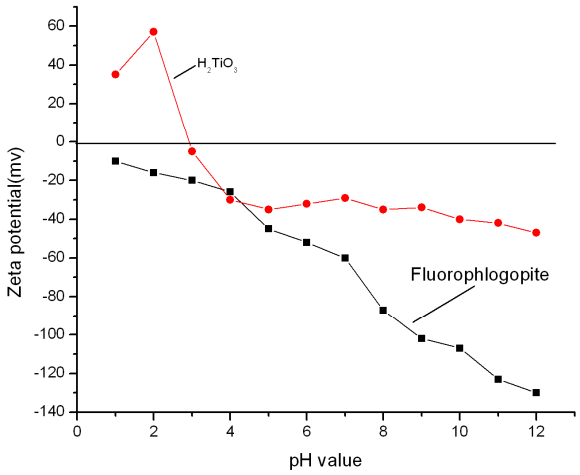

Figure 5. Effects of pH values on Zeta potential of metatitanic acid particles and fluorophlogopite flake

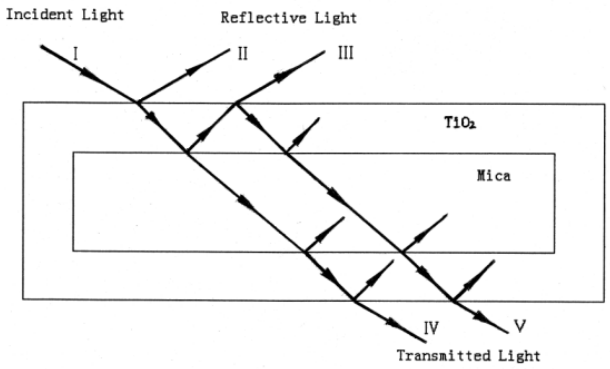

Figure 7. The reflection diagram of mica-based pearlescent pigment

Modern Applied Science

www.ccsenet.org/journal.html

Vol. 3, No. 6

June 2009

Vibration-Based Fault Diagnosis of Hydraulic Pump of Tractor Steering System by Using Energy Technique

Kaveh Mollazade (Corresponding author)

Department of Agricultural Machinery Engineering, Faculty of Biosystems Engineering

University of Tehran, P.O. Box 4111, Karaj 31587-77871, Iran

Tel: 98-918-972-0639 E-mail: kaveh.mollazade@gmail.com, mollazade@ut.ac.ir

Hojat Ahmadi

Department of Agricultural Machinery Engineering, Faculty of Biosystems Engineering

University of Tehran, P.O. Box 4111, Karaj 31587-77871, Iran

Mahmoud Omid

Department of Agricultural Machinery Engineering, Faculty of Biosystems Engineering

University of Tehran, P.O. Box 4111, Karaj 31587-77871, Iran

Reza Alimardani

Department of Agricultural Machinery Engineering, Faculty of Biosystems Engineering

University of Tehran, P.O. Box 4111, Karaj 31587-77871, Iran

Abstract

This paper focuses on a problem of vibration-based condition monitoring and fault diagnosis of pumps used in the tractor steering system. The vibration signal from a piezoelectric transducer was captured for the following conditions: normal pump, journal-bearing with inner face wear, gear with tooth face wear, and journal-bearing with inner face wear plus gear with tooth face wear for three working levels of pump speed (1000, 1500, and 2000 rpm). Then Power Spectral Density (PSD) of vibration spectra was then calculated. Results showed that peak value of PSD was occurred in the frequency range between 70-120 Hz for all conditions. Comparison of numerical data produced by calculation the area under PSD v. frequency diagram showed that energy technique is an effective method for fault diagnosis of external gear hydraulic pumps.

Keywords: Power spectral density, Vibration signal, External gear pump, Fault diagnosis

1. Introduction

Nowadays, hydraulic pumps are more widely used in the power transmission system of automobiles and tractors as a main part of their hydraulic system. Steering system of modern tractors is equipped with both mechanical and hydraulic systems. Use of hydraulic power in the steering system can provide a facilitated steering for driver of tractor in the hard condition of farm lands. Hydraulic pumps are available in several types and are consisting of rotating and reciprocating parts (Srivastava, 2006).

The detection and understanding of condition degradation in the pump is important for pump design and maintenance. For pump condition monitoring, the processing and analysis of the measured signal is the common way of extracting reliable feature representative of the pump condition (Mollazade et al., 2008).

Condition monitoring provides information on the health and maintenance requirement of machinery and is used in a wide range of industrial applications. Parameters such as vibration, temperature, lubricant quality and power

consumption can be used to monitor the mechanical status of equipment (James et al., 2004). In general, fault detection and diagnosis is a broad and active area of research. There are a large volume of papers that deal with this subject (Huang, 2001). In many applications the problem of fault detection and diagnosis is a crucial issue that has been theoretically and experimentally investigated with different types of approaches (Basseville and Nikiforov, 1993).

Monitoring and failure detection improves the reliability and availability of an existing system. Since various failures degrade relatively slowly, there is potential for fault detection at an early stage. This avoids the sudden, total system failure which can have serious consequences. It is important in the context of condition monitoring to distinguish fault detection from fault diagnosis. Fault detection is the decision if a fault is present or not while fault diagnosis provides more information about the nature or localization of the failure. This information can be used to minimize downtime and to schedule adequate maintenance action (Chafei et al., 2008).

The use of vibration and acoustic emission (AE) signals is quite common in the field of condition monitoring of rotating machinery. By comparing the signals of a machine running in normal and faulty conditions, detection of faults like mass unbalance, rotor rub, shaft misalignment, gear failures and bearing defects is possible. These signals can also be used to detect the incipient failures of the machine components, through the on-line monitoring system, reducing the possibility of catastrophic damage and the machine down time (Samanta et al., 2003). In recent years, on-line and automatic types of fault detection and diagnostic systems have been gaining considerable amount of business potential. The need for automating industrial processes and optimizing the cost of maintenance has stimulated the research and development of faster and robust fault diagnosis (Wuxing et al., 2004). Attempts have been made towards classification of the most common type of rotating machinery problems, defining their symptoms and search for remedial measures (Nalinaksh and Satishkumar, 2001).

Signal processing methods have been widely used to extract fault feature of vibration signals. Fast Fourier Transform (FFT), which has been the dominating analysis tool for feature extraction of stationary signals, could produce the statistical average characteristics over the entire duration of the data (Akaike, 1974; Haloui et al., 2006). However, it fails to provide the whole and local features of the signal in time and frequency domain. FFT suffers from some limitations. Among these limitations, the FFT is not efficient to describe the non-stationarities introduced by faults in the vibration signal. The second limitation and the most important one is the frequency resolution, which is the ability to distinguish the spectral responses to two or many harmonics. Another limitation is due to the windowing of data which appears during the FFT processing. In order to overcome these performance limitations inherent to the FFT approach, many modern spectral estimation techniques have been proposed during the last two decades (Jones, 1974; Cadzow, 1982; Bekka, and Chikouche, 1999). Power spectral density (PSD) is one of those methods that is reported by several research works (Gibson, 1972; Norton and Karczub, 2003).

Hence, the subject of this research was to diagnose the common faults of steering system hydraulic pump of Massey Ferguson MF 285 model tractor based on vibration monitoring and power spectral density method.

2. Material and Methods

2.1 Experimental works

A number of carefully designed experiments were carried out a hydraulic pump of steering system of Massey Ferguson MF 285 model tractor. This pump is an external gear hydraulic pump. This pump uses two rotating gears which un-mesh at the suction side of the pump to create voids which allow atmospheric pressure to force fluid into the pump. The spaces between the gear teeth transport the fluid along the outer perimeter of the housing to the discharge side, and then the gears re-mesh at the center to discharge the fluid. The gears are supported by Journal-bearings on both sides, which allow high discharge pressure capabilities. The motion of the motive gear is directly produced by tractor engine. Figure 1 shows the components of this pump.

Under the consideration of the degree of damage to the external gear pump, and the influence of economic cost, the faults were simulated mainly in the pump during the experiment. Vibration signals were collected for both normal condition and several different abnormal conditions (see Table 1 and Figure 2). Faulty parts were selected from the several pumps that were worked for a long time periods and their faults led to reduce of their efficiencies. The working speed of main shaft of the pump was set at approximately 1000, 1500, and 2000 rpm of engine rotational speed.

With the sensor mounted on body of gear housing of the pump, vibration signals were measured for various fault conditions by on-line monitoring when tractor was working at a stationary situation. The sensor used is a piezoelectric accelerometer (VMI-102 model) which was mounted on the flat surface of pump using hand mounting technique because of aluminized substance of the gear housing of the pump. The sensor was connected to the signal-conditioning unit (X-Viber FFT analyzer), where the signal goes through a charged amplifier and an analogue-to-digital converter (ADC). The vibration signal in digital form was saved on computer through a USB port for further analyses. The software SpectraPro-4 that accompanies the signal-conditioning unit was used for recording the signals directly in the computer's secondary memory. The signal was then read from the memory and processed to extract the Fast Fourier

Transform (FFT) of vibration spectrum. The sampling rate was 1000 Hz. After calculating FFT of vibration signals, power spectral density (PSD) was calculated and then graph of PSD versus frequency was plotted for each spectrum.

2.2 Theoretical principles

2.2.1 Fast Fourier Transform

FFT is applied in order to convert time domain signals X(n) into the frequency domain (Brigham, 1988; Yang and Penman, 2000):

$$X(f) = \frac{1}{N}\sum_{n=0}^{N-1} x(n) e^{-i2\pi n\frac{f}{N}}, \text{ f=0, 1, 2, …, N-1} \quad (1)$$

where f is the discrete frequency.

2.2.2. Power Spectral Density (PSD)

PSD function shows the strength of the variations (energy) as a function of frequency. In other words, it shows at which frequencies variations are strong and at which frequencies variations are weak (Irvine, 1998). It can be obtained from the FFT as follows.

The complex spectrum of a vibration *x(t)* in the time range (t_1, t_2) for any frequency f in the two-sided frequency domain (*-f*, *+f*) can be stated as (2) (Howard, 2002).

$$X(f) = \int_{t_1}^{t_2} x(t) e^{-2\pi i f t} dt \quad (2)$$

If *x(t)* is expressed in units of m/s^2, *X(f)* is expressed in units of $(m/s^2)/Hz$. From the complex spectrum, the one-sided PSD can be computed as (3).

$$PSD(f) = \frac{2|X(f)|^2}{(t_2 - t_1)} \quad (3)$$

where the factor 2 is due to adding the contributions from positive and negative frequencies.

The PSD divides up the total power of the vibration. To see this, we integrate it over its entire one-sided frequency domain (*0, f*):

$$\int_0^f PSD(f) df = \frac{\int_{t_1}^{t_2} |x(t)|^2 dt}{(t_2 - t_1)} \quad (4)$$

This is precisely the average power of the vibration in the time range (t_1, t_2). However, if the FFT of vibration signal be used, then the PSD may be calculated directly in the frequency domain by following formula (Irvine, 2000; Howard, 2002):

$$PSD = \frac{G^2_{rms}}{f} \quad (5)$$

where G_{rms} is the root-mean-square of acceleration at a given frequency *f*.

The most common set of erroneous units for PSD are $(m^2/s^4)/Hz$; which should instead be $(m^2/s^3)/Hz$. It must be noted that the (specific) power is really watts per kg per FFT component, which equals m^2/s^3 per FFT component (Peters, 2007). Here, Curve Expert v.1.3 software was used for estimating the area under PSD versus frequency curve. This software uses Trapezium rule in order to calculate the area under the curve (Davis and Rabinowitz, 2007).

3. Results and discussion

Figure 3 is an example of typical frequency spectra obtained from a vibration signal collected from various condition of pump. From this figure it can be observed that there are significant differences between spectral lines at each condition of pump. Also, frequencies that maximum amplitude is occurred are different.

Results show that the pumps dynamic responses, generated by a wide range of possible impulsive sources, are very complex. These sources may include the coincidence vibration in the hydraulic-end of the pump existing between fluid and the pipelines and cylinders, the whirlpool swash of fluid, the valve impact, the piston slap, the fluctuation of the fluid pressure in exhaust pipelines, the periodic impulsive inertial forces and moments, the shock coming from defective bearing, and mechanical events.

In the results, not only are individual samples of frequency spectra representing different faults often rather similar, but often rather similar having variability within a group of spectra that represent the same fault is significant. Figures 4 (a) and (b) show two frequency spectra that represent the same sample fault (GTFW at 1000 rpm). From this figure it can

be observed that there are obvious differences between these two samples of pump. For other conditions similar results were observed. The challenge is to provide early detection capability as well as distinction between fault types with a low risk of false alarms. In the fault diagnosis of pump, the frequency spectra of vibration signals contain complicated information of the running condition. Therefore it can be concluded that use of FFT is not suitable for diagnose of pump faults.

Similar findings were reported by Wang and Hu (2006) for five-plunger pumps and Wang and Chen (2007) for centrifugal pumps. They reported that in the early stages of a fault, effects of noise are so strong that the symptoms of a fault are not evident.

In order to devise a simple fault diagnosis, PSD function of frequency spectra was calculated. Diagram of PSD curves versus frequency for each condition of pump are shown in the figures 5 to 7. Results showed that peak value of PSD was occurred in the frequency range between 70-120 Hz for all conditions. At first glance it can be observed that the area under PSD-Frequency curves is different for different condition of pump. This characteristic can be used in the fault classification of pump. Therefore, the area under PSD-Frequency diagram for 10 spectra at each condition was calculated and the average of them is shown in Figure 8. According to this figure, area is increased by increasing the fault severity at each working speed. At GOOD and BIFW fault types of pump, maximum value of area was for 2000 rpm condition, but this value was at maximum for 1000 rpm condition at GTFW and G&BW condition.

4. Conclusion

The applications of the technique presented in this work are intended to be an analysis tool that can be used like an aid in the incipient detection problem of tractor steering pump faults. Summary of conclusion can be stated as follows:

1) Fault diagnosis of hydraulic pump is difficult using spectrum of vibration signals alone.

2) It is difficult to identify the symptom parameters for diagnosis by which all fault types can be distinguished perfectly.

3) Energy technique (calculation of area under PSD v. Frequency diagram) is suitable to diagnose several fault types that may be occurred at an external gear hydraulic pump. Therefore this technique can be used as a simple and reliable method for fault diagnosis of MF285 tractor steering pump.

4) Results of this study can be used as an input for automatic fault diagnosis systems such as neural network and fuzzy logic.

References

Akaike, H. (1974). A new look at the statistical model identification. *IEEE. Transactions on automatic control,* AC-19(6).

Basseville, M., & Nikiforov, I. V. (1993). *Detection of abrupt changes – theory and applications.* Englewood Cliffs: Prentice-Hall Inc., Simon & Schuster Company.

Bekka, R. E., &. Chikouche, D. (1999). Pouvoir de detection et de résolution de la méthode AR: Application aux signaux courts. *Revue Sciences &c Technologie, Univ. Constantine*, 12, 49- 53.

Brigham, E. (1988). *Fast fourier transform and its applications*. Prentice Hall Press.

Cadzow, J. A. (1982). Spectral estimation: an overdetermined rational model equation approach. *Proc. IEEE*, 70(9), 907-937.

Chafei, S., Zidani, F. R., Nait-said, M., & Boucherit, S. (2008). Fault detection and diagnosis on a PWM inverter by different techniques. *Journal of Electrical Systems,* 4(2), 1-12.

Davis, P. J., & Rabinowitz, P. (2007). *Methods of numerical integration*. (2nd Edition). Dover Publications.

Gibson, B. (1972). *Power Spectral Density: a fast, simple method with low core storage requirement*, M.I.T. Charles Stark Draper Laboratory Press.

Haloui, N., Chikouche D., Benidir, M., & Bekka,R. E. (2006). Diagnosis of gear systems by specral analysis of vibration signals using synchronous cepstre technique. *ESTS Internationl Transactions on Communication and Signal Processing*, 8 (1), 27 –36.

Huang, B. (2001). Detection of abrupt changes of total lest square models and application in fault detection. *IEEE Transactions on Control Systems Technology*, 9(2), 357-367.

Howard, R. M. (2002). *Principles of random signal analysis and low noise design: The power spectral density and its applications*. Wiley-IEEE Press.

Irvine, T. (1998). *An introduction to spectral functions*. Vibration Data Press.

Irvine, T. (2000). *Power spectral density Units: [G2 / Hz]*. Vibration Data Press.

James, E. P., Tudor, M. J., Beeby, S. P., Harris, N. R., Glynne-Jones, P., Ross, J. N., & White, N. M. (2004). An investigation of self-powered systems for condition monitoring applications. *Sensors Actuarors,* 110, 171-176.

Jones, R. H. (1974). Identification and autoregressive spectrum estimation, IEEE. *Transaction on automatic control,* AC-131(13).

Mollazade, K., Ahmadi, H., Omid, M., & Alimardani, R. (2008). An intelligent combined method based on power spectral density, decision trees and fuzzy logic for hydraulic pumps fault diagnosis. *International Journal of Intelligent Systems and Technologies*, 3(4), 251-263.

Nalinaksh, S., & Satishkumar, V. D. (2001). Artifcial neural network design for fault identification in a rotor-bearing system. *Mechanism and Machine Theory*, 36, 157-175.

Norton, M. P., & Karczub, D. G. (2003). *Fundamentals of noise and vibration analysis for engineers*. Cambridge University Press.

Peters, R. D. (2007). *A new tool for seismology-the cumulative spectral power.* Georgia: Mercer University Press.

Samanta, B., Al-Balushi, K. R., & Al-Araimi, S. A. (2003). Artificial neural networks and support vector machines with genetic algorithm for bearing fault detection. *Engineering Application of Artificial Intelligence*, 16, 657-665.

Srivastava, A. k., Georing, C. E., Rohrbach, R. P., & Buckmaster, D. R. (2006). *Engineering principles of agricultural machines.* (2nd ed.). Michigan: St. Joseph Press.

Wang, J., & Hu, H. (2006). Vibration-based fault diagnosis of pump using fuzzy technique. *Measurement,* 39: 176–185.

Wang, H. Q. & Chen. P. (2007). Fault diagnosis of centrifugal pump using symptom parameters in frequency domain. *Agricultural Engineering International: the CIGR Ejournal.* Manuscript IT 07 005. Vol. IX.

Wuxing, L., Tse Peter, W., Guicai, Z., & Tielin, S. (2004). Classification of gear faults using cumulants and the radial basis function network. *Mechanical Systems and Signal Processing*, 18, 381-389.

Yang, D. M., & Penman, J. (2000). Intelligent detection of induction motor bearing faults using current and vibration monitoring. *Proceedings of COMADEM 2000*, 1, 461-470.

Table 1. Pump faults taken into consideration

Number	Fault type	Label of Fault
1	Normal pump	GOOD
2	Journal-bearing with inner face wear	BIFW
3	Gear with tooth face wear	GTFW
4	Mixture of faults number 2 & 3	G&BW

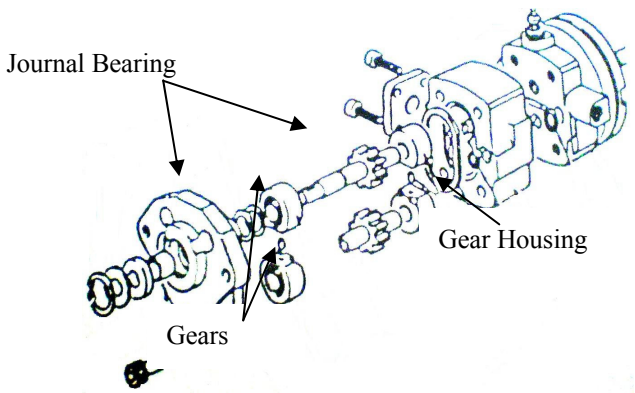

Figure 1. Main components of an external gear pump

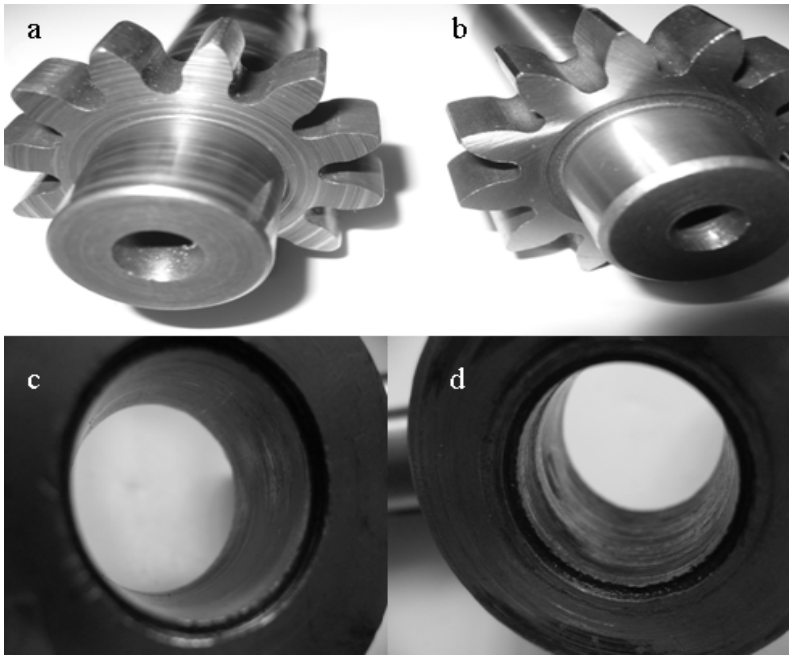

Figure 2. a. View of gear with tooth face wear, b. View of good gear,
c. View of good journal-bearing, d. View of journal-bearing with inner face wear

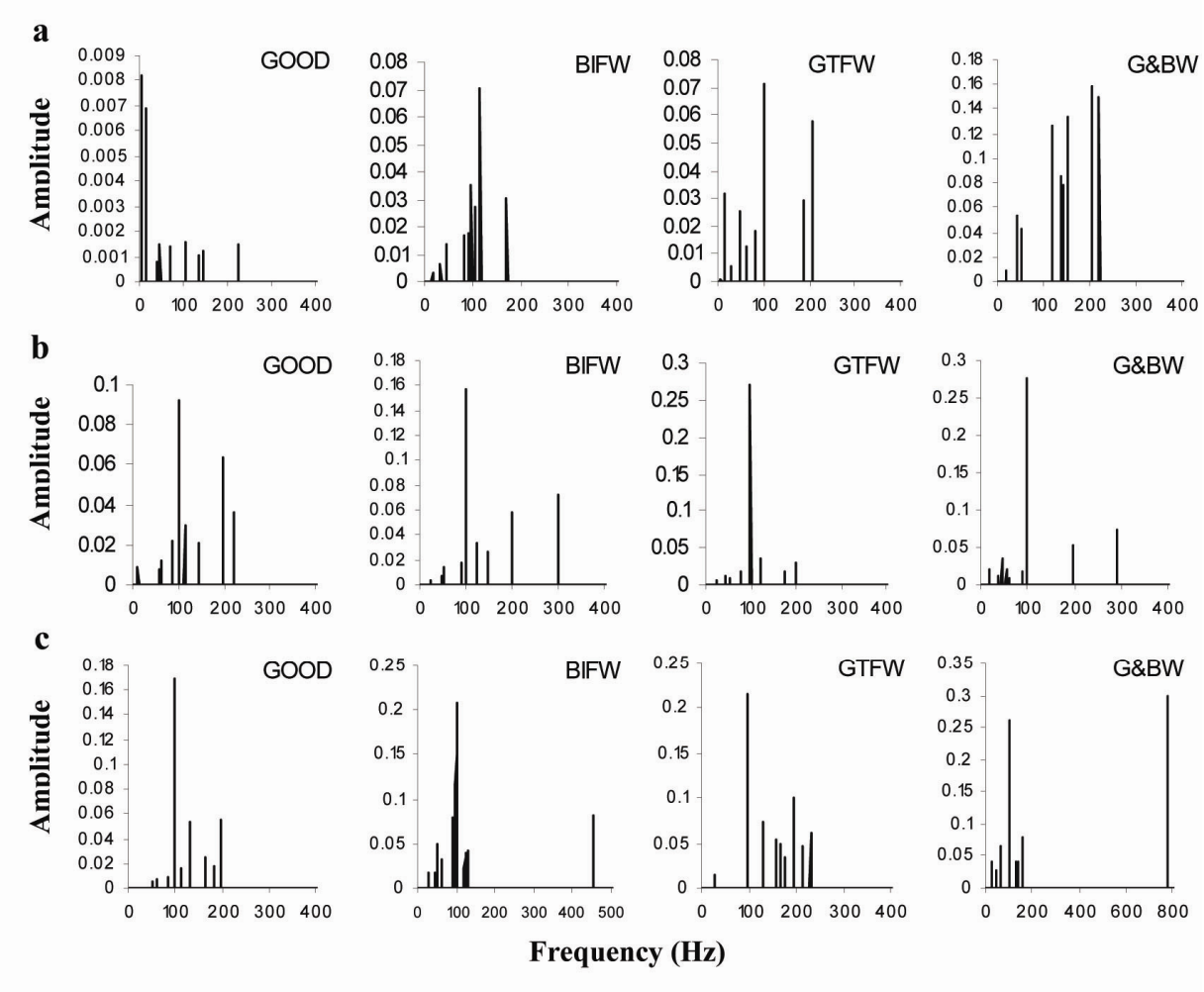

Figure 3. Frequency spectra of pump in a. 1000 rpm, b. 1500 rpm, and c. 2000 rpm

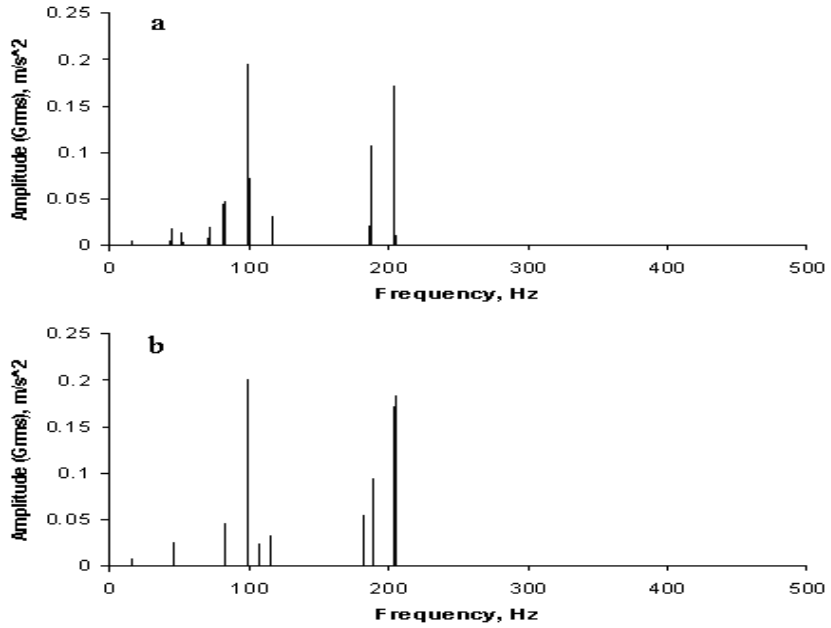

Figure 4. Two frequency spectra that represent the same sample fault.
(a) and (b) both show the GTFW fault at 1000 rpm

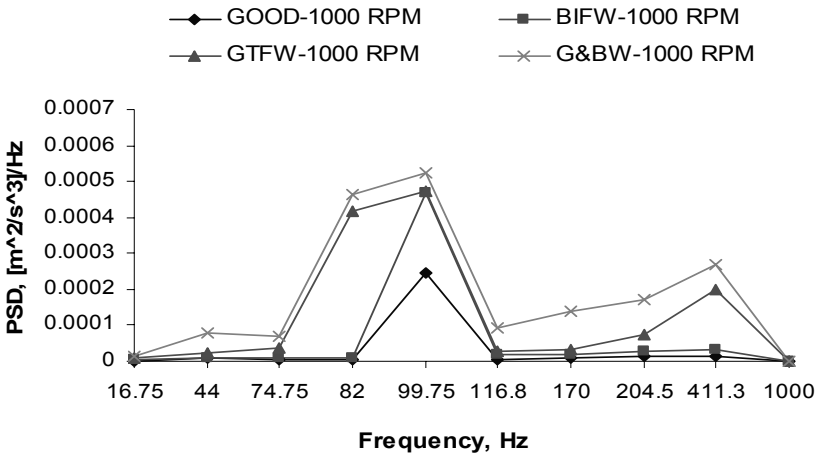

Figure 5. PSD versus frequency diagram for 1000 rpm condition

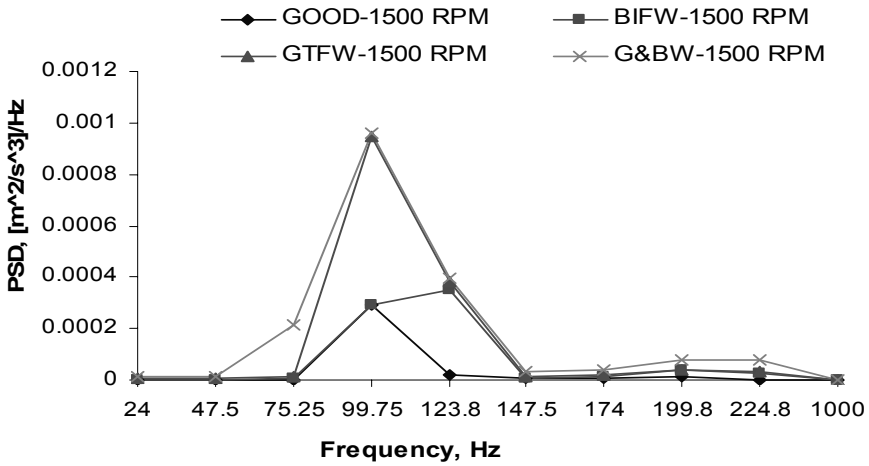

Figure 6. PSD versus frequency diagram for 1500 rpm condition

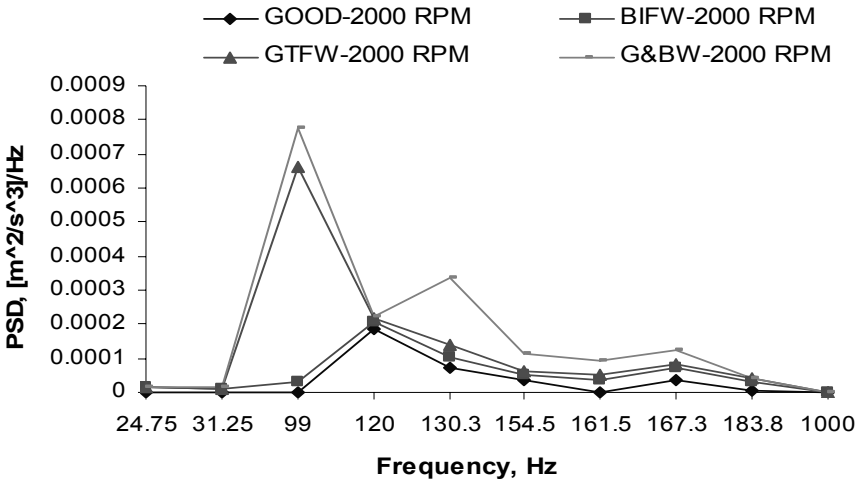

Figure 7. PSD versus frequency diagram for 2000 rpm condition

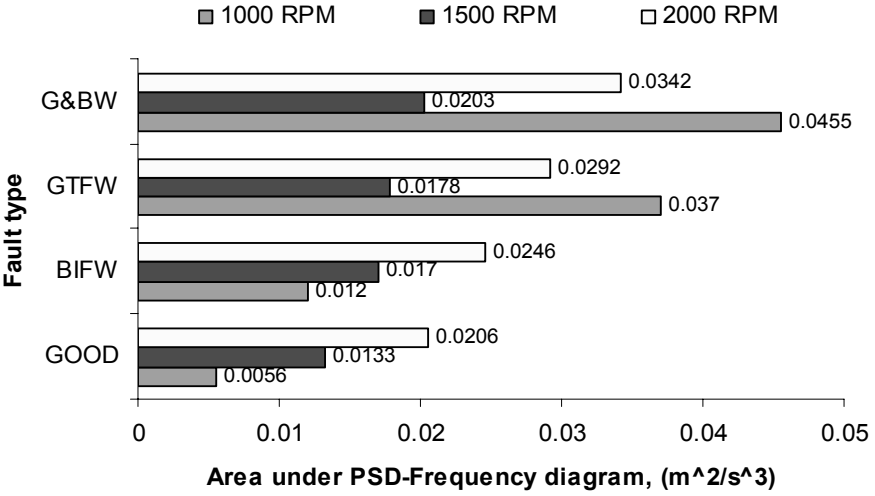

Figure 8. Average value of area under PSD-Frequency diagram at each condition of pump